

Die approbierte Originalversion dieser Diplom-/Masterarbeit ist an der Hauptbibliothek der Technischen Universität Wien aufgestellt (<http://www.ub.tuwien.ac.at>).

The approved original version of this diploma or master thesis is available at the main library of the Vienna University of Technology (<http://www.ub.tuwien.ac.at/englweb/>).



DIPLOMARBEIT

Fast Calibration in the Heston Model

ausgeführt am Institut für
Wirtschaftsmathematik
der Technischen Universität Wien

unter der Anleitung von
Dr. STEFAN GERHOLD

durch
RUDOLF BAUER

Lindenweg 5
3632 Bad Traunstein
bauer.r@hotmail.com

Wien, am 15. Februar 2012

Danksagung

Ich möchte mich an dieser Stelle bei allen bedanken, die direkt oder indirekt zur Entstehung dieser Diplomarbeit in Form fachlicher oder anderweitiger Unterstützung beigetragen haben.

Mein herzlicher Dank gilt Herrn Dr. Stefan Gerhold für die Betreuung meiner Arbeit und Herrn Dr. Richard Warnung, der mir die Daten für die empirische Untersuchung zur Verfügung gestellt hat.

Besonders bedanken möchte ich mich bei meinen Eltern, Hildegard und Rudolf, dass sie mir mein Studium ermöglicht und mich immer unterstützt haben. Auch meinen Geschwistern und ihren Partnern, Roman & Michaela, Gudrun & Helmut und Sandra & Johannes, gilt mein ganz besonderer Dank für ihre großartige Unterstützung im Laufe meines Studiums.

Einen großes Dankeschön geht außerdem an meine Freunde Alexander, Beatrice, Christoph, Florian, Johannes, Lukas, Magdalena, Martin, Michael, Sabrina, Stephanie und Thomas, und die Bib-Crew Bernhard, Gregor und Markus, für ihre Unterstützung und dass sie meine Studienzeit unvergesslich machten.

Weiters möchte ich mich noch bei Anita, Can, Christian und Julia bedanken, die mir durch ihre unzähligen Hilfestellungen das Studium erleichtert haben.

Vielen herzlichen Dank,
Rudolf Bauer

Abstract

The Heston model is one of the most popular stochastic volatility models for derivatives pricing. The model proposed by Heston (1993) takes into account non-lognormal distribution of the assets returns, leverage effect and the important mean-reverting property of volatility. In addition, it has a semi-closed form solution for European options. It therefore extends the Black and Scholes model and includes it as a special case.

The prices produced by the model are quite parameter sensitive, hence the calibration of the parameters is as crucial as the model itself. The calibration must be robust and stable and should not be too computer intensive, which rules out global optimisation algorithms. The general approach of applying a least-square type procedure is very sensitive to the choice of the initial point. Therefore, literature on closed-form asymptotic approximations has grown rapidly in the past few years. An overview of these approximations will be presented in this thesis and some will be proved for their accuracy in delivering a starting point for the calibration.

Contents

Abstract	v
Contents	vii
List of Figures	ix
1 Introduction	1
1.1 Motivation	1
1.2 Structure of Thesis	2
2 The Black-Scholes Theory of Derivative Pricing	5
2.1 Market Model	5
2.1.1 Brownian Motion	6
2.1.2 Stochastic Integral	7
2.1.3 Risky Asset Price Model	8
2.1.4 Itô's Formula	9
2.1.5 Lognormal Risky Asset Price	10
2.2 Derivative Contracts	11
2.2.1 European Call and Put Options	12
2.2.2 Moneyness of an Option	13
2.3 Replicating Strategies	14
2.3.1 Replicating Self-Financing Portfolios	15
2.3.2 The Black-Scholes Partial Differential Equation	15
2.3.3 The Black-Scholes Formula	17
2.3.4 Put-Call Parity	18
2.4 Volatility	19
2.4.1 Historical Volatility	20
2.4.2 Implied Volatility	20
2.5 Limitations of the Black-Scholes Model	21
2.5.1 Shortcomings of Gaussian distribution	22
2.5.2 Clustering and Leverage effect	23
2.5.3 Volatility Smile	24

3	Stochastic Volatility and the Heston Model	27
3.1	Moving to Stochastic Volatility Models	27
3.2	Derivation of the Valuation Equation	28
3.3	Base Equations of the Heston model	30
3.4	Incomplete Market in the Heston Model	32
3.5	Semi-closed Form Solution for European Options	33
3.6	Influence of Parameters	35
3.7	Advantages and Disadvantages of the Heston Model	39
4	Asymptotic Behaviour in the Heston model	43
4.1	Lee's Moment Formula	44
4.2	Short-maturity asymptotic behaviour	48
4.3	Large-maturity asymptotic behaviour	50
4.3.1	Large-maturity & Large-strike	50
4.3.2	Large-maturity & Fixed-strike	51
4.4	Extreme-strike asymptotic behaviour	52
4.4.1	Right Tail Asymptotics	53
4.4.2	Left Tail Asymptotics	54
5	Fast Calibration	57
5.1	Option Data	57
5.1.1	Austrian-Traded-Index	57
5.1.2	Data Description	57
5.2	Estimation Procedure	58
5.3	Empirical Findings	60
5.3.1	Short-maturity	61
5.3.2	All Asymptotic Formulas	77
5.4	Conclusion	96
A	Software	97
B	MATLAB Code	99
B.1	Calibration	99
B.2	Small-maturity	101
B.3	Small-maturity Leading Order Term	101
B.4	Large-maturity	101
B.5	Small-strike	102
B.6	Large-strike	104
B.7	Heston Model	105
C	Curriculum Vitae	107
	Bibliography	111

List of Figures

- 2.1 Sample path of a standard Brownian motion. 7
- 2.2 Lognormal density function with $\mu = 5$ and $\sigma = 0.5$ 11
- 2.3 Profit from buying a European *call option* on one share of a stock. Option price $C = 5$, strike price $K = 100$. Source: [34] 12
- 2.4 Profit from buying a European *put option* on one share of a stock. Option price $P = 7$, strike price $K = 70$. Source: [34] 13
- 2.5 Moneyness regions in a European call option (left) and in a European put option (right). Original Image Source: [34] 14
- 2.6 The Black-Scholes price for an European Call option with $K = 100, \sigma = 0.3, r = 0.05$. Source: [40] 18
- 2.7 Black-Scholes call and put option pricing function at time $t = 0$, with $K = 100, T = 0.5, \sigma = 0.1$ and $r = 0.04$. Source: [26] 19
- 2.8 Frequency distribution of 77 years of SPX daily log-returns compared with the normal distribution. Source: [28] 23
- 2.9 Q-Q plot of SPX daily log-returns compared with the normal distribution. Note the extreme tails. Source: [28] 24
- 2.10 SPX daily log-returns from December 31, 1984 to December 31, 2004. Note the -22.9% return on October 19, 1987. Source: [28] 25
- 2.11 Implied volatility of European ATX call options per moneyness group 26

- 3.1 The effect of changing the initial variance $v = \sqrt{v_0}$ (left) and the effect of changing the long run variance θ (right). Source: [29] 35
- 3.2 The effect of changing the mean reversion κ . Source: [29] 36
- 3.3 The effect of ρ on the skewness of the density function. Source: [51] 36
- 3.4 Implied volatility surface, $\rho = 0.5, \kappa = 2, \theta = 0.04, \sigma = 0.1, v_0 = 0.04, r = 1\%, S_0 = 1$, strikes: $0.8 - 1.2$, maturities: $0.5 - 3$ years. Source: [51] 37
- 3.5 Implied volatility surface, $\rho = 0, \kappa = 2, \theta = 0.04, \sigma = 0.1, v_0 = 0.04, r = 1\%, S_0 = 1$, strikes: $0.8 - 1.2$, maturities: $0.5 - 3$ years. Source: [51] 37
- 3.6 Implied volatility surface, $\rho = -0.5, \kappa = 2, \theta = 0.04, \sigma = 0.1, v_0 = 0.04, r = 1\%, S_0 = 1$, strikes: $0.8 - 1.2$, maturities: $0.5 - 3$ years. Source: [51] 38
- 3.7 The effect of σ on the kurtosis of the density function. Source: [51] 38
- 3.8 Implied volatility curve, $\rho = 0.5, \kappa = 2, \theta = 0.04, \sigma = 0.1, v_0 = 0.04, r = 1\%, S_0 = 1$, strikes: $0.8 - 1.2$, maturities: $0.5 - 3$ years. Source: [51] 39

3.9	Implied volatility curve, $\rho = 0$, $\kappa = 2$, $\theta = 0.04$, $\sigma = 0.1$, $v_0 = 0.04$, $r = 1\%$, $S_0 = 1$, strikes: 0.8 – 1.2, maturities: 0.5 – 3 years. Source: [51]	39
3.10	Implied volatility curve, $\rho = -0.5$, $\kappa = 2$, $\theta = 0.04$, $\sigma = 0.1$, $v_0 = 0.04$, $r = 1\%$, $S_0 = 1$, strikes: 0.8 – 1.2, maturities: 0.5 – 3 years. Source: [51]	40
4.1	The leading order term (grey) and correction term (blue) in the small-time limit for the Heston model for $\kappa = 1.15$, $\sigma = 0.2$, $y_0 = \theta = 0.04$, $\rho = -0.4$, $t = 0.25$. Source: [22]	49
5.1	Implied volatility of small-time calibration result per moneyness group	63
5.2	Implied volatility of small-time and small-time leading order term calibration result per moneyness group	63
5.3	Implied volatility of small-time calibration and corresponding Heston model calibration result per moneyness group	64
5.4	Implied volatility of small-time calibration and corresponding Heston model calibration result per moneyness group	64
5.5	Implied volatility of both small-time calibration and corresponding Heston model calibration results per moneyness group	65
5.6	Implied volatility of both small-time calibration and corresponding Heston model calibration results per moneyness group, on sample data with maturities ranging from 0.08 to 0.16 years	65
5.7	MAPE error per moneyness group from calibrating whole sample data with small-time formula and different initial parameters	67
5.8	MPE error per moneyness group from calibrating whole sample data with small-time formula and different initial parameters	67
5.9	MAE error per moneyness group from calibrating whole sample data with small-time formula and different initial parameters	68
5.10	MSE error per moneyness group from calibrating whole sample data with small-time formula and different initial parameters	68
5.11	MAPE error per moneyness group from calibrating whole sample data with small-time and Heston formula	69
5.12	MPE error per moneyness group from calibrating whole sample data with small-time and Heston formula	69
5.13	MAE error per moneyness group from calibrating whole sample data with small-time and Heston formula	70
5.14	MSE error per moneyness group from calibrating whole sample data with small-time and Heston formula	70
5.15	MAPE error per moneyness group from calibrating with small-time and Heston formula, using sample data with maturities ranging from 0.8 to 0.16 years	72
5.16	MPE error per moneyness group from calibrating with small-time and Heston formula, using sample data with maturities ranging from 0.8 to 0.16 years	72
5.17	MAE error per moneyness group from calibrating with small-time and Heston formula, using sample data with maturities ranging from 0.8 to 0.16 years	73

5.18	MSE error per moneyness group from calibrating with small-time and Heston formula, using sample data with maturities ranging from 0.8 to 0.16 years	73
5.19	Implied volatility surface of call option market data for the underlying price 2700	74
5.20	Implied volatility surface of call option market data for the underlying price 2900	74
5.21	Implied volatility surface of call option market data for the underlying price 3100	75
5.22	Implied volatility surface of small-time calibration result for call options with underlying price 2700	75
5.23	Implied volatility surface of small-time calibration result for call options with underlying price 2900	76
5.24	Implied volatility surface of small-time calibration result for call options with underlying price 3100	76
5.25	Implied volatility of various asymptotic formula calibration results per moneyness group, using whole sample data	77
5.26	MAPE error per moneyness group from calibrating whole sample data with various asymptotic formulas	78
5.27	MPE error per moneyness group from calibrating whole sample data with various asymptotic formulas	79
5.28	MAE error per moneyness group from calibrating whole sample data with various asymptotic formulas	79
5.29	MSE error per moneyness group from calibrating whole sample data with various asymptotic formulas	80
5.30	Implied volatility of various asymptotic formula calibration results per moneyness group, using sample data with maturities ranging from 0.08 to 0.16 years	80
5.31	MAPE error per moneyness group from calibrating with various asymptotic formulas, using sample data with maturities ranging from 0.08 to 0.16 years	81
5.32	MPE error per moneyness group from calibrating with various asymptotic formulas, using sample data with maturities ranging from 0.08 to 0.16 years	82
5.33	MAE error per moneyness group from calibrating with various asymptotic formulas, using sample data with maturities ranging from 0.08 to 0.16 years	82
5.34	MSE error per moneyness group from calibrating with various asymptotic formulas, using sample data with maturities ranging from 0.08 to 0.16 years	83
5.35	Implied volatility of various asymptotic formula calibration results per moneyness group, using options recorded in time period 1	84
5.36	Implied volatility of various asymptotic formula calibration results per moneyness group, using options recorded in time period 2	84
5.37	Implied volatility of various asymptotic formula calibration results per moneyness group, using options recorded in time period 3	85
5.38	Implied volatility of various asymptotic formula calibration results per moneyness group, using options recorded in time period 4	85
5.39	MAPE error per moneyness group from calibrating options from time period 1 with various asymptotic formulas	86
5.40	MPE error per moneyness group from calibrating options from time period 1 with various asymptotic formulas	87

5.41	MAE error per moneyness group from calibrating options from time period 1 with various asymptotic formulas	87
5.42	MSE error per moneyness group from calibrating options from time period 1 with various asymptotic formulas	88
5.43	MAPE error per moneyness group from calibrating options from time period 2 with various asymptotic formulas	89
5.44	MPE error per moneyness group from calibrating options from time period 2 with various asymptotic formulas	89
5.45	MAE error per moneyness group from calibrating options from time period 2 with various asymptotic formulas	90
5.46	MSE error per moneyness group from calibrating options from time period 2 with various asymptotic formulas	90
5.47	MAPE error per moneyness group from calibrating options from time period 3 with various asymptotic formulas	91
5.48	MPE error per moneyness group from calibrating options from time period 3 with various asymptotic formulas	92
5.49	MAE error per moneyness group from calibrating options from time period 3 with various asymptotic formulas	92
5.50	MSE error per moneyness group from calibrating options from time period 3 with various asymptotic formulas	93
5.51	MAPE error per moneyness group from calibrating options from time period 4 with various asymptotic formulas	94
5.52	MPE error per moneyness group from calibrating options from time period 4 with various asymptotic formulas	94
5.53	MAE error per moneyness group from calibrating options from time period 4 with various asymptotic formulas	95
5.54	MSE error per moneyness group from calibrating options from time period 4 with various asymptotic formulas	95

Chapter 1

Introduction

1.1 Motivation

Financial innovation has been the force driving global finance to greater economic efficiency since the late nineteenth century. Among all the innovations, derivative securities, such as options, futures, bonds, etc, have caused some of the most dramatic changes in the financial world. Although option agreements have been made for many centuries, a theoretically consistent frame work of option pricing did not become available until the 1970s when Fischer Black, Myron Scholes and Robert Merton derived the Black-Scholes model, which changed the way and impact the world of pricing derivatives using stocks as the underlying asset. It was now possible to price derivatives by a very simple closed form solution. But with the crude assumption on constant volatility and in lognormal returns really limits the model, and this is why the model only is used as a benchmark today.

In reality, the implied volatilities of traded options generally vary, both with strike price and with maturity of the option. The variation with strike price is called the volatility smile, or the volatility skew. The question then arises as to how to price options in a way which is consistent with this market-observed variation of implied volatility. One of the concepts used to cope with this problem is that of stochastic volatility. There are various models of stochastic volatility, although arguably the most popular is the Heston model.

The constant volatility of the Black-Scholes model corresponds to the assumption that the underlying asset follows a lognormal stochastic process. On the other hand, the basic assumption of stochastic volatility models is that the volatility (or possibly, the variance) of the underlying asset is itself a random variable. There are two Brownian motions: one for the underlying, and one for the variance; stochastic volatility models are thus at least two-factor models. Of course, the two processes are correlated and, at least in the equity world, the correlation is usually taken to be negative: increases/decreases in the asset price tend to be coupled to decreases/increases in the volatility. Once the variance of the underlying has been made stochastic, closed-form solutions for European call and put options will in general no longer exist. One of the attrac-

tive features of the Heston model, however, is that (quasi-) closed-form solutions do exist for European plain vanilla options. This feature, in turn, makes calibration of the model feasible.¹

The Heston model parameters can be determined by calibrating to a market observed implied volatility smile for European options. The calibration routine takes as its starting point the implied volatilities for a set of such options, with varying strikes and/or maturities. The volatilities are converted to option prices, and the parameters of the Heston model are chosen so as to best match this set of market data. All calibration algorithms search a region of parameter space in a more or less intelligent way, by minimizing an error metric.

This calibration must be robust and stable and should not be too computing intensive. This latter constraint often rules out global optimisation algorithms which are very slow despite their accuracy. The general approach to the calibration of parametric models, such as the Heston model, is to apply a least-square type procedure either in price or implied volatility. This kind of approach will in general be very sensitive to the choice of the initial point, which will often in practice drive the selection of the local minima the algorithm will converge to.

This is where asymptotic properties of the Heston model come into play, which have been thoroughly studied over the last years: small and large time behaviours, wings of the implied volatility for fixed maturity. These various explicit formulas are extremely useful in practice to determine initial points for the calibration of the model. Such algorithms will typically converge in a few seconds on a standard laptop and therefore improve the calibration efficiency.

These asymptotic approximations for short or long term asymptotics will be the main topic of this thesis. The accuracy of some selected approximations will be proofed by applying them to ATX option data.

1.2 Structure of Thesis

For a general understanding, the basic objects, ideas and results of the classical Black-Scholes theory of derivative pricing will be presented in *chapter 2*. The attention will be drawn to volatility and the limitations of the Black-Scholes model, which will lead to the assumption of stochastic volatility.

In *chapter 3* stochastic volatility models and in particular the Heston model will be discussed. Furthermore, the semi-closed form solution for European options will be presented and the Heston parameters will be analyzed in greater detail. The understanding of the parameter influence is important for accurate calibration of the model.

In *chapter 4* some selected closed-form asymptotic approximations for European option prices and implied volatility will be presented. The focus will be on the work of Forde & Jacquier [23],

¹FinCAD 2007, see [20]

Forde et al. [24], Forde et al. [25] and Friz et al. [27]. The explicit formulas provide information about the behaviour of option prices in extreme regions (small or large strikes and/or maturities) and help to improve calibration efficiency, since they can provide pertaining initial points for the model calibration.

Finally, in *chapter 5* some asymptotic approximations for implied volatility are applied to European ATX call options to calculate initial parameters for the calibration of the Heston model. The results of this empirical research will be presented in this chapter.

The *appendix* contains MATLAB Code used for the calculations throughout the paper and lists the software used.

Chapter 2

The Black-Scholes Theory of Derivative Pricing

The aim of the following chapter is to present the basic objects, ideas, and results of the now classical Black-Scholes theory of derivative pricing. The chapter is mainly based on [7], [26], [34] and [52], and it is intended for readers to enter the theory of derivative pricing or simply refresh their memory. This is not a complete treatment of this theory with detailed proofs, detailed presentations of the subject can be found in many books, some will be mentioned throughout the chapter.

2.1 Market Model

In this model, suggested by Samuelson [54] and used by Black and Scholes [9] in 1973, there are two assets. One is the *riskless asset (bond)* with price B_t at time t , described by the ordinary differential equation

$$dB_t = rB_t dt,$$

where the non-negative constant r is the instantaneous interest rate for lending or borrowing money. Setting $B_0 = 1$, the equation results in $B_t = e^{rt}$ for $t \geq 0$. The price X_t of the other asset, the *risky stock* or stock index, is described by the following stochastic differential equation

$$dX_t = \mu X_t dt + \sigma X_t dW_t \tag{2.1}$$

where $\mu \in \mathbb{R}$ is a constant *mean return rate*, $\sigma > 0$ is a constant *volatility*, and $(W_t)_{t \geq 0}$ is a *standard Brownian motion*. This fundamental model will be presented in the following sections.

2.1.1 Brownian Motion

The Brownian motion is a real-valued stochastic process with continuous trajectories (denoted by $t \rightarrow W_t$) that have independent and stationary increments. The standard Brownian motion is characterized by the following:

- (i) $W_0 = 0$,
- (ii) for any $0 < t_1 < \dots < t_n$, the random variables $(W_{t_1}, W_{t_2} - W_{t_1}, \dots, W_{t_n} - W_{t_{n-1}})$ are independent,
- (iii) for any $0 \leq s < t$, the increment $W_t - W_s$ is a centered (mean-zero) normal random variable with variance $\mathbb{E}[(W_t - W_s)^2] = t - s$. In particular, W_t is $\mathcal{N}(0, t)$ -distributed.

The probability space where the Brownian motion is defined is denoted by $(\Omega, \mathcal{F}, \mathbb{P})$ and the expectation $\mathbb{E}[\cdot]$ is computed. Let Ω be the space of all continuous trajectories $\mathcal{C}([0, \infty] : \mathbb{R})$, such that $W_t(\omega) = \omega(t)$. The σ -algebra \mathcal{F} contains all sets of the form $\{\omega \in \Omega : |\omega(s)| < R, s \leq t\}$. \mathbb{P} is the Wiener measure, which is the probability distribution of the standard Brownian motion.

The increasing family of σ -algebras \mathcal{F}_t generated by $(W_s)_{s \leq t}$, the information on W up to time t , and all the sets of probability 0 in \mathcal{F} is called the *natural filtration* of the Brownian motion. A stochastic process $(X_t)_{t \geq 0}$ is *adapted* to the filtration $(\mathcal{F}_t)_{t \geq 0}$ if the random variable X_t is \mathcal{F}_t -measurable (meaning that any event $\{X_t \leq x\}$ belongs to \mathcal{F}_t) for every t .

The independence of increments makes the Brownian motion an ideal candidate to define a complete family of independent infinitesimal increments dW_t , which are centered and normally distributed with variance dt and which will serve as a model of (Gaussian white) noise. The drawback is that the trajectories of (W_t) cannot be *nice* in the sense that they are not of bounded variation, as the following simple computation suggests.

Let $t_0 = 0 < t_1 < \dots < t_n = t$ be a subdivision of $[0, t]$, which one may suppose evenly spaced, so that $t_i - t_{i-1} = t/n$ for each interval. The quantity

$$\mathbb{E} \left[\sum_{i=1}^n |W_{t_i} - W_{t_{i-1}}| \right] = n \mathbb{E}[|W_{t/n}|] = n \sqrt{t/n} \mathbb{E}[|W_1|]$$

goes to $+\infty$ as $n \nearrow +\infty$, indicating that the integral with respect to dW_t cannot be defined in the usual way *trajectory by trajectory*. In the next section will be described how such integrals can be defined.

In figure 2.1 a simple simulation of the standard Brownian motion (Wiener process) is demonstrated. The simulation was done in Matlab with a chosen step size $\Delta = 1/1000$, by using the built in function `randn` for representing a $\mathcal{N}(0, 1)$ -distributed stochastic variable.

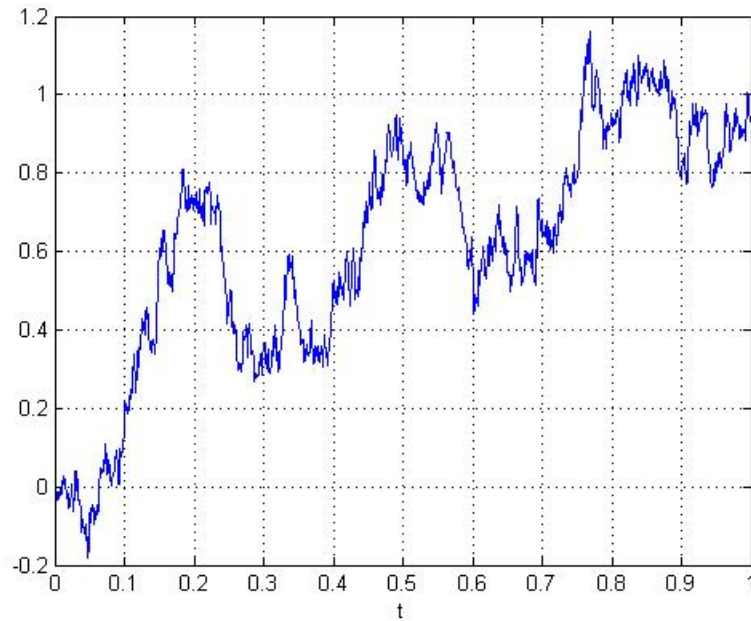


Figure 2.1: Sample path of a standard Brownian motion.

2.1.2 Stochastic Integral

For a fixed finite time T , let $(X_t)_{0 \leq t \leq T}$ be a stochastic process adapted to $(\mathcal{F}_t)_{0 \leq t \leq T}$, the filtration of the Brownian motion up to time T , such that

$$\mathbb{E} \left[\int_0^T (X_t)^2 dt \right] < +\infty.$$

The *stochastic integral* of (X_t) with respect to the Brownian motion (W_t) is defined as a limit in the mean-square sense ($L^2(\Omega)$),

$$\int_0^t X_s dW_s = \lim_{n \nearrow \infty} \sum_{i=1}^n X_{t_{i-1}} (W_{t_i} - W_{t_{i-1}}), \quad (2.2)$$

as the mesh size of the subdivision goes to zero. As a function of time t , this stochastic integral defines a continuous square integrable process such that

$$\mathbb{E} \left[\left(\int_0^t X_s dW_s \right)^2 \right] = \mathbb{E} \left[\int_0^t X_s^2 ds \right].$$

It has the *martingale property*

$$\mathbb{E} \left[\int_0^t X_u dW_u \mid \mathcal{F}_s \right] = \int_0^s X_u dW_u \quad (\mathbb{P}\text{-a.s.}, s \leq t), \quad (2.3)$$

as can easily be deduced from the definition (2.2). The *quadratic variation* $\langle Y_t \rangle$ of the stochastic integral $Y_t = \int_0^t X_u dW_u$ is

$$\langle Y_t \rangle = \lim_{n \nearrow \infty} \sum_{i=1}^n (Y_{t_i} - Y_{t_{i-1}})^2 = \int_0^t X_s^2 ds \quad (2.4)$$

in the mean-square sense.

Stochastic integrals are mean-zero, continuous, and square integrable martingales. Also the converse is true, meaning every mean-zero, continuous, and square integrable martingale is a Brownian stochastic integral.

2.1.3 Risky Asset Price Model

The Black-Scholes model for the risky asset price corresponds to a continuous process (X_t) such that, in an infinitesimal amount of time dt , the infinitesimal return dX_t/X_t has mean μdt , proportional to dt with a constant *rate of return* μ and centered random fluctuations that are independent of the past up to time t . These fluctuations are modeled by σdW_t where σ is a positive constant *volatility* and dW_t the infinitesimal increments of the Brownian motion. The corresponding formula for the infinitesimal return is

$$\frac{dX_t}{X_t} = \mu dt + \sigma dW_t \quad (2.5)$$

which is the stochastic differential equation (2.1). The right side has the natural financial interpretation of a return term plus a risk term. For simplicity, it is also assumed that there are no dividends paid in the time interval being considered. In integral form, this equation is

$$X_t = X_0 + \mu \int_0^t X_s ds + \sigma \int_0^t X_s dW_s$$

where the last integral is a stochastic integral as described in the previous section. The initial value X_0 is assumed to be independent of the Brownian motion and square integrable. This equation, or in the differential form (2.1), is a particular case of a general class of stochastic differential equations driven by a Brownian motion:

$$dX_t = \mu(t, X_t)dt + \sigma(t, X_t)dW_t, \quad (2.6)$$

or in integral form,

$$X_t = X_0 + \int_0^t \mu(s, X_s) ds + \int_0^t \sigma(s, X_s) dW_s. \quad (2.7)$$

In the Black-Scholes model, $\mu(t, x) = \mu x$ and $\sigma(t, x) = \sigma x$, these are independent of t , differentiable in x , and linearly growing at infinity.

It is very tempting to write X_t/X_0 in equation (2.5) explicitly as the exponential of $(\mu t + \sigma W_t)$, but this is not correct because the usual chain rule is not valid for stochastic differentials. For example, W_t^2 is not equal to $2 \int_0^t W_s dW_s$, since by the martingale property (2.3), this last integral has an expectation equal to zero but $\mathbb{E}[W_t^2] = t$. This discrepancy is corrected by Itô's formula and will be explained in the following section.

2.1.4 Itô's Formula

The function $g(W_t)$ of the Brownian motion W_t defines a new stochastic process. In the following will be supposed that the function g is twice continuously differentiable bounded, and has bounded derivatives. The purpose of the chain rule is to compute the differential $dg(W_t)$ or equivalently its integral $g(W_t) - g(W_0)$. Using the subdivision $t_0 = 0 < t_1 < \dots < t_n = t$ of $[0, t]$, one can write

$$g(W_t) - g(W_0) = \sum_{i=1}^n (g(W_{t_i}) - g(W_{t_{i-1}})).$$

Applying Taylor's formula to each term results in

$$\begin{aligned} g(W_t) - g(W_0) &= \sum_{i=1}^n g'(W_{t_{i-1}})(W_{t_i} - W_{t_{i-1}}) \\ &\quad + \frac{1}{2} \sum_{i=1}^n g''(W_{t_{i-1}})(W_{t_i} - W_{t_{i-1}})^2 + R, \end{aligned}$$

where R contains all the higher-order terms.

If (W_t) were differentiable only the first sum would contribute to the limit as the mesh size of the subdivision goes to zero, leading to the chain rule $dg(W_t) = g'(W_t)W_t' dt$ of calculus. In the Brownian case (W_t) is not differentiable and, by (2.2), the first sum converges to the stochastic integral

$$\int_0^t g'(W_s) dW_s.$$

The correction comes from the second sum, which converges like (2.4) to the following:

$$\frac{1}{2} \int_0^t g''(W_s) dW_s.$$

This can be seen by comparing it in L^2 with $\frac{1}{2} \sum_{i=1}^n g''(\bar{W}_{t_{i-1}})(t_i - t_{i-1})$. The higher-order terms contained in R converge to zero and do not contribute to the limit, which is

$$g(W_t) - g(W_0) = \int_0^t g'(W_s) dW_s + \frac{1}{2} \int_0^t g''(W_s) ds.$$

This is the simplest version of Itô's formula and it is often written in differential form:

$$dg(W_t) = g'(W_t) dW_t + \frac{1}{2} g''(W_t) dt.$$

In the next step a similar formula for $dg(X_t)$ will be derived, where X_t is the solution of a stochastic differential equation like (2.6). The general formula for a function g depending also on time t is the following:

$$dg(t, X_t) = \frac{\partial g}{\partial t}(t, X_t) dt + \frac{\partial g}{\partial x}(t, X_t) dX_t + \frac{1}{2} \frac{\partial^2 g}{\partial x^2}(t, X_t) d\langle X \rangle_t,$$

where dX_t is given by the stochastic differential equation (2.6) and $\langle X \rangle_t = \int_0^t \sigma^2(s, X_s) ds$ is the quadratic variation of the martingale part of X_t , which is the stochastic integral on the right side of (2.7). In terms of dt and dW_t , the formula is

$$dg(t, X_t) = \left(\frac{\partial g}{\partial t} + \mu(t, X_t) \frac{\partial g}{\partial x} + \frac{1}{2} \sigma^2(t, X_t) \frac{\partial^2 g}{\partial x^2} \right) dt + \sigma(t, X_t) \frac{\partial g}{\partial x} dW_t, \quad (2.8)$$

where all the partial derivatives of g are evaluated at (t, X_t) .

2.1.5 Lognormal Risky Asset Price

For the evolution of the stock price X_t , the focus will be on the stochastic differential equation (2.5) again. It is natural to suspect from the ordinary calculus formula $\int dx/x = \log x$ that $\log X_t$ might satisfy an equation that can be integrated explicitly. The differential of $\log X_t$ will be computed by applying Itô's formula (2.8) with $g(t, x) = \log x$, $\mu(t, x) = \mu x$ and $\sigma(t, x) = \sigma x$:

$$d \log X_t = \left(\mu - \frac{1}{2} \sigma^2 \right) dt + \sigma dW_t.$$

The logarithm of the stock price is then given explicitly by

$$\log X_t = \log X_0 + \left(\mu - \frac{1}{2} \sigma^2 \right) t + \sigma W_t,$$

which leads to the following formula for the stock price:

$$X_t = X_0 \exp\left(\left(\mu - \frac{1}{2}\sigma^2\right)t + \sigma W_t\right). \quad (2.9)$$

The return X_t/X_0 is *lognormal*, it is the exponential of a non-standard Brownian motion that is normally distributed with mean $(\mu - \frac{1}{2}\sigma^2)t$ and variance $\sigma^2 t$ at time t . The process (X_t) is also called *geometric* Brownian motion. The stock price given by (2.9) satisfies equation (2.5). It can also be obtained as a diffusion limit of binomial tree models, which arise when Brownian motion is approximated by a random walk.

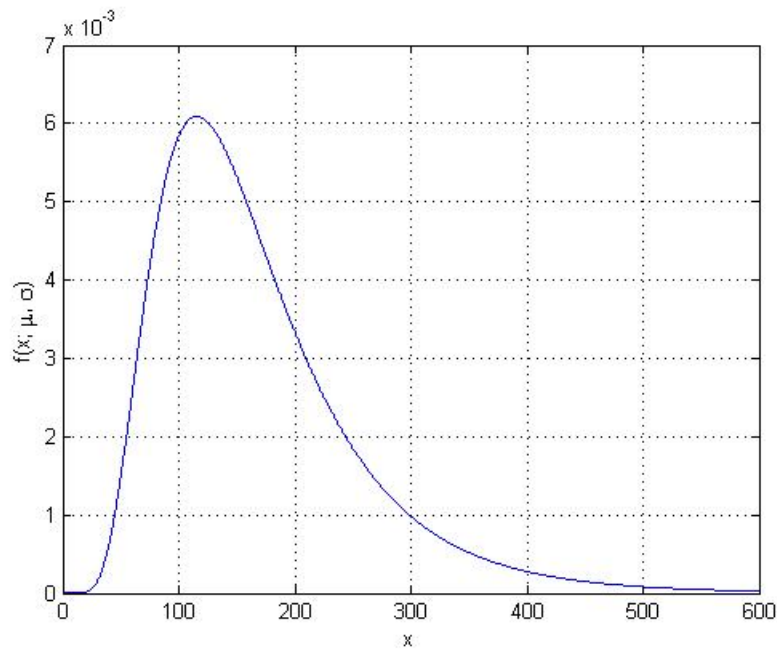


Figure 2.2: Lognormal density function with $\mu = 5$ and $\sigma = 0.5$.

Notice that, if X_t becomes zero, it stays at zero for all times thereafter. Thus, bankruptcy (zero stock price) is a permanent state in this model. However, $\frac{1}{t}W_t$ tends to zero as t tends to infinity with probability 1, so it follows that if X_0 is not zero then (with probability 1) X_t does not go to zero in a finite time.

2.2 Derivative Contracts

Derivatives are contracts based on the underlying asset price (X_t). They are also called *contingent claims* and can be applied to almost any type of asset, e.g. stocks, interest rates or

commodities.

2.2.1 European Call and Put Options

A **European call option** is a contract that gives its holder the right, but not the obligation, to *buy* one unit of an underlying asset for a predetermined *strike price* K on the *maturity date* T . If X_T denotes the price of the underlying asset at maturity time T , then the value of this contract at maturity, its *payoff*, is

$$h(X_T) = (X_T - K)^+ = \begin{cases} X_T - K & \text{if } X_T > K, \\ 0 & \text{if } X_T \leq K. \end{cases} \quad (2.10)$$

In the first case of the equation, the holder will exercise the option and make a profit of $X_T - K$ by buying the stock for K and selling it immediately at the market price X_T . In the second case, the holder does not exercise the option, since the market price of the asset is less than the strike price and the payoff is therefore 0.

A **European put option** is a contract that gives its holder the right to *sell* a unit of the asset for a strike price K at the maturity date T . Its payoff is

$$h(X_T) = (K - X_T)^+ = \begin{cases} K - X_T & \text{if } X_T < K, \\ 0 & \text{if } X_T \geq K. \end{cases} \quad (2.11)$$

In the first case, buying the stock at the market price X_T and exercising the put option yields a profit of $K - X_T$. In the second case, the holder will not exercise the option.

Figures 2.3 and 2.4 show the way in which the investor's profit or loss on an European option varies with the terminal stock price. The expiration date of the two options is in 2 months.

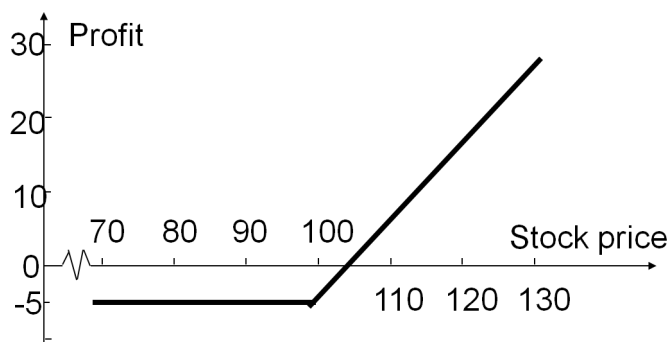


Figure 2.3: Profit from buying a European *call option* on one share of a stock. Option price $C = 5$, strike price $K = 100$. Source: [34]

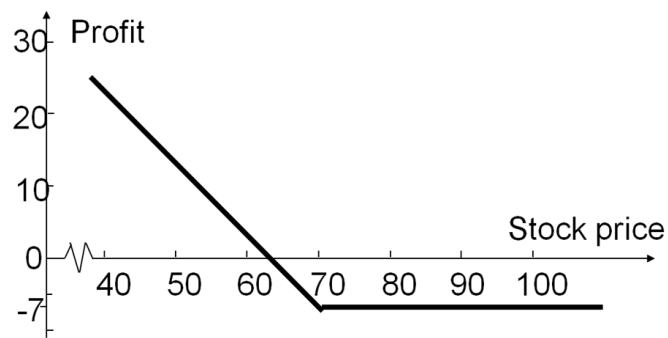


Figure 2.4: Profit from buying a European *put option* on one share of a stock. Option price $P = 7$, strike price $K = 70$. Source: [34]

2.2.2 Moneyness of an Option

Moneyness of an option indicates whether an option is worth exercising or not. Moneyness of an option at any given time depends on where the price of the underlying asset is at that point of time relative to the strike price. The following three terms are used to define the moneyness of an option:

An option is **ITM (in-the-money)** if on exercising the option, it would produce a cash inflow for the holder. Thus, call options are ITM at time t when the value of the price of the underlying exceeds the strike price, $X_t > K$. On the other hand, put options are ITM when the price of the underlying is lower than the strike price, $X_t < K$.

An **OTM (out-of-the-money)** option is an opposite of an ITM option. A holder will not exercise the option when it is OTM. A call option is OTM when its strike price is greater than the price of the underlying and a put option is OTM when the price of the underlying is greater than the option's strike price.

An **ATM (at-the-money)** is one in which the price of the underlying is equal to the strike price. It is at the stage where with any movement in the price of the underlying, the option will either become ITM or OTM.

In figure 2.5 the moneyness regions are displayed in the European call and put options, which have already been presented in section 2.2.1 above.

The moneyness for call and put options is defined by

$$M_t = \frac{K}{X_t},$$

and the moneyness categories listed in table 2.1 will be used throughout this thesis.

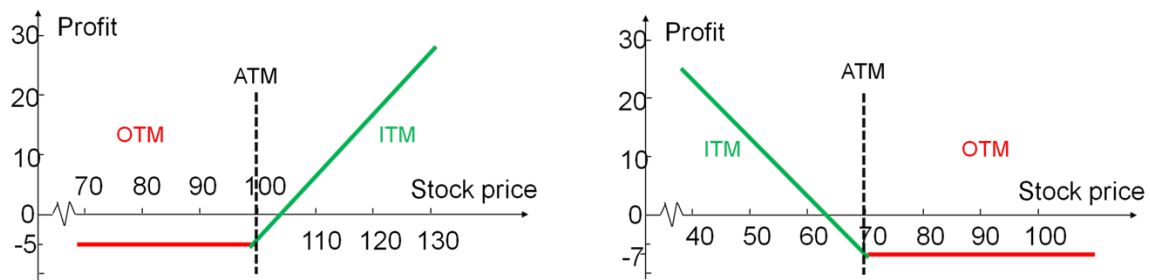


Figure 2.5: Moneyiness regions in a European call option (left) and in a European put option (right). Original Image Source: [34]

Moneyiness	Call	Put
< 0.94	deep ITM	deep OTM
$0.94 - 0.97$	ITM	OTM
$0.97 - 1.00$	ATM	ATM
$1.00 - 1.03$	ATM	ATM
$1.03 - 1.06$	OTM	ITM
> 1.06	deep OTM	deep ITM

Table 2.1: Moneyiness of call and put options

2.3 Replicating Strategies

The Black-Scholes analysis of a European-style derivative yields an explicit trading strategy in the underlying risky asset and riskless bond whose terminal payoff is equal to the payoff of the derivative at maturity. The path the stock price takes does not matter. Thus, an investor can cover against all risk of eventual loss, by selling the derivative and holding a dynamically adjusted portfolio according to this trading strategy. This *replicating strategy* therefore provides an insurance policy against the risk of being short the derivative: A loss incurred at the final time from one part of this portfolio will be exactly compensated by a gain in the other part. It is called a *dynamic hedging strategy* since it involves continuous trading, where to hedge means to eliminate risk. The essential step in the Black-Scholes methodology is the construction of this replicating strategy and arguing, based on *no arbitrage*, that the value of the replicating portfolio at time t is the fair price of the derivative. This argument will be developed in the following sections.

2.3.1 Replicating Self-Financing Portfolios

In this chapter a European-style derivative will be considered. Its payoff $h(X_T)$ is a function of the underlying asset price at maturity time T . The stock price (X_t) follows the geometric Brownian motion model (2.9), which describes a solution of the stochastic differential equation (2.1). The pair $\phi = (\phi^1, \phi^2)$ of adapted processes is called a *trading strategy*. ϕ_t^1 is specifying the number of units of the underlying asset held at time t , whereas ϕ_t^2 is describing the number of units of the riskless bond. In order to have the stochastic integral involving ϕ_t^1 and the usual integral involving ϕ_t^2 well-defined, suppose that $\mathbb{E}[\int_0^T (\phi_t^1)^2]dt$ and $\int_0^T |\phi_t^2|dt$ are finite.

Assume $B_t = e^{rt}$ for the price of the bond at time t , then the value at time t of this portfolio is $\phi_t^1 X_t + \phi_t^2 e^{rt}$. If its value at time T is almost surely equal to the payoff

$$\phi_T^1 X_T + \phi_T^2 e^{rT} = h(X_T), \quad (2.12)$$

it will *replicate* the derivative at maturity. Furthermore, this portfolio is assumed to be *self-financing*: the variations of its value are due only to the variations of the stock and bond prices (variations of the market). After the initial investment, no further funds are required. For example, if more of the asset is bought, bonds have to be sold to pay for it. In differential form this is described by the following:

$$d(\phi_t^1 X_t + \phi_t^2 e^{rt}) = \phi_t^1 dX_t + r\phi_t^2 e^{rt} dt. \quad (2.13)$$

2.3.2 The Black-Scholes Partial Differential Equation

The goal is to construct a self-financing portfolio $\phi = (\phi^1, \phi^2)$ that will replicate the derivative at maturity (2.12). Assume that a pricing function $P(t, x)$ exists, that relates the option price to the present risky asset price, and is regular enough to apply Itô's formula (2.8). To exclude possible arbitrage opportunities assume

$$\phi_t^1 X_t + \phi_t^2 e^{rt} = P(t, X_t) \quad \text{for any } 0 \leq t \leq T. \quad (2.14)$$

For example, if the left-hand side in the equation is less than the right-hand side, one can create arbitrage by selling the overpriced derivative security immediately and investing in the underpriced asset-bond trading strategy. Since the terminal payoff of the trading strategy is equal to the payoff of the derivative, this yields an immediate profit with no exposure to future loss.

Differentiating (2.14) and using the self-financing property (2.13), one obtains for the left hand-side

$$\phi_t^1 dX_t + r\phi_t^2 e^{rt} dt,$$

and in addition using equation (2.1) results in

$$(\phi_t^1 \mu X_t + \phi_t^2 r e^{rt}) dt + \phi_t^1 \sigma X_t dW_t.$$

Using Itô's formula (2.8) on the right-hand side, yields in total:

$$(\phi_t^1 \mu X_t + \phi_t^2 r e^{rt}) dt + \phi_t^1 \sigma X_t dW_t = \left(\frac{\partial P}{\partial t} + \mu X_t \frac{\partial P}{\partial x} + \frac{1}{2} \sigma^2 X_t^2 \frac{\partial^2 P}{\partial x^2} \right) dt + \sigma X_t \frac{\partial P}{\partial x} dW_t, \quad (2.15)$$

where all the partial derivatives of P are evaluated at (t, X_t) . Equating the coefficients of the dW_t terms gives

$$\phi_t^1 = \frac{\partial P}{\partial x}(t, X_t), \quad (2.16)$$

and from (2.14) one obtains

$$\phi_t^2 = (P(t, X_t) - \phi_t^1 X_t) e^{-rt}. \quad (2.17)$$

Equating the dt terms in (2.15) gives

$$r \left(P - X_t \frac{\partial P}{\partial x} \right) = \frac{\partial P}{\partial t} + \frac{1}{2} \sigma^2 X_t^2 \frac{\partial^2 P}{\partial x^2},$$

which is satisfied for any stock price X_t if $P(x, t)$ is the solution of the *Black-Scholes partial differential equation*

$$\mathcal{L}_{BS}(\sigma)P = 0, \quad (2.18)$$

where

$$\mathcal{L}_{BS}(\sigma) = \frac{\partial}{\partial t} + \frac{1}{2} \sigma^2 x^2 \frac{\partial^2}{\partial x^2} + r \left(x \frac{\partial}{\partial x} - \cdot \right).$$

This equation holds in the domain $t \leq T$ and $x > 0$, since the stock price remains positive in the model. It is to be solved *backward in time* with the final condition $P(T, x) = h(x)$, because at expiration the price of the derivative is simply its payoff.

The partial differential equation (2.18) with its final condition has a unique solution $P(t, x)$, which is the value of a self-financing replicating portfolio. Knowing P , the portfolio $\phi = (\phi^1, \phi^2)$ is uniquely determined by (2.16) and (2.17).

Notice, the rate of return μ does not enter in the valuation of this portfolio. It is a remarkable feature of the Black-Scholes theory that if two investors have different speculative views about the growth rate of the risky asset (meaning that they have different values of μ but agree that the historical volatility σ will prevail), then they will agree on the no-arbitrage price of the derivative, since P does not depend on μ .

2.3.3 The Black-Scholes Formula

For European call options the Black-Scholes partial differential equation (2.18) is solved with the final condition $(x - K)^+ = h(x)$. The Price of a European call option depends on the following:

- current stock price x
- time-to-maturity $T - t$
- strike price K
- volatility σ
- interest rate r

At time t and for an observed risky asset price $X_t = x$, the price of a European call option $C_{BS}(t, x)$ is given by a closed-form solution known as the *Black-Scholes Formula*:

$$C_{BS}(t, x) = xN(d_1) - Ke^{-r(T-t)}N(d_2), \quad (2.19)$$

where

$$d_1 = \frac{\log(x/K) + (r + \frac{1}{2}\sigma^2)(T - t)}{\sigma\sqrt{T - t}}, \quad (2.20)$$

$$d_2 = d_1 - \sigma\sqrt{T - t}. \quad (2.21)$$

Furthermore, let N stand for the standard Gaussian cumulative distribution function, then it is given by

$$N(z) = \frac{1}{\sqrt{2\pi}} \int_{-\infty}^z e^{-y^2/2} dy. \quad (2.22)$$

This convenient formula for the price of a European call option explains the popularity of the model in the financial services industry since the mid-1970s. Only the volatility σ , the standard deviation of the returns scaled by the square root of the time increment, needs to be estimated from data, assuming that the interest rate r is known. There is a similar formula for European put options, as will be shown in the next section.

Figure 2.6 demonstrates how the Black-Scholes price changes when strike price K , volatility σ , and interest rate r are kept constant while time-to-maturity T and the stock price x vary. One can observe that the option price increases as the stock price and time-to-maturity increase.

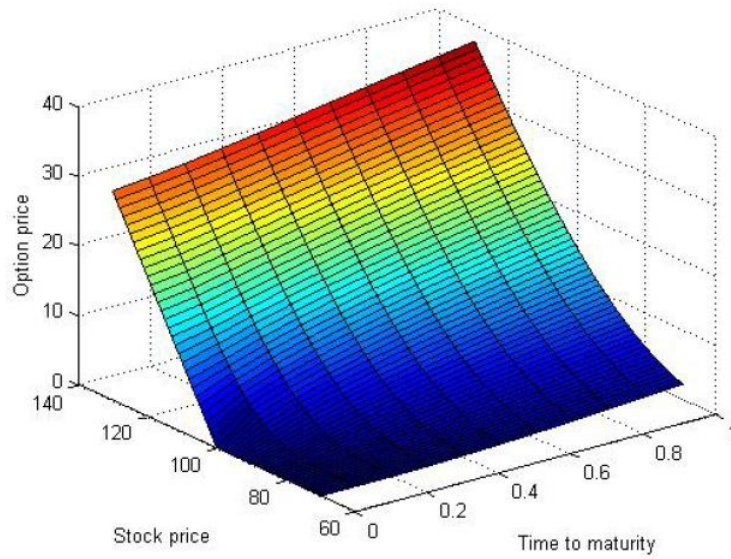


Figure 2.6: The Black-Scholes price for an European Call option with $K = 100$, $\sigma = 0.3$, $r = 0.05$. Source: [40]

2.3.4 Put-Call Parity

The *put-call parity* describes the important relationship between European call and put options, which can be used to derive a closed-form expression for the price of a European put option. It is satisfied in any arbitrage-free, continuous-time model of a security market, provided that the savings account, the risk less bond is given by $B_t = e^{rt}$.

Let $C_{BS}(t, x)$ be the price of a European call and $P_{BS}(t, x)$ of a European put option. The prices of European call and put options with the same expiry date T and strike price K satisfy the put-call parity relationship

$$C_{BS}(t, X_t) - P_{BS}(t, X_t) = X_t - Ke^{-r(T-t)}. \quad (2.23)$$

The relationship is preserved under the lognormal model because the difference $C_{BS} - P_{BS}$ satisfies the partial differential equation (2.18) with the final condition $h(x) = x - K$. This problem has the simple solution $x - Ke^{-r(T-t)}$. To derive a closed-form expression for the price of a European put option, use the Black-Scholes formula (2.19) for C_{BS} and the put-call parity relation (2.23). Thus, the following explicit formula for the price of a European put option is obtained:

$$P_{BS}(t, x) = Ke^{-r(T-t)}N(-d_2) - xN(-d_1), \quad (2.24)$$

where d_1 , d_2 and N are as in (2.20), (2.21) and (2.22), respectively.

Figure 2.7 shows the pricing function $C_{BS}(0, x; 100, 0.5; 0.1)$ and $P_{BS}(0, x; 100, 0.5; 0.1)$ plotted against the present ($t = 0$) stock price x . Notice how the call option function is a smoothed version of the “ramp” terminal payoff function. For the put option function one can see that it crosses over its terminal payoff for some (small enough) x .

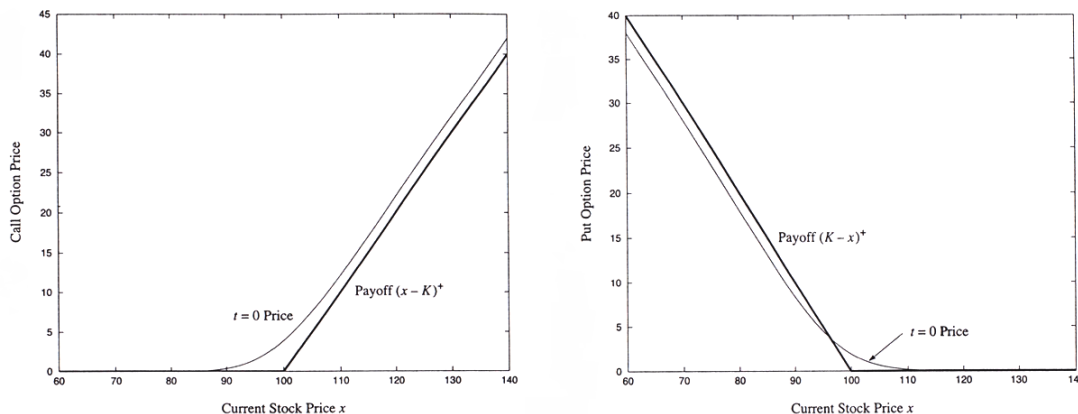


Figure 2.7: Black-Scholes call and put option pricing function at time $t = 0$, with $K = 100$, $T = 0.5$, $\sigma = 0.1$ and $r = 0.04$. Source: [26]

Other types of options, in general, do not lead to such explicit formulas. Solving numerically the partial differential equation (2.18) with appropriate boundary conditions is required, to determine their prices. More information, e.g. on the determination of American option prices, can be found in [26] and in many other books.

2.4 Volatility

For practical application of the Black-Scholes Theory, one needs to have numerical estimates of all the input parameters. The input data consists of the string x, r, T, t and σ . Out of these five parameters, x, r, T and t can be observed directly, which leaves the problem of obtaining an estimate of the volatility σ . The volatility of a stock is a measure of the uncertainty about the returns provided by the stock. Stocks typically have a volatility between 15% and 60%. Two basic approaches for the estimation are used, namely *historical volatility* or *implied volatility*.

2.4.1 Historical Volatility

To value an European option, an obvious idea is to use historical data in order to estimate σ . Since, in real life, the volatility is not constant over time, one standard practice is to use historical data for a period of the same length as the time to maturity. This approach takes the standard deviation of the underlying's log-returns and times the time length. The log-return of the underlying asset is

$$R_t = \log \frac{X_t}{X_{t-1}}.$$

Using elementary statistical theory, an estimate of σ is given by

$$\hat{\sigma}^H = \sqrt{\frac{\vartheta}{\Delta t}},$$

where the sample variance ϑ is given by

$$\vartheta = \frac{1}{n-1} \sum_{t=1}^n (R_t - \bar{R}_n)^2,$$

with $\bar{R}_n = \frac{1}{n} \sum_{t=1}^n R_t$ being the sample mean.

An argument against the use of historical volatility is that in real life volatility is not constant, but changes over time. It should be an estimate of the volatility for the coming time period, but this approach only yields an estimate for the volatility over the past time period.

2.4.2 Implied Volatility

Implied volatility of an option is calculated from its market price observed on an exchange and not from the prices of the underlying as it is the case for the historical volatility. In this thesis its defined as the volatility, that is obtained when equating the option's market value to its Black-Scholes value, given the same strike price and time to maturity. It is extracted numerically due to the fact that the Black-Scholes formula cannot be solved for σ in terms of the other parameters.

Given an observed European call option price C^{obs} (market price) for a contract with strike K and expiration date T , the implied volatility $\hat{\sigma}^I$ is defined to be the value of the volatility parameter that must go into the Black-Scholes formula (2.19) to match this price:

$$C_{BS}(t, x; K, T; \hat{\sigma}^I) = C^{obs}.$$

Remark (1) A unique non-negative implied volatility $\hat{\sigma}^I > 0$ can be found given $C^{obs} > C_{BS}(t, x; K, T; 0)$ because of the monotonicity of the Black-Scholes formula in the volatility parameter:

$$\frac{\partial C_{BS}}{\partial \sigma} = \frac{x e^{-d_1^2/2} \sqrt{T-t}}{\sqrt{2\pi}} > 0.$$

(2) The implied volatilities from put and call options of the same strike price and time to maturity are the same because of put-call parity (2.23).

Thus implied volatilities are embedded in option prices, which in turn reflect the future expectations of the market participants. Whereas historical volatilities are backward looking, implied volatilities are forward looking. Traders often quote the implied volatility of an option rather than its price. This is convenient because the implied volatility tends to be less variable than the option price.

Note, that implied volatilities can be used to test (in a non-standard way) the Black-Scholes model. Suppose, e.g. the market prices of a number of European calls with the same exercise date on a single underlying stock were observed. If the model is correct (with a constant volatility) then, if one plots implied volatility as a function of the strike price, one should obtain a horizontal straight line. Contrary to this, it is often observed that options deep OTM or deep ITM are traded at higher implied volatilities than ATM options. The graph of the observed implied volatility function thus often looks like a smile, and for this reason the implied volatility curve is termed the *volatility smile*, see figure 2.11; but more on this in the following section.

2.5 Limitations of the Black-Scholes Model

The Black-Scholes model has set such an important foundation in financial engineering in the past 30 years and has been really recognized by both academia and practitioners, but it is also well known and accepted that this model is not that accurate in capturing the features in the stock markets in reality. There are several major drawbacks of the Black-Scholes model, mainly because the idealized assumptions do rarely hold in the real world. First of all, the assumption of a normal distribution of log-returns is under critique ever since 1963 by Mandelbrot.¹ Combined factors of extreme events, fat tails, high peak and the volatility clustering effects make the assumption of non-Gaussian distribution more appropriate. Secondly, the volatility smile is simply a violation of the constant volatility assumption. The mentioned drawbacks will be discussed in greater detail in the following sections.

¹Mandelbrot (1963a, 1963b), see [44] and [45] respectively

2.5.1 Shortcomings of Gaussian distribution

Economists believed that prices in speculative markets, such as grain and securities markets, behave very much like random walks,² which is based on two assumptions: (1) price changes are independent random variables, and (2) the changes conform to some probability distribution.

Mandelbrot (1963) challenged this long existing believe, that the price changes in a speculative market are approximately Gaussian. First, some features of Gaussian distribution will be presented. In the study of financial time-series, it is a concept to describe the actual return distribution, where data or the variable turns to cluster around the mean. The two important parameters are the mean μ and the variance σ^2 . For a Gaussian distribution the probability density function is given by

$$f(x) = \frac{1}{\sqrt{2\pi\sigma^2}} e^{-\frac{(x-\mu)^2}{2\sigma^2}}.$$

Some notable properties of the Gaussian distribution are the following:

- symmetry around its mean μ , therefore the skewness of the distribution is 0,
- both the mode and the median are the same as the mean μ ,
- the inflection points (points where the curve changes sign) of the curve occur one standard deviation away from the mean, e.g. at $\mu - \sigma$ and $\mu + \sigma$,
- the kurtosis (describes the peakedness of a distribution) is equal to 3.

Unfortunately, these properties are not suitable in capturing the probability of extreme events in the market. Take for example the stock market crash of October 1987. Following the standard paradigm, the stock market returns are lognormally distributed with a annualized volatility of 20% (as was already mentioned in section 2.4, it is usually believed to be between 15% and 60%). On October 19, 1987, the two month S&P 500 futures price fell 29 percent. Under the lognormal assumption and according to the calculation from the probability density function, the probability of this event is 10^{-160} , which is virtually impossible.³ In the history of stock market this is not the only event with little probability that actually did happen.

Besides the difficulty in dealing with historical extreme events, empirical research has shown that the actual return distributions in stock market have fatter tails and higher peak than the normal distribution. In figure 2.8, the frequency distribution of SPX daily log-returns over a 77-year period from 1928 to 2005 is plotted and compared with the normal distribution. Note the -22.9% return on October 19, 1987 in figure 2.10, which is not directly visible in figure 2.8, but the x-axis has been extended to the left to accommodate it. It is quite obvious that

²Fama (1965), p2, see [18]

³This example is extracted from Jackwerth & Rubinstein (1996), p1611, see [36]

the distribution of log-returns of SPX is highly peaked and fat-tailed relative to the normal distribution. The Q-Q plot in figure 2.9 shows just how extreme the tails of the empirical distribution of returns are relative to the normal distribution. This plot would be a straight line, if the empirical distribution were normal. Fat tails and the high central peak are characteristics of mixture of distributions with different variances.⁴

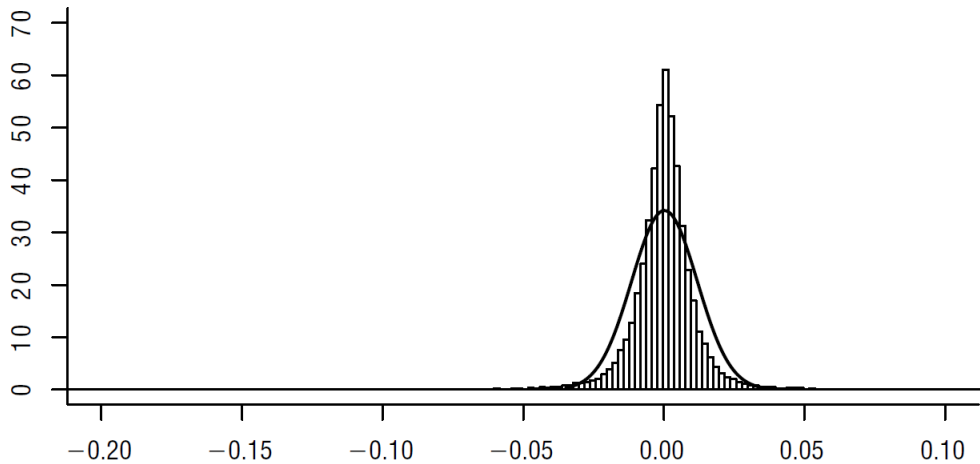


Figure 2.8: Frequency distribution of 77 years of SPX daily log-returns compared with the normal distribution. Source: [28]

All mentioned factors above are against the assumption of a Gaussian distribution and point out the necessity to move from assumption of constant volatility to stochastic volatility.

2.5.2 Clustering and Leverage effect

Another drawback is the so-called *volatility clustering*. It means, that large market moves are followed by large moves, while small moves are followed by small moves, a feature which obviously cannot be captured by a model assuming constant volatility. One can observe this trend in figure 2.10, where the log-returns of SPX over a 15-year period are plotted. This implies that actually the volatility of the log-returns is auto-correlated. In the model, this is a consequence of mean reversion of volatility.⁵

This strong negative correlation between stock's current prices and their future volatilities, called the *leverage effect* was first noted by Black [8] in 1976, who also mentions: "I have believed for a long time that stock returns are related to volatility changes. When stocks go up, volatility seem to go down; and when stocks go down, volatilities seem to go up."⁶ This

⁴Gatheral (2006), page 2, see [28]

⁵Gatheral (2006), page 2, see [28]

⁶Black (1976), pp. 177, see [8]

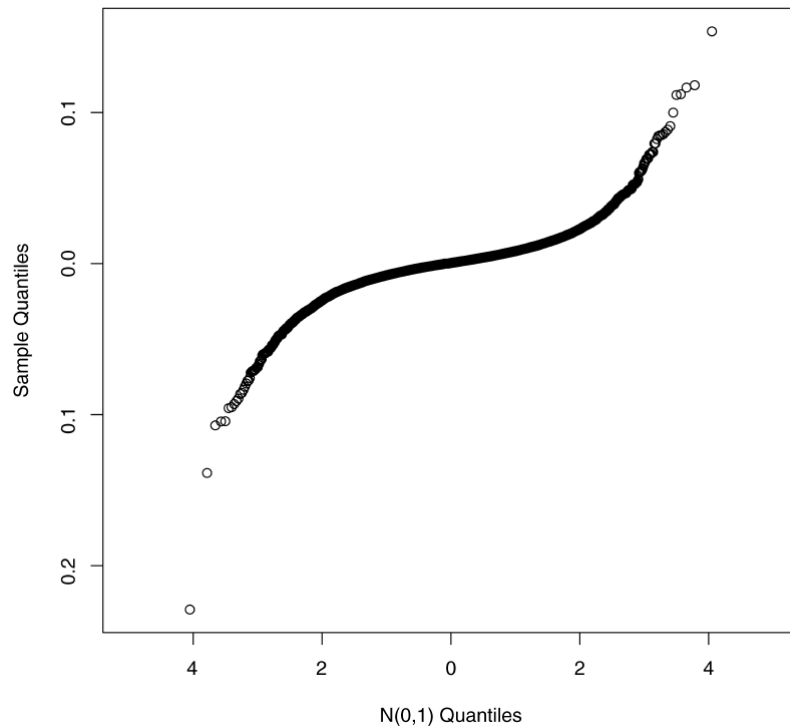


Figure 2.9: Q-Q plot of SPX daily log-returns compared with the normal distribution. Note the extreme tails. Source: [28]

could also be explained from intuition. When the return of equity becomes negative, the reactions from the investors will be more volatile, thus the volatility will increase. Otherwise, when the return becomes positive, investors will gain more confidence in the speculative market; therefore the volatility in the near future would decrease. Therefore, this is also an implication that the constant volatility assumption is far away from the reality.

2.5.3 Volatility Smile

Recall the definition of the implied volatility from section 2.4.2 as the volatility of the underlying assets which, when substituted into the Black-Scholes formula, gives a theoretical price equal to the market price. If the assumption of constant volatility in the Black-Scholes model would hold in the market, the implied volatility of the underlying one could get given an underlying price with different maturities and strikes should be the same. In other words, using Black-Scholes option pricing model, for options with the same expiration date, the implied volatility is expected to be the same regardless the value of the strike price.

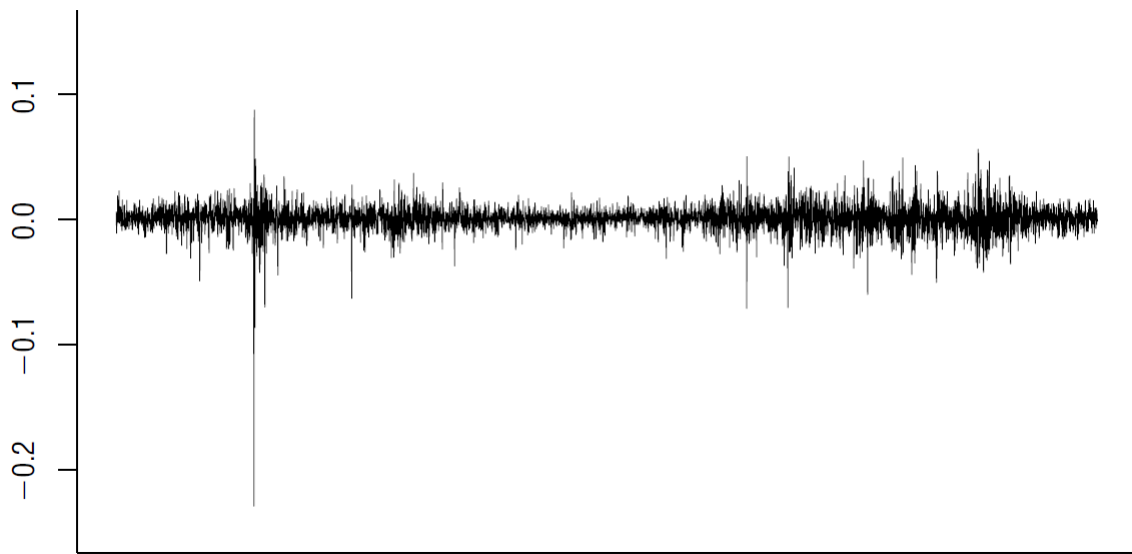


Figure 2.10: SPX daily log-returns from December 31, 1984 to December 31, 2004. Note the -22.9% return on October 19, 1987. Source: [28]

As seen in figure 2.11, where one can observe a so-called *volatility smile*, this contradicts the market reality. The characteristic shape of the curve indicates, that implied volatilities for OTM options are typically higher than those of ATM options. Closely related to this phenomenon is the so-called *skew*, an asymmetry which can also be observed in the market. In figure 2.11, for European ATX call options from the market data described in 5.1, the Black-Scholes implied volatility for each option and then the average per moneyness group (introduced in section 2.2.2) were calculated.

Jackwerth & Rubinstein [36] in 1996, and many other researchers have studied the phenomenon of volatility smile for equity options. Table 2.2 shows how implied volatility changes through different time-to-maturity. This has become more widely observed after the stock market crash in October 1987, because the volatility surface was rarely flat afterwards.

But despite these limitations of idealistic assumptions, which are clearly not suitable to the real market, the Black-Scholes model is still widely used. The main reason is simply its easy analytical tractability, which results in simple formulas for most pricing problems. It is also quite accurate for ATM vanilla options, but one should be careful when using Black-Scholes prices for deep OTM options or exotic options; in these cases market prices can show huge deviations from the theoretical Black-Scholes prices. However, the content of the following chapter will digress from the Black-Scholes world to stochastic volatility world.

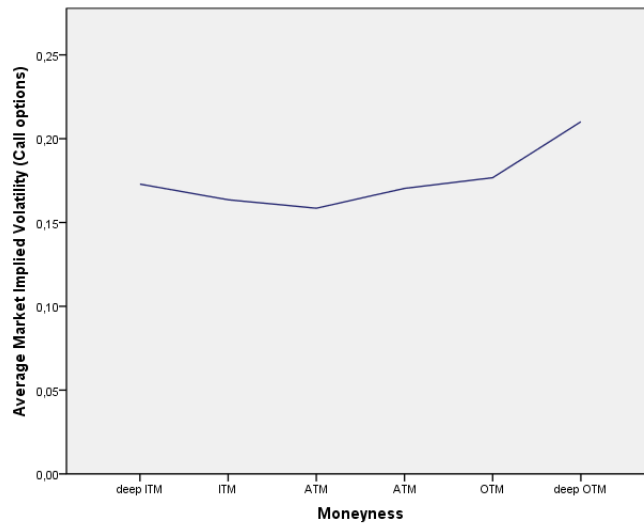


Figure 2.11: Implied volatility of European ATX call options per moneyness group

	At-the-money	Historical Volatility: Prior Sampling Period			
Date	Implied Volatility	28 Days	91 Days	364 Days	1092 Days
04/02/86	0.193	0.137	0.133	0.108	0.118
04/02/87	0.199	0.145	0.143	0.170	0.136
04/04/88	0.262	0.149	0.220	0.348	0.233
04/03/89	0.153	0.116	0.115	0.141	0.238
04/02/90	0.194	0.108	0.136	0.137	0.231
04/02/91	0.196	0.139	0.169	0.167	0.149
04/02/92	0.153	0.073	0.095	0.127	0.145
04/02/93	0.133	0.122	0.108	0.100	0.134

The first column displays the Black-Scholes implied volatility for the ATM option on the S&P 500 index. The option with a time-to-expiration between 135 and 225 days is chosen. 8 dates from April 2, 1986 through April 2, 1993 are used and the date closest to April 2 is chosen for each year. The remaining four columns report the historical volatility for those dates, sampling the prior 28, 91, 364 and 1092 days, respectively.

Table 2.2: Black-Scholes Implied and Historical Time Series Volatilities. Source: Jackwerth & Rubinstein, page 1613, see [36].

Chapter 3

Stochastic Volatility and the Heston Model

In the previous chapter, the Black-Scholes world and its limitations have been discussed. The phenomenon of the implied volatility smile points to a more realistic assumption of stochastic volatility model. In this chapter some alternative option pricing models will be discussed, before the widely used Heston model will be presented. This chapter is based on [1], [28], [29], [33], [37], [51], [53] and [60].

3.1 Moving to Stochastic Volatility Models

Due to its inconsistency with reality and existence of implied volatility smile, Black-Scholes framework leaves much room for improvement by loosening its idealized assumptions. Different researchers have contributed various models to deal with its drawbacks to their individual and specific focus. One category of alternative models are models with the assumptions of stochastic interest rate instead of constant interest rate, presented by Merton [48] and Amin & Jarrow [3]. Also a possibility is to retain the property that the asset price changes continuously, but assume a process other than geometric Brownian motion. Another alternative is to assume a process where all the asset price changes that take place are jumps.

These three types of processes are known as *Levy processes*.¹ A model where stock prices change continuously is known as a *diffusion model*. A model where continuous changes are overlaid with jumps is known as a *mixed jump-diffusion model* and was suggested by Merton [49] in 1976. A model where all stock price changes are jumps is known as a *pure jump model*, an example is the *variance-gamma model* by Carr et al. [10].

¹Roughly speaking, a Levy process is a continuous-time stochastic process with stationary independent increments.

The *constant elasticity of variance* (CEV) model is an example for a diffusion model where the risk-neutral process for a stock price S is

$$dS = (r - q)Sdt + \sigma S^\alpha dz$$

where r is the risk-free rate, q is the dividend yield, dz is a Wiener process, σ is a volatility parameter, and α is a positive constant.²

When $\alpha = 1$, the CEV model is the geometric Brownian motion model, which has been used in the last chapter. When $\alpha < 1$, the volatility increases as the stock price decreases. This creates a probability distribution similar to that observed for equities with a heavy left tail and a less heavy right tail. When $\alpha > 1$, the volatility increases as the stock price increases. This creates a probability distribution with a heavy right tail and a less heavy left tail.

These models have been developed to fit the volatility smiles that are observed in practice.

The CEV model is more suitable for catching the volatility smile similar to that observed for equity options, while jump-diffusion models are better for currency options.

Finally, the limitation of constant volatility leads to models with assumption of stochastic volatility. The volatility is related to a square root process, Cox-Ingersoll-Ross (CIR) process, which was first introduced by Cox, Ingersoll and Ross in 1985.³ There are a number of models, including models by Hull & White [35], Scott [56], Wiggins [59], Stein & Stein [57] and Heston [33]. Stochastic volatility models are useful because they explain in a self-consistent way why options with different strikes and expirations have different Black-Scholes implied volatilities. An important paper on the empirical performance analysis of alternative options pricing models by Bakshi et al. [5] gives the overall conclusion that the stochastic volatility feature is the most important. Other measurement, such as adding jumps and assumption of stochastic interest rate are not as significant as the assumption of stochastic volatility.

In the following section the derivation of the valuation equation in stochastic volatility models will be described and in section 3.3 the base equations of the Heston model will be presented.

3.2 Derivation of the Valuation Equation

This section is based on [28] and [60]. Suppose that the stock price S and its variance v satisfy the following SDEs:

$$dS_t = \mu_t S_t dt + \sqrt{v_t} S_t dW_t, \tag{3.1}$$

$$dv_t = \alpha(S_t, v_t, t) dt + \sigma \beta(S_t, v_t, t) \sqrt{v_t} dZ_t, \tag{3.2}$$

²Cox & Ross (1976), see [13]

³Cox et al. (1985), see [14]

with

$$dW_t dZ_t = \rho dt,$$

where μ_t is the (deterministic) instantaneous drift of stock price returns, σ is the volatility of volatility and ρ is the correlation between random stock price returns and changes in v_t . $W(t)$ and $Z(t)$ are standard Brownian motions (Wiener processes).

The stochastic process (3.1) followed by the stock price is equivalent to the one assumed in the derivation of Black and Scholes (2.1). This ensures that the standard time-dependent volatility version of the Black-Scholes formula may be retrieved in the limit $\eta \rightarrow 0$. In practical applications, this is a key requirement of a stochastic volatility option pricing model as practitioners' intuition for the behaviour of options prices is invariably expressed within the framework of the Black-Scholes formula.

In contrast, the stochastic process (3.2) followed by the variance is very general. Nothing will be assumed about the functional form of $\alpha(\cdot)$ and $\beta(\cdot)$. In particular, a square root process for variance will not be assumed.

In the Black-Scholes case, there is only one source of randomness, the stock price, which can be hedged with stock. In the present case, random changes in volatility also need to be hedged in order to form a riskless portfolio. Set up a portfolio Π containing the option being priced, denote the value by $U(S, v, t)$, a quantity $-\Delta$ of the stock and a quantity $-\Delta_1$ of another asset whose value U_1 depends on volatility. One receives

$$\Pi = U - \Delta S - \Delta_1 U_1.$$

The change in this portfolio in a time dt is given by

$$\begin{aligned} d\Pi = & \left\{ \frac{\partial U}{\partial t} + \frac{1}{2} v S^2 \frac{\partial^2 U}{\partial S^2} + \rho \sigma v \beta S \frac{\partial^2 U}{\partial v \partial S} + \frac{1}{2} \sigma^2 v \beta^2 \frac{\partial^2 U}{\partial v^2} \right\} dt \\ & - \Delta_1 \left\{ \frac{\partial U_1}{\partial t} + \frac{1}{2} v S^2 \frac{\partial^2 U_1}{\partial S^2} + \rho \sigma v \beta S \frac{\partial^2 U_1}{\partial v \partial S} + \frac{1}{2} \sigma^2 v \beta^2 \frac{\partial^2 U_1}{\partial v^2} \right\} dt \\ & + \left\{ \frac{\partial U}{\partial S} - \Delta_1 \frac{\partial U_1}{\partial S} - \Delta \right\} dS \\ & + \left\{ \frac{\partial U}{\partial v} - \Delta_1 \frac{\partial U_1}{\partial v} \right\} dv \end{aligned}$$

where, for clarity, the explicit dependence of the state variables S_t and v_t on t and the dependence of α and β on the state variables have been eliminated. To make the portfolio instantaneously risk-free, choose

$$\frac{\partial U}{\partial S} - \Delta_1 \frac{\partial U_1}{\partial S} - \Delta = 0$$

to eliminate dS terms, and

$$\frac{\partial U}{\partial v} - \Delta_1 \frac{\partial U_1}{\partial v} = 0$$

to eliminate dv terms. This leaves

$$\begin{aligned} d\Pi &= \left\{ \frac{\partial U}{\partial t} + \frac{1}{2}vS^2 \frac{\partial^2 U}{\partial S^2} + \rho\sigma v\beta S \frac{\partial^2 U}{\partial v\partial S} + \frac{1}{2}\sigma^2 v\beta^2 \frac{\partial^2 U}{\partial v^2} \right\} dt \\ &\quad - \Delta_1 \left\{ \frac{\partial U_1}{\partial t} + \frac{1}{2}vS^2 \frac{\partial^2 U_1}{\partial S^2} + \rho\sigma v\beta S \frac{\partial^2 U_1}{\partial v\partial S} + \frac{1}{2}\sigma^2 v\beta^2 \frac{\partial^2 U_1}{\partial v^2} \right\} dt \\ &= r\Pi dt \\ &= r(U - \Delta S - \Delta_1 U_1) dt \end{aligned}$$

where the fact has been used, that the return on a risk-free portfolio must equal the risk-free rate r , which will be assumed to be deterministic for this purpose. Collecting all U terms on the left-hand side and all U_1 terms on the right-hand side, one gets

$$\begin{aligned} &\frac{\frac{\partial U}{\partial t} + \frac{1}{2}vS^2 \frac{\partial^2 U}{\partial S^2} + \rho\sigma v\beta S \frac{\partial^2 U}{\partial v\partial S} + \frac{1}{2}\sigma^2 v\beta^2 \frac{\partial^2 U}{\partial v^2} + rS \frac{\partial U}{\partial S} - rU}{\frac{\partial U}{\partial v}} \\ &= \frac{\frac{\partial U_1}{\partial t} + \frac{1}{2}vS^2 \frac{\partial^2 U_1}{\partial S^2} + \rho\sigma v\beta S \frac{\partial^2 U_1}{\partial v\partial S} + \frac{1}{2}\sigma^2 v\beta^2 \frac{\partial^2 U_1}{\partial v^2} + rS \frac{\partial U_1}{\partial S} - rU_1}{\frac{\partial U_1}{\partial v}} \end{aligned}$$

The left-hand side is a function of U only and the right-hand side is a function of U_1 only. The only way that this can be is for both sides to be equal to some function f of the *independent* variables S , v and t . Deduce that

$$\begin{aligned} &\frac{\partial U}{\partial t} + \frac{1}{2}vS^2 \frac{\partial^2 U}{\partial S^2} + \rho\sigma v\beta S \frac{\partial^2 U}{\partial v\partial S} + \frac{1}{2}\sigma^2 v\beta^2 \frac{\partial^2 U}{\partial v^2} + rS \frac{\partial U}{\partial S} - rU \\ &= -(\alpha - \phi\beta\sqrt{v}) \frac{\partial U}{\partial v} \end{aligned}$$

where, without loss of generality, the arbitrary function f of S , v and t has been written as $(\alpha - \phi\beta\sqrt{v})$, where α and β are the drift and volatility functions from the SDE (3.2) for instantaneous variance.

3.3 Base Equations of the Heston model

The stochastic volatility model proposed by Heston [33] in 1993, extends the Black and Scholes model and includes it as a special case. Heston's setting take into account non-lognormal distribution of the assets returns, leverage effect, important mean-reverting property of volatility and it remains analytically tractable. Furthermore, the Black-Scholes volatility surfaces generated by Heston's model look like empirical implied volatility surfaces.

The Heston model corresponds to choosing $\alpha(S, v_t, t) = \kappa(\theta - v_t)$ and $\beta(S, v, t) = 1$ in equations (3.1) and (3.2). Therefore, the underlying asset price S at time t with dividend q and risk-free interest rate r is assumed to follow the following stochastic process:

$$dS_t = (r - q)S_t dt + \sqrt{v_t}S_t dW_t, \quad S_0 \geq 0, \quad (3.3)$$

where $v(t)$ is the variance and follows the process:

$$dv_t = \kappa(\theta - v_t)dt + \sigma\sqrt{v_t}dZ_t, \quad v_0 = \sigma_0^2 = 0, \quad (3.4)$$

where $W(t)$ and $Z(t)$ are two standard Brownian motions, correlated with each other by

$$dW_t dZ_t = \rho dt, \quad (3.5)$$

where $\kappa, \theta, \sigma > 0$ and $|\rho| < 1$ are the model parameters:

- v_0 Initial variance
- κ Mean reversion rate
- θ Long run variance
- σ Volatility of variance
- ρ Correlation parameter

Note that $v_0 > 0$ is assumed to be non random at time 0, and accounts for the short-term at-the-money implied variance observed on the market. The parameter ρ represents the correlation between the asset price and its instantaneous volatility, and corresponds to the *leverage effect* introduced in section 2.5.2.

The variance process $(v_t)_{t \geq 0}$ is called a Feller diffusion (or a CIR process) and the Yamada-Watanabe conditions⁴ ensure that a non-negative unique strong solution exists. Since the process $(S_t)_{t \geq 0}$ can be written as the exponential of a smooth functional of the variance process, it also has a unique strong solution. Since the square-root function is not smooth at the origin, understanding the behaviour of the variance process at this point is fundamental. The Feller classification of boundaries for one-dimensional diffusions⁵ implies the following:

- (i) if $2\kappa\theta \geq \sigma^2$, then the origin is unattainable;
- (ii) if $2\kappa\theta < \sigma^2$, then the origin is a regular, attainable and reflecting boundary; this means that the variance process can touch 0 in finite time, but does not spend time there;

⁴Karatzas & Shreve (1991), Section 5.2.C, see [38]

⁵Karlin & Taylor (1981), Chapter 15, Section 6, see [39]

- (iii) infinity is a natural boundary, i.e. it can not be attained in finite time and the process can not be started there.

In the rest of the paper, to the inequality $2\kappa\theta \geq \sigma^2$ will be referred to as the *Feller condition*. The interested reader may refer to [43] for the implications of such a boundary classification when pricing options using finite difference schemes.

3.4 Incomplete Market in the Heston Model

By looking at the Heston model and comparing the number of random sources (two standard Brownian motions) with the number of the risky traded assets (only the underlying spot since volatility is not traded) one can easily see that the model is an incomplete model.⁶ Therefore, it is not possible to obtain an unique price for any contingent claim using only the underlying asset and a bank account, which is normally the case for complete models such as the Black-Scholes model. To complete the market in the Heston model, one has to add an European call option for example.

In a complete (frictionless) market framework, contingent claims written on the existing primitive assets are redundant. Assuming that their introduction in the economy does not affect equilibrium prices,⁷ the agent utility cannot be increased by trading in such redundant assets. However in incomplete markets, contingent claims can improve the market efficiency by reducing the dimensionality of unhedgeable risks (see Hart [31]).

Bajoux & Rochet [4] addressed this problem in a continuous-time incomplete market model. Considering the stochastic volatility model studied by Hull & White [35], they showed that any European option completes the market. A pricing rule of the option is required in order to check its redundancy at any time.

Romano & Touzi [53] show that a sufficient condition for a contingent claim to complete the market is the strict convexity of its price function in the current underlying asset price at any time (strictly) before maturity. Such a sufficient condition is satisfied by European call and put option. In general, given a contingent claim with convex payoff function, such a sufficient condition is satisfied by any admissible arbitrage price induced by an equivalent martingale measure under which the volatility process is Markov.

Thus, they extended the result of Bajoux & Rochet [4] to a large class of contingent claims and allow a possible correlation between the asset price and its volatility variations.

⁶Björk (2004), p118, Meta-theorem 8.3.1, see [7]

⁷Detemple & Selden (1991) showed that trading in options does affect the equilibrium prices since the agents' demand is changed, see [15]

3.5 Semi-closed Form Solution for European Options

The above mentioned equations (3.3)-(3.5) are still insufficient to price contingent claims because no assumptions that give the *price of volatility risk* have been made. Standard arbitrage arguments⁸ demonstrate that the value of any asset $U(S, v, t)$ must satisfy the partial differential equation

$$\begin{aligned} \frac{1}{2}vS^2\frac{\partial^2 U}{\partial S^2} + \rho\sigma vS\frac{\partial^2 U}{\partial S\partial v} + \frac{1}{2}\sigma^2v\frac{\partial^2 U}{\partial v^2} + rS\frac{\partial U}{\partial S} \\ + \kappa(\theta - v_t) - \lambda(S, v, t)\frac{\partial U}{\partial v} - rU + \frac{\partial U}{\partial t} = 0. \end{aligned} \quad (3.6)$$

The function $\lambda(S, v, t)$ represents the market price of the volatility risk. Without loss of generality its functional form can be reduced to $\lambda(S, v, t) = \lambda v$.

A European call option with strike price K and maturing at time T satisfies the PDE (3.6) subject to the following boundary conditions:

$$\begin{aligned} U(S, v, T) &= \max(0, S - K), \\ U(0, v, t) &= 0, \\ \frac{\partial U}{\partial S}(\infty, v, t) &= 1 \\ rS\frac{\partial U}{\partial S}(S, 0, t) + \kappa\theta\frac{\partial U}{\partial v}(S, 0, t) - rU(S, 0, t) + U_t(S, 0, t) &= 0, \\ U(S, \infty, t) &= S. \end{aligned} \quad (3.7)$$

By analogy with the Black-Scholes formula, the solutions have the form

$$C(S, v, t) = SP_1 - KP(t, T)P_2, \quad (3.8)$$

where the first term is the present value of the underlying (spot) asset, and the second term is the present value of the strike price payment. Both of these terms must satisfy the original PDE (3.6). It is convenient to write them in terms of the logarithm of the spot price $x = \ln[S]$.

$$\begin{aligned} \frac{1}{2}v\frac{\partial^2 P_j}{\partial x^2} + \rho\sigma v\frac{\partial^2 P_j}{\partial x\partial v} + \frac{1}{2}\sigma^2v\frac{\partial^2 P_j}{\partial v^2} + (r + u_jv)\frac{\partial P_j}{\partial x} \\ + (a_j - b_jv)\frac{\partial P_j}{\partial v} + \frac{\partial P_j}{\partial t} = 0. \end{aligned} \quad (3.9)$$

⁸Black & Scholes (1973) and Merton (1973), see [9] and [48] respectively

for $j = 1, 2$, where

$$u_1 = \frac{1}{2}, \quad u_2 = -\frac{1}{2}, \quad a = \kappa\theta, \quad b_1 = \kappa + \lambda - \rho\sigma, \quad b_2 = \kappa + \lambda.$$

For the option price to satisfy the terminal condition in equation (3.7), these PDEs (3.9) are subject to the terminal condition

$$P_j(x, v, T; \ln[K]) = \mathbb{I}_{\{x \leq \ln[K]\}}$$

Thus, they may be interpreted as *adjusted* or *risk-neutralized* probabilities.⁹ The probabilities P_j are not immediately available in closed form, but one can receive them by inverting the characteristic functions. Their characteristic functions satisfy the same PDE (3.9) and the characteristic function solution is

$$f_j(x, v, t; \phi) = \exp(C(T-t; \phi) + D(T-t; \phi)v + i\phi x), \quad (3.10)$$

where

$$C(\tau, \phi) = r\phi i\tau + \frac{a}{\sigma^2} \left\{ (b_j - \rho\sigma\phi i + d)\tau - 2 \ln \left[\frac{1 - ge^{d\tau}}{1 - g} \right] \right\}$$

$$D(\tau, \phi) = \frac{b_j - \rho\sigma\phi i + d}{\sigma^2} \left[\frac{1 - e^{d\tau}}{1 - ge^{d\tau}} \right]$$

and

$$g = \frac{b_j - \rho\sigma\theta i + d}{b_j - \rho\sigma\theta i - d},$$

$$d = \sqrt{(\rho\sigma\phi i - b_j)^2 - \sigma^2(2u_j\phi i - \phi^2)}.$$

One can invert the characteristic functions to get the desired probabilities:

$$P_j(x, v, T; \ln[K]) = \frac{1}{2} + \frac{1}{\pi} \int_0^\infty \operatorname{Re} \left[\frac{e^{-i\phi \ln[K]} f_j(x, v, T; \phi)}{i\phi} \right] d\phi. \quad (3.11)$$

The integrand in equation (3.11) is a smooth function that decays rapidly and presents no difficulties. Equations (3.8), (3.10) and (3.11) give the solutions for European call options.

⁹Cox & Ross (1976), see [13]

3.6 Influence of Parameters

It is important to understand the meaning of the Heston parameters, since the effective utilisation of the stochastic volatility model depends on the initial parameters and calibration parameters:

Initial variance v_0 Changing the initial variance allows adjustment in the height of the smile curve rather than the shape. Increasing the initial volatility level, $\sqrt{v_0}$ moves the implied volatility smile upwards, see figure 3.1 (left). This behaviour is quite intuitive, hence will not be commented further.

Long run variance θ As a matter of fact, long run variance θ and initial variance v_0 have a similar influence upon the implied volatility smile. In figure 3.1 (right) the effect of changing long run variance is shown.

Mean reversion κ The mean reversion rate can be interpreted as representing the degree of *volatility clustering*. As mentioned in section 2.5.2, volatility clustering can be observed in the market, it means that large moves are followed by large moves, while small moves are more likely to be followed by small moves. The mean reversion parameter controls the curvature of the curve. Increasing the mean reversion parameter flattens the implied volatility smile, see figure 3.2. Decreasing the mean reversion has a similar effect as increasing the volatility of variance in terms of curvature, the effect is shown in figure 3.9.

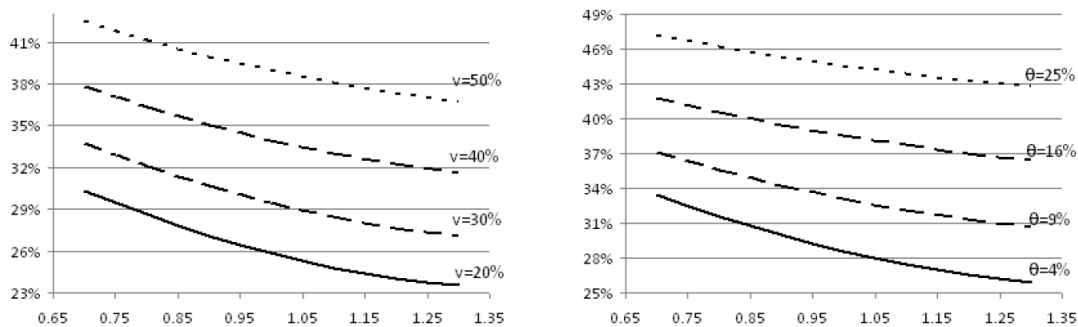


Figure 3.1: The effect of changing the initial variance $v = \sqrt{v_0}$ (left) and the effect of changing the long run variance θ (right). Source: [29]

Correlation ρ The correlation, which can be interpreted as the correlation between the log-returns and volatility of the asset, affects the heaviness of the tails. Intuitively, if $\rho > 0$, then volatility will increase as the asset price/return increases. This will spread the right tail and squeeze the left tail of the distribution creating a fat right-tailed distribution. Conversely, if $\rho < 0$, then volatility will increase when the asset price/return decreases, thus spreading the

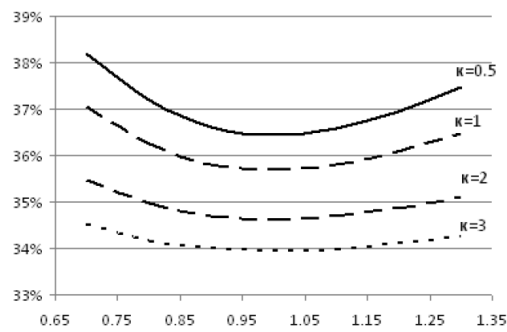


Figure 3.2: The effect of changing the mean reversion κ . Source: [29]

left tail and squeezing the right tail of the distribution creating a fat left-tailed distribution (emphasising the fact that equity returns and its related volatility are negative correlated). The correlation, therefore, affects the skewness of the distribution. Figure 3.3 shows this effect for different values ρ on the skewness of the density function.

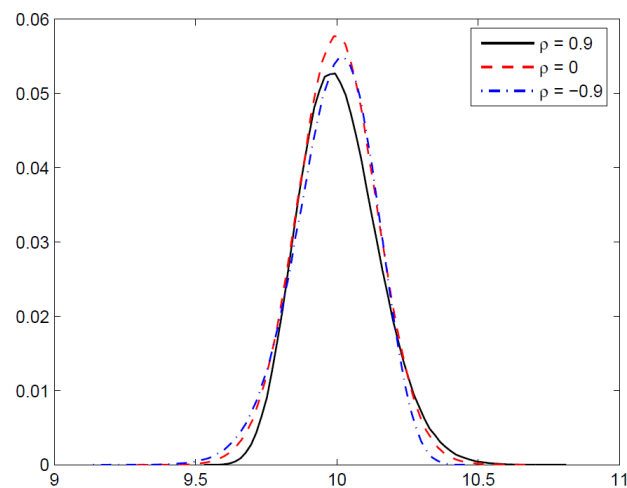


Figure 3.3: The effect of ρ on the skewness of the density function. Source: [51]

The effect of changing the skewness of the distribution also impacts on the shape of the implied volatility surface. Hence, ρ also affects this. Figures 3.4, 3.5 and 3.6 show the effect of varying ρ . As can be seen, the model can imply a variety of volatility surfaces and hence addresses the shortcoming of constant volatility across differing strike levels in the Black-Scholes model.

Volatility of variance σ The Volatility of variance σ affects the kurtosis (peak) of the distribution. When σ is 0 the volatility is deterministic and hence the log-returns will be

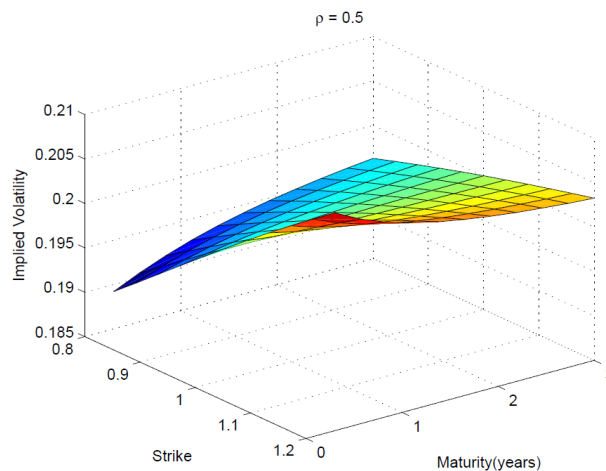


Figure 3.4: Implied volatility surface, $\rho = 0.5$, $\kappa = 2$, $\theta = 0.04$, $\sigma = 0.1$, $v_0 = 0.04$, $r = 1\%$, $S_0 = 1$, strikes: 0.8 – 1.2, maturities: 0.5 – 3 years. Source: [51]

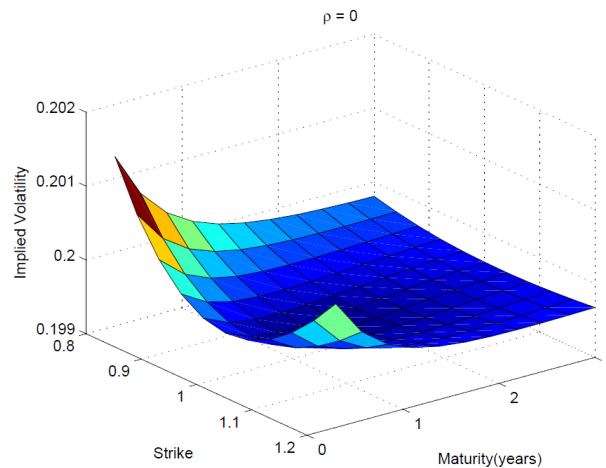


Figure 3.5: Implied volatility surface, $\rho = 0$, $\kappa = 2$, $\theta = 0.04$, $\sigma = 0.1$, $v_0 = 0.04$, $r = 1\%$, $S_0 = 1$, strikes: 0.8 – 1.2, maturities: 0.5 – 3 years. Source: [51]

normally distributed. Increasing σ will then increase the kurtosis only, creating heavy tails on both sides. The effect of varying σ on the kurtosis of the density function is shown in figure 3.7. Again, the effect of changing the kurtosis of the distribution impacts on the implied volatility. Figures 3.8 - 3.10 show how σ affects the *significance* of the smile/skew. Higher σ makes the skew/smile more prominent. This makes sense relative to the leverage effect. Higher σ means that the volatility is more volatile. This means that the market has a greater change of extreme movements. So, writers of puts must charge more and those of calls less, for a given strike.

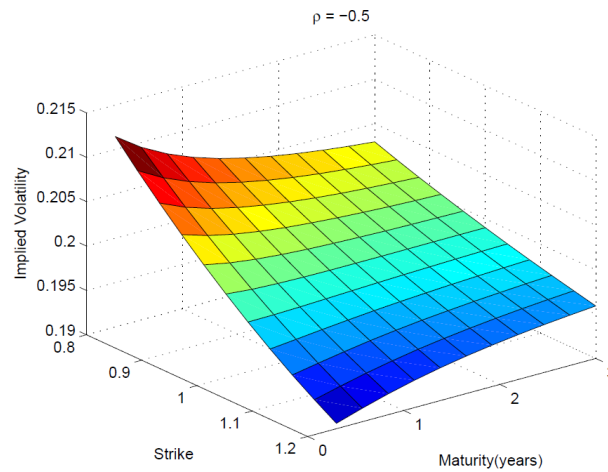


Figure 3.6: Implied volatility surface, $\rho = -0.5$, $\kappa = 2$, $\theta = 0.04$, $\sigma = 0.1$, $v_0 = 0.04$, $r = 1\%$, $S_0 = 1$, strikes: 0.8 – 1.2, maturities: 0.5 – 3 years. Source: [51]

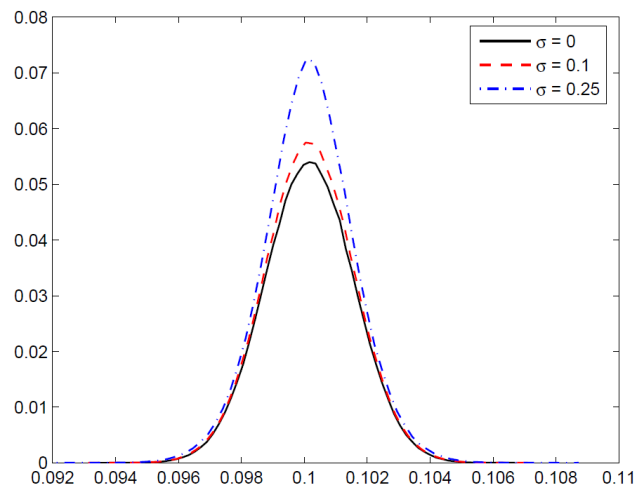


Figure 3.7: The effect of σ on the kurtosis of the density function. Source: [51]

The aforementioned features of this model enables it to produce a barrage of distributions. This makes the model very robust and hence addresses the shortcomings of the Black-Scholes model. It provides a framework to price a variety of options that is closer to reality.

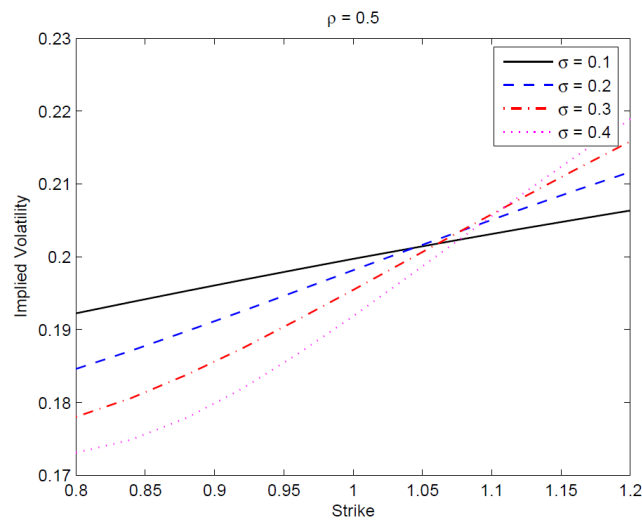


Figure 3.8: Implied volatility curve, $\rho = 0.5$, $\kappa = 2$, $\theta = 0.04$, $\sigma = 0.1$, $v_0 = 0.04$, $r = 1\%$, $S_0 = 1$, strikes: 0.8 – 1.2, maturities: 0.5 – 3 years. Source: [51]

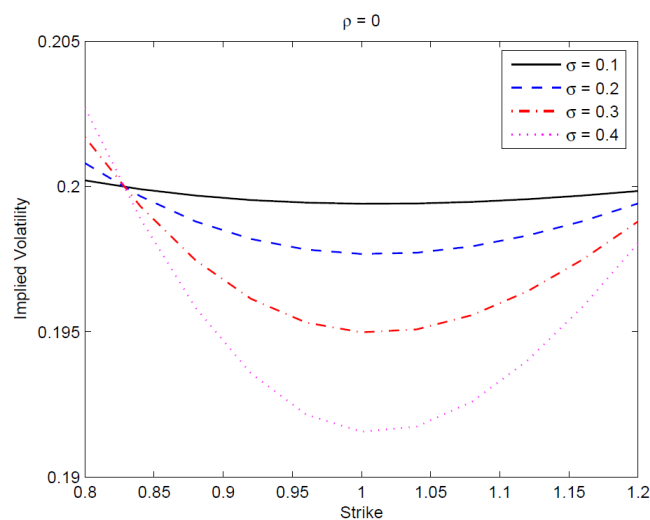


Figure 3.9: Implied volatility curve, $\rho = 0$, $\kappa = 2$, $\theta = 0.04$, $\sigma = 0.1$, $v_0 = 0.04$, $r = 1\%$, $S_0 = 1$, strikes: 0.8 – 1.2, maturities: 0.5 – 3 years. Source: [51]

3.7 Advantages and Disadvantages of the Heston Model

Both academia and practitioners have recognized the significance of the Heston Model, nevertheless, it is not a model without any drawbacks. A brief summary of its advantages and disadvantages will be presented in this section.

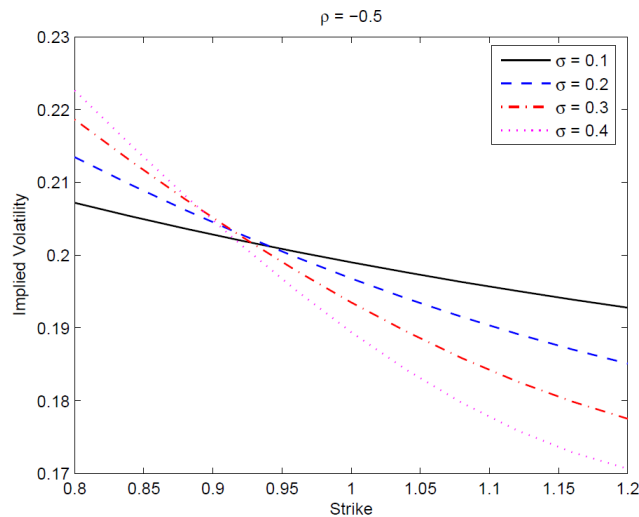


Figure 3.10: Implied volatility curve, $\rho = -0.5$, $\kappa = 2$, $\theta = 0.04$, $\sigma = 0.1$, $v_0 = 0.04$, $r = 1\%$, $S_0 = 1$, strikes: 0.8 – 1.2, maturities: 0.5 – 3 years. Source: [51]

Advantages of the Heston model:

- Semi-closed form solution for European options and thus the model allows a fast calibration to given market data.
- Unlike the Black-Scholes model, the price dynamics in the Heston model allows for non-lognormal probability distribution (high peak, fat tails).
- The model fits the implied volatility surface of option prices in the market, when the maturity is not too small.
- The volatility is mean reverting.
- It takes into account leverage effect (negative correlation of equity returns and implied volatility), and in addition, it permits the correlation between the asset and the volatility to be changed

Disadvantages of the Heston model:

- Since volatility is unobservable, the parameter values in the Heston model (and other SV models) are not easily estimated.
- The prices produced by the model are quite parameter sensitive, hence the fitness of the model depends on the calibration. In other words, the price to pay for more realistic models is the increased complexity of model calibration.

- The Heston model fails to produce decent results for short maturities as the model fails to create a short term skew as strong as the one given by the market. To perform well, further extensions of the model are necessary, such as adding jumps.¹⁰

The first two drawbacks display the importance of calibration in the Heston model. Often, the estimation method for the parameters becomes as crucial as the model itself.¹¹

In the last years asymptotic properties of the model have been thoroughly studied: small and large time behaviours, wings of the implied volatility for fixed maturity. They are extremely useful in practice to determine initial points for the calibration of the model. On this calibration issue, least-square minimisation methods based on these asymptotical results as a proxy should be very accurate. In the next chapters some asymptotic results will be presented, and used for the calibration of initial parameters.

¹⁰Mikhailov & Nögel (2003), see [50]

¹¹Mikhailov & Nögel (2003), see [50]

Chapter 4

Asymptotic Behaviour in the Heston model

This chapter is based on [21], [22], [23], [24], [25] and [27]. Stochastic models are used extensively by traders and quantitative analysts in order to price and hedge financial products. Once a model has been chosen for its realistic features, one has to calibrate it. This calibration must be robust and stable and should not be too computer intensive. This latter constraint often rules out global optimisation algorithms which are very slow despite their accuracy. For this matter closed-form asymptotic approximations have grown rapidly in the past few years. They have proved to be very efficient

- (i) to provide some information about the behaviour of option prices in some extreme regions such as small or large strikes and/or maturities (where standard numerical schemes lose their accuracy),
- (ii) to improve calibration efficiency.

Indeed one can first perform an instantaneous calibration on the closed-form first and then use this result as a starting point to calibrate the whole model. In practice calibration is often performed using the implied volatility, i.e. the volatility parameter to be used in the Black-Scholes formula in order to match the observed market price, rather than option prices. The general approach to the calibration of parametric models, such as the Heston model, is to apply a least-square type procedure in implied volatility. This kind of approach will in general be very sensitive to the choice of the initial point, which will often in practice drive the selection of the local minima the algorithm will converge to. The various explicit formulae for short or long term asymptotics, conveniently inverted, come into play to get a pertaining initial point.

In this chapter an overview of the many recent results concerning the asymptotic properties of the Heston model, with a main focus on the work of Forde & Jacquier [23], Forde et al. [24], Forde et al. [25] and Friz et al. [27] will be presented. Finally, in chapter 5 the results on

calibrating the initial points in the Heston model with the afore mentioned asymptotic properties will be provided.

Note, in the following sections $\sigma_t(x)$ shall denote the implied volatility of a European Call option written on the (forward) asset price S_t , with strike $K = S_0 e^x$ maturing at time T . With $X_t = \log(S_t)$ the log-forward price will be denoted for convenience, the log-moneyness of an option is denoted with x . Many results in this section will be based on the knowledge and the properties of the Laplace transform of the model. It hence worth recalling its exact form. For any $t > 0$, define the moment generating function Λ_t of the Heston model by

$$\Lambda_t(u) := \log \mathbb{E}(e^{u(X_t - x_0)}), \quad \text{for all } u \in \mathbb{R} \text{ such that the expectation exists.}$$

4.1 Lee's Moment Formula

First, Lee's moment formula will be presented. Lee [42] proved in 2004 the existence of bounds for the implied volatility skew at extreme, i.e. deep in-the-money or out-of-the-money. He shows that implied volatility is bounded by two functions that are linear in the log-strike $k = \log(K/S_0)$. He shows also how to relate the gradients of the wings of the upper bound of the implied volatility skew to the maximal finite moments of the underlying process. The main results will be presented in theorem 4.1.3 and 4.1.5.

Let B_t be the time- t price of a discount bond maturing at T , and S_T a nonnegative underlying randomness. Write C and P for the time-0 call and put prices as a function of strike:

$$\begin{aligned} C(K) &= B_0 \mathbb{E}(S_T - K)^+ \\ P(K) &= B_0 \mathbb{E}(K - S_T)^+ \end{aligned}$$

for $K > 0$ and define $F_0 = \mathbb{E}S_T$, which one interprets as today's T -forward price of the payoff S_T . Note also the following Corollary.

Corollary 4.1.1. *If $\mathbb{E}S_T^{p+1} < \infty$, then $C(K) = O(K^{-p})$ as $K \rightarrow \infty$.
If $\mathbb{E}S_T^{-q} < \infty$, then $P(K) = O(K^{1+q})$ as $K \rightarrow 0$.*

Consider the right-hand (or large K or positive x or out-of-the-money call) tail of the square of implied volatility. First it will be shown that this tail slope is no larger than 2.

Lemma 4.1.2. *There exists $x^* > 0$ such that for all $x > x^*$*

$$I(x) < \sqrt{2|x|/T}$$

Proof. By the strict monotonicity of C_{BS} in its second argument, it is only necessary to establish that

$$C_{BS}(x, I(x)) < C_{BS}(x, \sqrt{2|x|/T}) \quad (4.1)$$

whenever $x > x^*$. On the left-hand side of 4.1, one gets

$$\lim_{x \rightarrow \infty} C(K(x)) = \lim_{K \rightarrow \infty} B_0 \mathbb{E}(S_T - K)^+ = 0$$

by dominated convergence, because $\mathbb{E}S_T < \infty$. On the right-hand side,

$$\lim_{x \rightarrow \infty} C_{BS}(x, \sqrt{2|x|/T}) = B_0 F_0 [\Phi(0) - \lim_{x \rightarrow \infty} e^x \Phi(-\sqrt{2|x|})] = B_0 F_0 / 2$$

by L'Hôpital's rule. This proves 4.1.2 □

The explicit formula relating the right-hand tail slope to how many finite moments the underlying possesses is given by the following:

Theorem 4.1.3 (The Moment Formula, part 1). *Let*

$$\tilde{p} := \sup \left\{ p : \mathbb{E}S_T^{1+p} < \infty \right\} \quad \beta_R := \limsup_{k \rightarrow \infty} \frac{\sigma_{BS}^2(K, T)T}{|k|}.$$

Then $\beta_R \in [0, 2]$,

$$\tilde{p} = \frac{1}{2} \left(\frac{1}{\sqrt{\beta_R}} - \frac{\sqrt{\beta_R}}{2} \right)^2$$

where $1/0 := \infty$. Equivalently,

$$\beta_R = 2 - 4(\sqrt{\tilde{p}^2 + \tilde{p}} - \tilde{p})$$

where the right-hand expression is to be read as zero, in the case $\tilde{p} = \infty$.

Proof. Lemma 4.1.2 implies $\beta_R \in [0, 2]$. Show that $\tilde{p} = f_-(\beta_R)/2$.

For any $\beta \in (0, 2)$, L'Hôpital's rule implies that

$$\limsup_{x \rightarrow \infty} \frac{e^{-cx}}{C_{BS}(x, \sqrt{\beta|x|/T})} = \begin{cases} 0 & \text{for } c > f_-(\beta)/2 \\ \infty & \text{for } c \leq f_-(\beta)/2 \end{cases}$$

which will be used in both stages of the proof.

To prove $\tilde{p} \leq f_-(\beta_R)/2$, note that $f_- : (0, 2) \xrightarrow{\text{onto}} (0, \infty)$ is strictly decreasing. So it suffices to show that for any $\beta \in (0, 2)$ with $f_-(\beta)/2 < \tilde{p}$, one has $\beta_R \leq \beta$. Choose $p \in (f_-(\beta)/2, \tilde{p})$. By Corollary 4.1.1, as $x \rightarrow \infty$,

$$\frac{C_{BS}(x, I(x))}{C_{BS}(x, \sqrt{\beta|x|/T})} = \frac{O(e^{-px})}{C_{BS}(x, \sqrt{\beta|x|/T})} \rightarrow 0.$$

The result follows from the monotonicity of C_{BS} in its second argument.

To prove $\tilde{p} \geq f_-(\beta_R)/2$, it suffices to show that for any $p \in (0, f_-(\beta)/2)$, one has $\mathbb{E}S_T^{1+p} < \infty$. Choose

$$\frac{C_{BS}(K(x))}{e^{-Qx}} \leq \frac{C_{BS}(x, \sqrt{\beta|x|/T})}{e^{-Qx}} \rightarrow 0 \quad \text{as } x \rightarrow \infty,$$

so there exists K_* such that for all $K > K_*$, one has $C(K) < K^{-Q}$. Then, as claimed,

$$\begin{aligned} \mathbb{E}S_T^{1+p} &= \mathbb{E} \int_0^\infty (p+1)pK^{p-1}(S_T - K)^+ dK \\ &\leq p(p+1)B_0^{-1} \left[\int_0^{K_*} K^{p-1}C(K)dK + \int_{K_*}^\infty K^{p-Q-1}dK \right] < \infty, \end{aligned}$$

where the first step uses a mixture of calls to span the twice-differentiable payoff S^{1+p} ; see the appendix of [11]. \square

Consider the left-hand (or small K or negative x or out-of-the-money put) tail of the square of implied volatility. First it will be shown, that this tail slope is no larger than 2.

Lemma 4.1.4. *For any $\beta > 2$ there exists x^* such that for all $x < x^*$,*

$$I(x) < \sqrt{\beta|x|/T}$$

For $\beta = 2$, the same conclusion holds, if and only if S_T satisfies $\mathbb{P}(S_T = 0) < 1/2$.

Proof. For case $\beta > 2$ and the “if” part of case $\beta = 2$: There exists x^* such that for all $x < x^*$,

$$\mathbb{P}(S_T < F_0e^x) < \Phi(-\sqrt{f_-(\beta)|x|}) - e^{-x}\Phi(-\sqrt{f_+(\beta)|x|})$$

because as $x \rightarrow -\infty$, the left-hand side approach $\mathbb{P}(S_T = 0)$, while the right-hand side approaches either 1 (in case $\beta > 2$) or 1/2 (in case $\beta = 2$). So

$$P_{BS}(x, I(x)) = B_0\mathbb{E}(K(x) - S_T)^+ \leq B_0K(x)\mathbb{P}(S_T < F_0e^x) < P_{BS}(x, \sqrt{\beta|x|/T})$$

for all $x < x^*$. The result follows from strict monotonicity of P^{BS} in its second argument.

For the “only if” part of case $\beta = 2$: By monotonicity of P_{BS} , on has

$$B_0K(x)/2 > P_{BS}(x, \sqrt{2|x|/T}) > B_0\mathbb{E}(K(x) - S_T)^+ \geq B_0K(x)\mathbb{P}(S_T = 0)$$

for arbitrary $x > x^*$. Divide by $B_0K(x)$ to obtain the result. \square

The explicit formula relating the left-hand tail slope to how many finite moments the underlying’s reciprocal possesses is given by the following:

Theorem 4.1.5 (The Moment Formula, part 2). *Let*

$$\tilde{q} := \sup \left\{ q : \mathbb{E}S_T^{-q} < \infty \right\} \quad \beta_L := \limsup_{k \rightarrow -\infty} \frac{\sigma_{BS}^2(K, T)T}{|k|}.$$

Then $\beta_L \in [0, 2]$,

$$\tilde{q} = \frac{1}{2} \left(\frac{1}{\sqrt{\beta_L}} - \frac{\sqrt{\beta_L}}{2} \right)^2$$

where $1/0 := \infty$. Equivalently,

$$\beta_L = 2 - 4(\sqrt{\tilde{q}^2 + \tilde{q}} - \tilde{q})$$

where the right-hand expression is to be read as zero, in the case $\tilde{q} = \infty$.

Proof. Lemma 4.1.4 implies $\beta_L \in [0, 2]$. Show that $\tilde{q} = f_-(\beta_L)/2$.

For any $\beta \in (0, 2)$, L'Hôpital's rule implies that

$$\limsup_{x \rightarrow -\infty} \frac{e^{(1+c)x}}{P_{BS}(x, \sqrt{\beta|x|/T})} = \begin{cases} 0 & \text{for } c > f_-(\beta_L)/2 \\ \infty & \text{for } c \leq f_-(\beta_L)/2 \end{cases}$$

which will be used in both stages of the proof.

To prove $\tilde{q} \leq f_-(\beta_L)/2$, note that $f_- : (0, 2) \xrightarrow{\text{ontQ}} (0, \infty)$ is strictly decreasing. So it suffices to show that for any $\beta \in (0, 2)$ with $f_-(\beta)/2 < \tilde{q}$, one has $\beta_L \leq \beta$. Choose $q \in (f_-(\beta)/2, \tilde{q})$. By Corollary 4.1.1, as $x \rightarrow -\infty$,

$$\frac{P_{BS}(x, I(x))}{P_{BS}(x, \sqrt{\beta|x|/T})} = \frac{O(e^{(1+q)x})}{P_{BS}(x, \sqrt{\beta|x|/T})} \rightarrow 0.$$

The result follows from the monotonicity of P_{BS} in its second argument.

To prove $\tilde{q} \geq f_-(\beta_L)/2$, it suffices to show that for any $q \in (0, f_-(\beta_L)/2)$, one has $\mathbb{E}S_T^{-q} < \infty$. Choose β such that $Q := f_-(\beta)/2 \in (q, f_-(\beta_L)/2)$. For $|x|$ sufficiently large,

$$\frac{P(K(x))}{e^{(1+Q)x}} \leq \frac{P_{BS}(x, \sqrt{\beta|x|/T})}{e^{(1+Q)x}} \rightarrow 0 \quad \text{as } x \rightarrow -\infty,$$

so there exists K_* such that for all $K < K_*$, one has $P(K) < K^{1+Q}$. Then, as claimed,

$$\begin{aligned} \mathbb{E}S_T^{-q} &= \mathbb{E} \int_0^\infty -q(-q-1)K^{-q-2}(K - S_T)^+ dK \\ &\leq q(q+1)B_0^{-1} \left[\int_0^{K_*} K^{Q-q-1} dK + \int_{K_*}^\infty K^{-q-2} P(K) dK \right] < \infty, \end{aligned}$$

where the first step uses a mixture of puts to span the twice-differentiable payoff S^{-q} ; see the appendix of [11]. \square

4.2 Short-maturity asymptotic behaviour

In this section the main results of Forde et al. [24] will be presented. The short-maturity behaviour of the Heston model has recently attracted quite a few people, with a focus on applications of Varadhan's seminal work [58] on short-time behaviour of diffusion processes. Berestycki et al. [6] showed that, in a fairly general stochastic volatility model, the short-time implied volatility is the viscosity solution to a certain PDE; Durrleman [17] characterised and solved this PDE in the Heston model, and Henry-Labordère [32] characterised the small-time behaviour of the implied volatility using the heat kernel expansion on a Riemannian manifold. Finally, in [19], Feng et al. worked out the short-time behaviour of the Heston model in a fast mean-reverting regime using large deviations theory, Alòs & Ewald [2] in a small volatility of volatility regime using Malliavin calculus, and Medvedev & Scaillet [46] obtained the short-time behaviour of general stochastic volatility models by means of asymptotic expansion of the corresponding pricing PDE.

Using the affine properties of the Heston model, Forde & Jacquier [21] developed a large deviation approach to obtain the small-time behaviour of the implied volatility. In [24] Forde et al. refined this analysis by providing the first-order correction of the small-maturity expansion for the implied volatility in this model. Their methodology in use is, similar to the one used in [25] for the large-maturity case, is based on saddlepoint expansions in the complex plane and the properties of holomorphic functions.

The attention will now be drawn to Forde et al. [24], which results hold in both correlation regimes. The analysis in this work relies on the Laplace transform of the process and not on its path properties, so it is not necessary to assume the Feller condition. The limiting moment generation function $\Lambda : \mathcal{D} \rightarrow \mathbb{R}$ is defined by $\Lambda(p) := \lim_{t \rightarrow 0} t\Lambda_t(p/t)$, for all $p \in \mathcal{D}$, where \mathcal{D} is a closed interval of the real line containing the origin. The function Λ has the following representation:

$$\Lambda(p) := \frac{y_0 p}{\sigma(\sqrt{1 - \rho^2} \cot(\frac{1}{2}\sigma p \sqrt{1 - \rho^2}) - \rho)}, \quad \text{for all } p \in \mathcal{D}. \quad (4.2)$$

The Fenchel-Legendre transform $\Lambda^* : \mathbb{R} \rightarrow \mathbb{R}$ of the function Λ is defined by

$$\Lambda^*(x) := \sup_{p \in \mathcal{D}} \{px - \Lambda(p)\}, \quad \text{for all } x \in \mathbb{R}. \quad (4.3)$$

Then the following small-time expansions for European call option prices and implied volatilities in the Heston model hold.

Theorem 4.2.1. *In the Heston model (3.3) the asymptotic behaviour for European call options*

$$\frac{\mathbb{E}(e^{X_t} - S_0 e^x)_+}{S_0} = \begin{cases} (1 - e^x)_+ + \exp\left(-\frac{\Lambda^*(x)}{t}\right) \left(\frac{A(x)}{\sqrt{2\pi}} t^{3/2} + \mathcal{O}(t^{5/2})\right), & \text{if } x \neq 0 \\ \sqrt{\frac{y_0 t}{2\pi}} - B t^{3/2} + \mathcal{O}(t^{5/2}), & \text{if } x = 0, \end{cases} \quad (4.4)$$

holds as the maturity $t \rightarrow 0$, where

$$\begin{aligned} A(x) &:= \frac{e^x U(p^*(x))}{p^*(x)^2 \sqrt{\Lambda''(p^*(x))}}, \\ U(p) &:= \exp\left(\frac{\kappa\theta}{\sigma^2} \left((i\rho\sigma - d_0)ip - 2 \log\left(\frac{1 - g_0 e^{id_0 p}}{1 - g_0}\right) \right)\right) \\ &\quad \exp\left(\frac{y_0 e^{-id_0 p}}{(1 - g_0 e^{-id_0 p})\sigma^2} \left((i\rho\sigma - d_0)ip d_1 + (d_1 - \kappa)(1 - e^{id_0 p}) - \frac{(i\rho\sigma - d_0)(1 - e^{-id_0 p})(g_1 - id_1 g_0 p)}{1 - g_0 e^{-id_0 p}} \right)\right), \\ B &:= \frac{1}{48} \sqrt{\frac{2}{y_0 \pi}} \left(\sigma^2 \left(1 - \frac{\rho^2}{4}\right) + y_0(y_0 - 3\rho\sigma) - 6\kappa(\theta - y_0) \right), \end{aligned}$$

where the functions Λ and Λ^* are defined in (4.2) and (4.3), and

$$d_0 := \sigma\bar{\rho}, \quad d_1 := \frac{2\kappa\rho - \sigma}{2\bar{\rho}}i, \quad g_0 := \frac{i\rho - \bar{\rho}}{i\rho + \bar{\rho}}, \quad g_1 := \frac{(2\kappa - \rho\sigma)}{\sigma\bar{\rho}(i\rho + \bar{\rho})^2}.$$

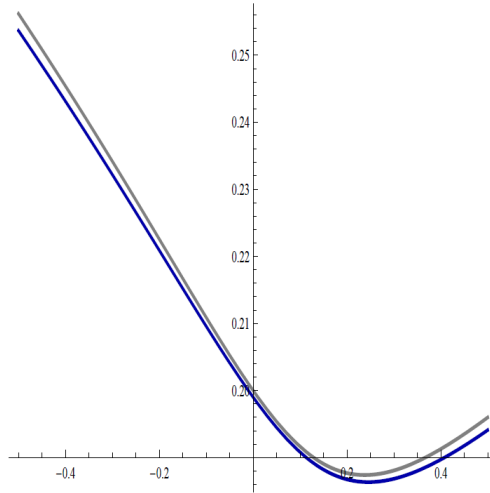


Figure 4.1: The leading order term (grey) and correction term (blue) in the small-time limit for the Heston model for $\kappa = 1.15$, $\sigma = 0.2$, $y_0 = \theta = 0.04$, $\rho = -0.4$, $t = 0.25$. Source: [22]

The following theorem gives the out-of-the-money and in-the-money ($x \neq 0$), and the at-the-money ($x = 0$) implied volatility for small maturities.

Theorem 4.2.2. *The small-time implied volatility has the asymptotic behaviour*

$$\sigma_t^2(x) = \begin{cases} \sigma_0^2(x) + a(x)t + o(t) & \text{if } x \neq 0 \\ y_0 + \left(\kappa(\theta - y_0) - \frac{\sigma^2}{6} \left(1 - \frac{\rho^2}{4} \right) + \frac{\rho\sigma y_0}{2} \right) \frac{t}{2} + o(t) & \text{if } x = 0, \end{cases} \quad (4.5)$$

as the maturity $t \rightarrow 0$, where the following expansions for the functions σ_0 and a hold when x is close to zero,

$$\begin{aligned} \sigma_0(x) &= \sqrt{y_0} \left(1 + \frac{\rho\sigma x}{4y_0} + \frac{1}{24} \left(1 - \frac{5\rho^2}{2} \right) \frac{\sigma^2 x^2}{y_0^2} \right) + \mathcal{O}(x^3) \\ a(x) &= -\frac{\sigma^2}{12} \left(1 - \frac{\rho^2}{4} \right) + \frac{y_0\rho\sigma}{4} + \frac{\kappa}{2}(\theta - y_0) + \frac{\rho\sigma}{24y_0}(\sigma^2\rho^2 - 2\kappa(\theta + y_0) + y_0\rho\sigma)x \\ &\quad + \frac{176\sigma^2 - 480\kappa\theta - 712\rho^2\sigma^2 + 521\rho^4\sigma^2 + 40y_0\rho^3\sigma + 1040\kappa\theta\rho^2 - 80y_0\kappa\rho^2}{7680} \frac{\sigma^2 x^2}{y_0^2} + \mathcal{O}(x^3). \end{aligned}$$

Note that the two functions σ_0 and a are symmetric when the correlation parameter ρ is null. This is consistent with the fact that uncorrelated stochastic volatility models generate symmetric smiles.

4.3 Large-maturity asymptotic behaviour

4.3.1 Large-maturity & Large-strike

The section is based on Forde and Jacquier [23]. The two theorems show the asymptotic behaviour for European call options and the implied volatility in the large-time, large-strike regime.

Theorem 4.3.1. *For the Heston model (3.3) let $\bar{\theta} = \frac{\kappa\theta}{\kappa - \rho\sigma}$ and assume the good correlation regime $\bar{\kappa} = \kappa - \rho\sigma > 0$. Then the large-time behaviour for the price of a call option of strike $S_0 e^{xt}$ on $S_t = e^{X_t}$ is*

$$\begin{aligned} \frac{1}{S_0} \mathbb{E}(S_t - S_0 e^{xt})^+ &= (1 - e^{xt}) \mathbf{1}_{\{x < -\frac{1}{2}\bar{\theta}\}} + \mathbf{1}_{\{-\frac{1}{2}\bar{\theta} < x < \frac{1}{2}\bar{\theta}\}} \\ &\quad + \frac{1}{2} \mathbf{1}_{\{x = \frac{1}{2}\bar{\theta}\}} + (1 - \frac{1}{2} e^{-\frac{1}{2}\bar{\theta}t}) \mathbf{1}_{\{x = -\frac{1}{2}\bar{\theta}\}} \end{aligned} \quad (4.6)$$

as $t \rightarrow \infty$, where

$$V(p) = \frac{\kappa\theta}{\sigma^2} (\kappa - \rho\sigma p - d(-ip)),$$

$$d(k) = \sqrt{(\kappa - \rho\sigma ik)^2 + \sigma^2(ik + k^2)},$$

where $p^*(x) = \frac{\sigma - 2\kappa\rho}{2(1-\rho^2)\sigma} + \frac{\kappa\theta\rho + x\sigma}{2(1-\rho^2)\sigma} \sqrt{\frac{\sigma^2 + 4\kappa^2 - 4\kappa\rho\sigma}{x^2\sigma^2 + 2x\kappa\theta\rho\sigma + \kappa^2\theta^2}}$ and $V^*(x) = p^*(x)x - V(p^*(x))$ is the Legendre transform of V .

Theorem 4.3.2. *Let $\sigma_t(x)$ denote the implied volatility at maturity t for a log-moneyness x . Then the large-time expansion for the large-time, large-strike regime is*

$$\begin{aligned} \sigma_\infty^2(x) &= \lim_{t \rightarrow \infty} \sigma_t^2(x) \\ &= \begin{cases} 2(2V^*(x) - x - 2\sqrt{V^*(x)^2 - V^*(x)x}) & \text{if } x > \frac{1}{2}\bar{\theta} \text{ or } x < -\frac{1}{2}\theta \\ 2(2V^*(x) - x + 2\sqrt{V^*(x)^2 - V^*(x)x}) & \text{if } x \in (-\frac{1}{2}\theta, \frac{1}{2}\bar{\theta}), \end{cases} \end{aligned} \quad (4.7)$$

where V^* is given in theorem 4.3.1.

Note, the next term in the expansion for the implied volatility is calculated in Forde et al. [25].

4.3.2 Large-maturity & Fixed-strike

The section is based on Forde et al. [25]. The following two theorems show the asymptotic behaviour for European call options and the implied volatility in the large-time, fixed-strike regime.

Theorem 4.3.3. *For the Heston model (3.3) for any $x \in \mathbb{R}$, the following asymptotic behaviour for the price of a call option on $S = e^X$ with fixed strike $K = S_0 \exp(x)$*

$$\frac{1}{S_0} \mathbb{E}(S_t - K)^+ = 1 + \frac{A(0)}{\sqrt{2\pi t}} \exp((1 - p^*(0))x - V^*(0)t) (1 + \mathcal{O}(1/t)) \quad (4.8)$$

holds as the maturity $t \rightarrow \infty$, where

$$A(x) = \frac{1}{\sqrt{V''(p^*)}} \begin{cases} \frac{U(p^*(x))}{(p^{*2}(x) - p^*(x))} & \text{if } x \in \mathbb{R} \setminus \{-\frac{1}{2}\theta, \frac{1}{2}\bar{\theta}\} \\ -1 - \operatorname{sgn}(x) \left(\frac{1}{6} \frac{V'''(p^*(x))}{V''(p^*(x))} - U'(p^*(x)) \right) & \text{if } x \in \{-\frac{1}{2}\theta, \frac{1}{2}\bar{\theta}\}, \end{cases}$$

$$V(p) = \frac{\kappa\theta}{\sigma^2} (\kappa - \rho\sigma p - d(-ip)),$$

$$U(p) = \exp\left(\frac{V(p)y_0}{\kappa\theta} + \frac{2\kappa\theta}{\sigma^2} \log(1 - g(-ip))\right),$$

$$g(k) = \frac{\kappa - \rho\sigma ik - d(k)}{\kappa - \rho\sigma ik + d(k)},$$

$$d(k) = \sqrt{(\kappa - \rho\sigma ik)^2 + \sigma^2(ik + k^2)},$$

where $p^*(x) = \frac{\sigma - 2\kappa\rho}{2(1-\rho^2)\sigma} + \frac{\kappa\theta\rho + x\sigma}{2(1-\rho^2)\sigma} \sqrt{\frac{\sigma^2 + 4\kappa^2 - 4\kappa\rho\sigma}{x^2\sigma^2 + 2x\kappa\theta\rho\sigma + \kappa^2\theta^2}}$, $V^*(x) = p^*(x)x - V(p^*(x))$ is the Legendre transform of V and $\operatorname{sgn}(x)$ equals 1 if x is positive and -1 otherwise.

Theorem 4.3.4. *Let $\sigma_t(x)$ denote the implied volatility corresponding to a call option with maturity t and fixed strike $K = S_0 \exp(x)$ in the Heston model. Then the following behaviour for the implied volatility in the fixed-strike case*

$$\sigma_t(x)^2 = 8V^*(0) + a_1(x)/t + \mathcal{O}(1/t) \quad (4.9)$$

holds for all $x \in \mathbb{R}$, as $t \rightarrow \infty$,

where the correction term $a_1 : \mathbb{R} \rightarrow \mathbb{R}$ is defined by

$$a_1(x) := -8 \log\left(-A(0)\sqrt{2V^*(0)}\right) + 4(2p^*(0) - 1)x, \quad \text{for all } x \in \mathbb{R},$$

and where V^* , A and p^* are given in theorem 4.3.3. The error term $|\sigma_t^2(x) - 8V^*(0) - a_1(x)/t|t$ tends to zero as t goes to infinity uniformly on compact subsets of \mathbb{R} .

4.4 Extreme-strike asymptotic behaviour

In this section the main results of Friz et al. [27] will be presented. It is known that Heston's stochastic volatility model exhibits moment explosion, and that the critical moment s_+ can be obtained by solving (numerically) a simple equation. This yields a leading order expansion for the implied volatility at large strikes: $\sigma_{BS}(k, T)^2 T \sim \Psi(s_+ - 1) \times k$ (Roger Lee's moment formula [42]). Friz et al. first derive a novel tail expansion for the Heston density, sharpening previous work of Drăgulescu & Yakovenko [16], and then showed the validity of a refined expansion of the type $\sigma_{BS}(k, T)^2 T = (\beta_1 k^{1/2} + \beta_2 + \dots)^2$, where all the constants are explicitly known as functions of s_+ , the Heston model parameters, spot vol and maturity T . In the case

of the *zero-correlation* Heston model such an expansion was derived by Gulisashvili & Stein [30]. The entire quantitative analysis in Friz et al. is based on affine principles, at no point do they need knowledge of the (explicit, but cumbersome) closed form expression of the Fourier transform of $\log S_T$ (equivalently: Mellin transform of S_T); what matters is that these transforms satisfy ordinary differential equations of Riccati type. Secondly, the analysis of Friz et al. reveals a new parameter (*critical slope*), defined in a model free manner, which drives the second and higher order terms in tail- and implied volatility expansions.

The novel right and left tail expansion for the Heston density and the refined expansion of the implied volatility of Friz et al. [27] will be presented in the following two subsections.

4.4.1 Right Tail Asymptotics

As mentioned above, the Heston model, as many other stochastic volatility models, exhibits *moment explosion* in the sense that

$$T^*(s) = \sup\{t \geq 0 : \mathbb{E}[S_t^s] < \infty\}$$

is finite for s large enough. Differently put, for fixed maturity T there will be a (finite) *critical moment*

$$s_+ := \sup\{s \geq 1 : \mathbb{E}[S_T^s] < \infty\}.$$

Note, in the Heston model, and many other affine stochastic volatility models, T^* is explicitly known. The critical moment, for fixed T , is then found numerically from $T^*(s_+) = T$.

A model free result due to Lee [42] (see moment formula section 4.1) then yields

$$\limsup_{k \rightarrow \infty} \sigma_{BS}(k, T)^2 T = \Psi(s_+ - 1) \times k,$$

where $k = \log(K/S_0)$ denotes the log-strike, σ_{BS} the Black-Scholes implied volatility, and

$$\Psi(x) = 2 - 4(\sqrt{x^2 + x} - x) \in [0, 2].$$

Theorem 4.4.1. *For every fixed $T > 0$, the distribution density D_T of the stock price S_T in a correlated Heston model with $\rho \leq 0$ satisfies the following asymptotic formula:*

$$D_T(x) = A_1 x^{-A_3} e^{A_2 \sqrt{\log x}} (\log x)^{-3/4 + a/c^2} (1 + \mathcal{O}((\log x)^{-1/2})) \quad (4.10)$$

as $x \rightarrow \infty$. The constants A_3 and A_2 are expressed explicitly in terms of critical moments s_+ and critical slope

$$\sigma := - \left. \frac{\partial T^*(s)}{\partial s} \right|_{s=s_+}$$

as

$$A_3 = s_+ + 1 \quad \text{and} \quad A_2 = 2 \frac{\sqrt{2v_0}}{c\sqrt{\sigma}}.$$

For the constant factor A_1 the following explicit expression is obtained:

$$\begin{aligned} A_1 &= \frac{1}{2\sqrt{\pi}} (2v_0)^{1/4 - a/c^2} c^{2a/c^2} \sigma^{-a/c^2 - 1/4} \\ &\times \exp \left(-v_0 \left(\frac{b + s_+ \rho c}{c^2} + \frac{\kappa}{c^2 \sigma^2} \right) - \frac{aT}{c^2} (b + c\rho s_+) \right) \\ &\times \left(\frac{2\sqrt{b^2 + 2bc\rho s_+ + c^2 s_+ (1 - (1 - \rho^2) s_+)}}{c^2 s_+ (s_+ - 1) \sinh T \frac{1}{2} \sqrt{b^2 + 2bc\rho s_+ + c^2 s_+ (1 - (1 - \rho^2) s_+)}} \right)^{2a/c^2}. \end{aligned}$$

Theorem 4.4.2. *Under the assumptions of Theorem 4.4.1, the Black-Scholes implied volatility admits the expansion*

$$\sigma_{BS}(k, T)^2 T = \left(\beta_1 k^{1/2} + \beta_2 + \beta_3 \frac{\log k}{k^{1/2}} + \mathcal{O} \left(\frac{1}{k^{1/2}} \right) \right)^2 \quad (4.11)$$

as $k \rightarrow \infty$, where

$$\begin{aligned} \beta_1 &= \sqrt{2} \left(\sqrt{A_3 - 1} - \sqrt{A_3 - 2} \right), \\ \beta_2 &= \frac{A_2}{\sqrt{2}} \left(\frac{1}{\sqrt{A_3 - 2}} - \frac{1}{\sqrt{A_3 - 1}} \right), \\ \beta_3 &= \frac{1}{\sqrt{2}} \left(\frac{1}{4} - \frac{a}{c^2} \right) \left(\frac{1}{\sqrt{A_3 - 1}} - \frac{1}{\sqrt{A_3 - 2}} \right). \end{aligned}$$

4.4.2 Left Tail Asymptotics

First the behaviour of the Heston density $D_T(x)$ near zero will be discussed. The lower critical moment is defined by

$$s_- := \inf \{ s \leq 0 : \mathbb{E}[S_T^s] < \infty \}$$

and the corresponding slope and curvature by

$$\sigma_- := \partial_s T^*|_{s_-} \geq 0 \quad \text{and} \quad \kappa_- := \partial_s^2 T^*|_{s_-}.$$

Theorem 4.4.3. *For every fixed $T > 0$, the distribution density D_T of the stock price S_T in a correlated Heston model with $\rho \leq 0$ satisfies the following asymptotic formula:*

$$D_T(x) = B_1 x^{B_3} e^{B_2 \sqrt{-\log x}} (-\log x)^{a/c^2 - 3/4} (1 + \mathcal{O}((-\log x)^{-1/2})) \quad (4.12)$$

as $x \downarrow 0$, where

$$\begin{aligned} B_3 &= -(s_- + 1), \quad B_2 = \frac{2\sqrt{2v_0}}{c\sqrt{\sigma_-}} \\ B_1 &= \frac{1}{2\sqrt{\pi}} (2v_0)^{1/4 - a/c^2} c^{2a/c^2 - 1/2} \sigma_-^{-a/c^2 - 1/4} \\ &\quad \times \exp\left(-v_0 \left(\frac{b + s_- \rho c}{c^2} + \frac{\kappa_-}{c^2 \sigma_-^2}\right) - \frac{aT}{c^2} (b + c\rho s_-)\right) \\ &\quad \times \left(\frac{2\sqrt{b^2 + 2bc\rho s_- + c^2 s_- (1 - (1 - \rho^2)s_-)}}{c^2 s_- (s_- - 1) \sinh \frac{1}{2} \sqrt{b^2 + 2bc\rho s_- + c^2 s_- (1 - (1 - \rho^2)s_-)}}\right)^{2a/c^2}. \end{aligned}$$

Theorem 4.4.4. *Under the assumptions of this section, the Black-Scholes implied volatility admits the expansion*

$$\sigma_{BS}(k, T) \sqrt{T} = \rho_1 (-k)^{1/2} + \rho_2 + \rho_3 \frac{\log(-k)}{(-k)^{1/2}} + \mathcal{O}\left(\frac{\varphi(-k)}{(-k)^{1/2}}\right) \quad (4.13)$$

as $k \rightarrow -\infty$. The constants are given by

$$\begin{aligned} \rho_1 &= \sqrt{2} \left(\sqrt{B_3 + 2} - \sqrt{B_3 + 1} \right), \\ \rho_2 &= \frac{B_2}{\sqrt{2}} \left(\frac{1}{\sqrt{B_3 + 1}} - \frac{1}{\sqrt{B_3 + 2}} \right), \\ \rho_3 &= \frac{1}{\sqrt{2}} \left(\frac{1}{4} - \frac{a}{c^2} \right) \left(\frac{1}{\sqrt{B_3 + 2}} - \frac{1}{\sqrt{B_3 + 1}} \right). \end{aligned}$$

Chapter 5

Fast Calibration

In this chapter some of the asymptotic formulas from chapter 4 will be applied to market data and proofed for their accuracy. As mentioned before, the asymptotic formulas can be applied to receive a pertaining initial point. The calculation will only take a few seconds on a standard computer and these initial points can later be used as a starting point to calibrate the whole Heston model (3.11), e.g. with a least-square method. This approach improves the calibration efficiency.

First, the market data used for the empirical research will be described, second the results of the estimation procedures will be analyzed. This chapter is based on [61] and [41].

5.1 Option Data

5.1.1 Austrian-Traded-Index

The Austrian-Traded-Index (ATX) is the most important stock market index of the Wiener Börse and the largest trading place in the Austrian economy. The ATX is, like most European indices, defined as a price index and it contains the 20 largest and most actively-traded stocks on the exchange. The index is reviewed twice a year, and as many as three companies might be removed and replaced. Large companies listed on the ATX are for example the Erste Group, OMV, Voestalpine, Telekom Austria and Andritz, which combined amount about 60% of the index.

5.1.2 Data Description

For the empirical investigation in the next chapter, data on European ATX options from March 10, 2011 to May 9, 2011 was used. This comprises a sample of 576 daily collected data.

The data contains information on the mid price, strike price, underlying price, maturity and the corresponding 3-M EURIBOR rate.

	Call		Put	
	\bar{x}	s	\bar{x}	s
deep ITM	241.85	48.06	274.73	41.19
ITM	137.48	18.25	190.72	28.88
ATM	94.07	30.22	123.65	30.11
ATM	57.62	27.58	78.83	33.23
OTM	31.07	19.47	45.87	25.89
deep OTM	19.83	13.87	14.56	13.21

Table 5.1: Average mid prices \bar{x} and standard deviation s per moneyness.

The option data was categorized into moneyness groups, according to the definition in section 2.2.2. The data consists of 19.2% ITM, 35.2% ATM and 45.6% OTM options. In table 5.1 the average mid price and its standard deviation per moneyness group are displayed. The average call option prices vary between 19.83 and 241.85, whereas the put options vary between 14.56 and 274.72.

	Call		Put	
	\bar{x}	s	\bar{x}	s
deep ITM	0.17	0.03	0.26	0.03
ITM	0.17	0.02	0.28	0.04
ATM	0.16	0.04	0.25	0.02
ATM	0.17	0.02	0.25	0.02
OTM	0.18	0.02	0.24	0.18
deep OTM	0.21	0.03	0.23	0.18

Table 5.2: Average implied volatility \bar{x} and standard deviation s per moneyness.

Table 5.2 shows the implied volatility calculated with the Black-Scholes model from the market data per moneyness group. The implied volatility was calculated for each option and then the average per moneyness group was calculated. One can recognize that the ATM option data displays a volatility smile as described in section 2.5.3, and therefore points out the necessity of an option pricing model with stochastic volatility, capable of taking this effect into account.

5.2 Estimation Procedure

As mentioned in chapter 4, calibration of the Heston model is very sensitive to the choice of the initial point. The various explicit formulas come into play to receive a pertaining initial

point. Therefore, calibration efficiency can be improved and carried out on a standard computer in a few seconds. Estimates for the volatility parameter v_0 with the structural parameters $\{\kappa, \theta, \sigma, \rho\}$ will be needed.

Since closed-form solutions are available for the Black-Scholes implied volatility from the asymptotic formulas, a natural candidate for the estimation of the initial parameters is a non-linear least squares procedure involving minimization of the sum of squared errors between the model implied volatility and the market implied volatility.

Let $\sigma_i(t, S_t, K)$ denote the market implied volatility of option i on day t , and let $\sigma_i^*(t, S_t, K)$ denote the model implied volatility of the option i on day t . To estimate the parameters, the sum of squared percentage errors between model and market implied volatilities will be minimized:

$$\min_{\Phi_t} \sum_{i=1}^N \left[\frac{\sigma_i(t, S_t, K) - \sigma_i^*(t, S_t, K)}{\sigma_i(t, S_t, K)} \right]^2, \quad t = 1, \dots, T; \quad (5.1)$$

where N denotes the number of options on day t , and T denotes the number of days in the sample. For the calculation MATLAB function `lsqnonlin` was used. The function `lsqnonlin(fun,x0,lb,ub)` starts at the point x_0 and finds a minimum of the sum of squares of the functions described in `fun`. In `lb` and `ub` a vector of lower and upper bounds is defined, so that the solution x is always in the range $lb \leq x \leq ub$, which means that Heston's calibrated initial parameters will be between `lb` and `ub`.

The market implied volatility $\sigma_i(t, S_t, K)$ from the data described in section 5.1 was calculated using `blsimpv` from the Financial Toolbox of MATLAB. The function returns the implied volatility values for the given parameters: underlying price S , strike K , risk-free rate of return r , time-to-maturity $T - t$ and the observed option price.

Since the results for the estimation, might again depend on the choice of the starting point x_0 , five different sets of reasonable parameters have been used, see table 5.3. With each of these parameters five suitable options for the prevailing asymptotic formula were calibrated, meaning an equation with five unknown was solved. In section 5.3.1 the results of calibrating with different starting values will be discussed in greater detail for the short-maturity formula.

	κ	θ	σ	ρ	v_0
Starting point A	6.5482	0.0731	2.3012	-0.4176	0.1838
Starting point B	1.1500	0.0400	0.2000	-0.4000	0.0400
Starting point C	3.0000	0.0500	0.5000	-0.5000	0.1500
Starting point D	1.3784	0.2319	1.0359	-0.2051	0.0231
Starting point E	0.6067	0.0707	0.2928	-0.7571	0.0654

The parameters B, C and E were taken from [24], [51] and [54] respectively, the parameters A and D are from [47].

Table 5.3: Starting points for calibration of five options

5.3 Empirical Findings

In this section the results of the empirical research will be presented. In section 5.3.1 the small-time regime will be examined in greater detail, before in section 5.3.2 the results of the various implied volatility asymptotics will be presented. For the calibration only European call options from the sample data described in 5.1 were used, the MATLAB code for the various calibrations can be found in appendix B.

With the parameter sets received from the calibration procedures, option price, with Heston's semi-closed form solution (3.11), and Black-Scholes implied volatility were calculated. The results are displayed as volatility surfaces and smiles, and in addition the empirical performance was analyzed using four measures for the option prices:

- MAE: Mean absolute errors

$$MAE = \frac{1}{N} \sum_{n=1}^N (|O_n - O_n^*|)$$

- MPE: Mean percentage errors

$$MPE = \frac{1}{N} \sum_{n=1}^N \frac{(O_n - O_n^*)}{O_n}$$

- MAPE: Mean absolute percentage errors

$$MAPE = \frac{1}{N} \sum_{n=1}^N \frac{(|O_n - O_n^*|)}{O_n}$$

- MSE: Mean squared errors

$$MSE = \frac{1}{N} \sum_{n=1}^N (O_n - O_n^*)^2,$$

where O_n is the mid price of the option n and O_n^* is the option price calculated with the Heston model (3.11). MAEs and MAPEs measure the magnitude of pricing errors, while MPEs indicate the direction of the pricing errors. MSEs measure the volatility of errors.

5.3.1 Short-maturity

For the calibration, the closed form for the small-time implied volatility (4.5) without the error term, was used. The data was also calibrated using only the leading order term of the small-time implied volatility formula. Furthermore, parameter results were also used as actual initial parameters for a calibration with the Heston model. Heston's semi-closed form solution (3.11) for option prices was used for this calibration.

First, attention will be drawn to the choice of the starting values. The parameter sets in table 5.3 were used for calibrating five options only, to receive a reasonable starting point for the calibration. Sets A, C and D lead to the same result, starting point IP1, and the initial parameter set IP2 is the result of using set B or E (see table 5.4). To receive more starting points, this procedure was done three times, using a different option mix every time. In total four parameters which differ significantly were received from the calculations, and are displayed in table 5.4. Note, that κ and σ differ more often than the other parameters.

	κ	θ	σ	ρ	v_0
Starting point IP1	0.2542	0.9998	0.8096	-0.0000	0.0119
Starting point IP2	19.9992	0.0271	0.9599	-0.7567	0.0125
Starting point IP3	0.0909	0.9714	0.6773	-0.0000	0.0228
Starting point IP4	2.7262	0.1711	0.0001	-0.5419	0.0000

The parameter sets were calculated by calibrating five call options, using the starting points from table 5.3.

Table 5.4: Initial Parameters for the small-time calibration

The initial points in table 5.4 were finally used to calibrate the sample data with the small-time formula (4.5). The parameter results are displayed in table 5.5. Note, that calibration with the initial parameter sets IP1 and IP3, yielded the same result S1. One can also see some similarities between the three results, e.g. v_0 is almost the same for all of them.

	κ	θ	σ	ρ	v_0
Small-time result S1	0.2372	1.0000	0.7064	-0.0000	0.0099
Small-time result S2	19.9990	0.0178	0.0079	-1.0000	0.0005
Small-time result S3	2.5131	0.1393	0.0051	-0.9864	0.0003

The parameter sets were calculated by calibrating all call options from the sample data with the formula for the small-time implied volatility (4.5).

Table 5.5: Parameter results from small-time calibration

Figure 5.1 shows the average implied volatility per moneyness group calculated for the three results and the market implied volatility. The error measures for the Heston option prices are

displayed in table 5.6 and plotted in figures 5.7 to 5.10. Note, that the result S2 is not as good as the other results.

Using only the leading order term from the small-time regime for the calibration with the initial parameters IP1 and IP3 (which yielded both the small-time result S1 before), a result quite similar to S1 and one differing were received. The implied volatilities are shown in figure 5.2 and in table 5.6 one can see that the differing result (lead-term 2) is not as accurate but still quite good.

The small-time results (S1-S3) were also used as actual initial parameters for the calibration with the Heston model (3.11). From the initial sets S1 and S2 a similar result was received, in figure 5.3 the implied volatilities are plotted. It is interesting to note, that S2 was a poor quality small-time result, but still serves as a very good initial parameter for the Heston calibration. In figure 5.4 the third small-time result S3 is plotted with its corresponding Heston calibration result.

In figure 5.5 the implied volatility for the corresponding (using same initial point) small-time, small-time leading order term and Heston calibration result is shown. Their error measures are plotted in figures 5.11 to 5.14. The same comparison was also calculated in a smaller time interval, using only call options with maturities ranging from 0.08 to 0.16 years from the sample. See figure 5.6 and for the error measures see table 5.7 and figures 5.15 to 5.18.

Furthermore the volatility surfaces for the call options from the sample data have been plotted for the underlying prices 2700, 2900 and 3100. Figures 5.19 to 5.21 display the market volatility surfaces and in figures 5.22 to 5.24 the volatility surface produced by small-time calibration result S1 is plotted. The good fit of the surface produced by the Heston model to the one generated by the market is obvious.

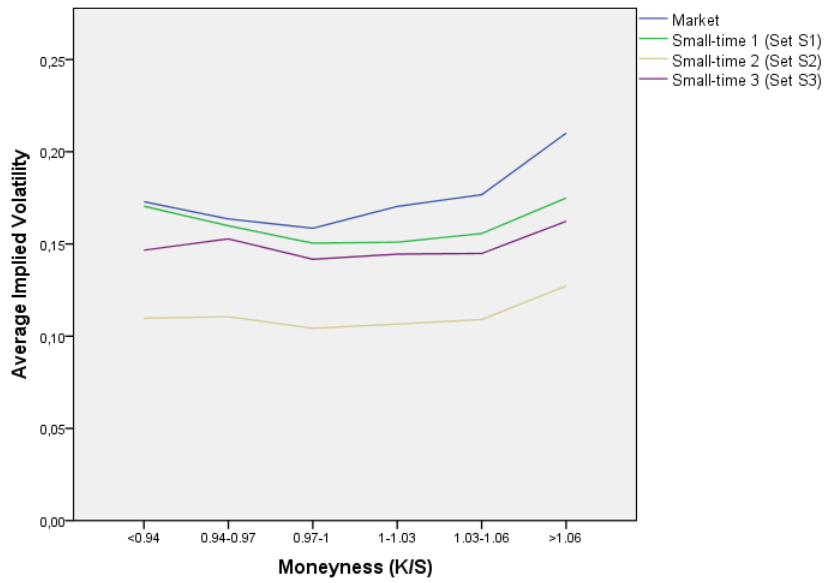


Figure 5.1: Implied volatility of small-time calibration result per moneyness group

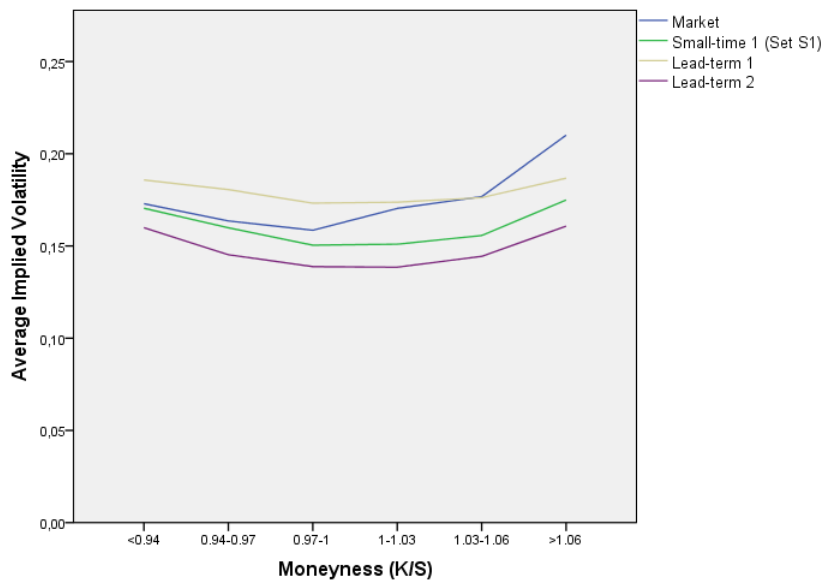


Figure 5.2: Implied volatility of small-time and small-time leading order term calibration result per moneyness group

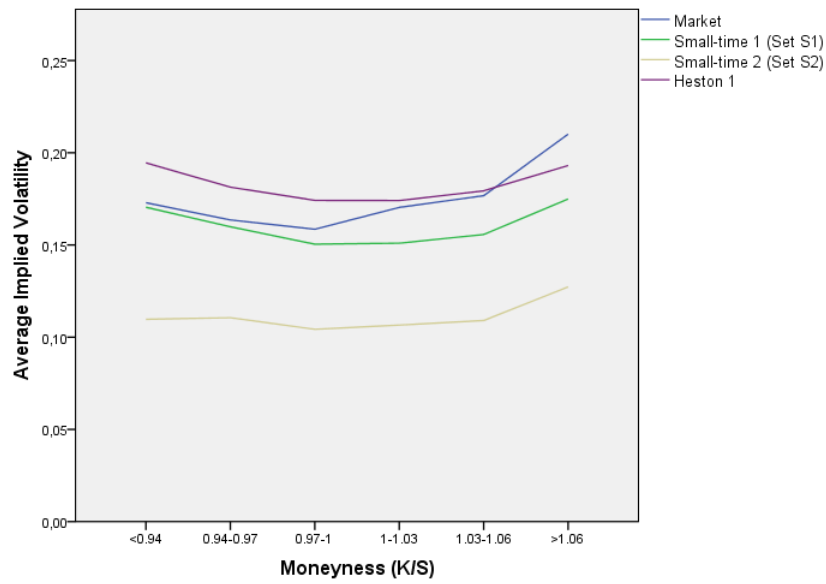


Figure 5.3: Implied volatility of small-time calibration and corresponding Heston model calibration result per moneyness group

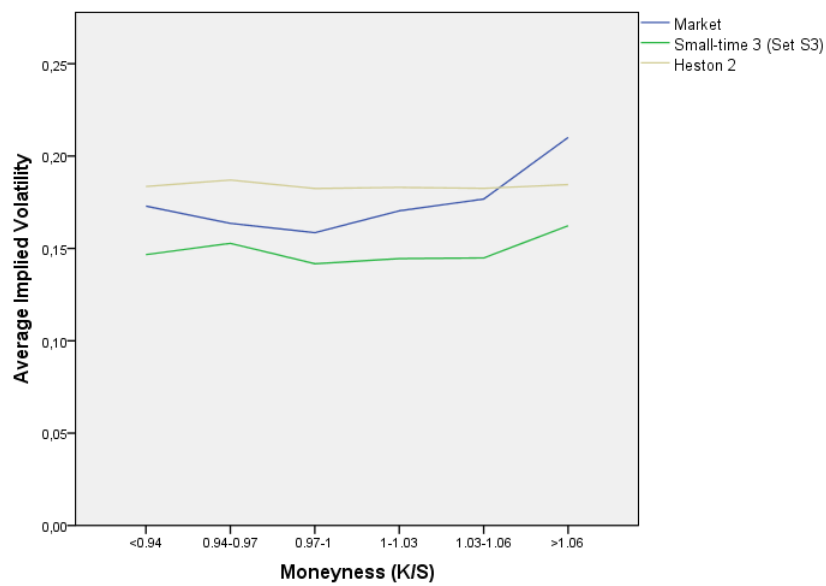


Figure 5.4: Implied volatility of small-time calibration and corresponding Heston model calibration result per moneyness group

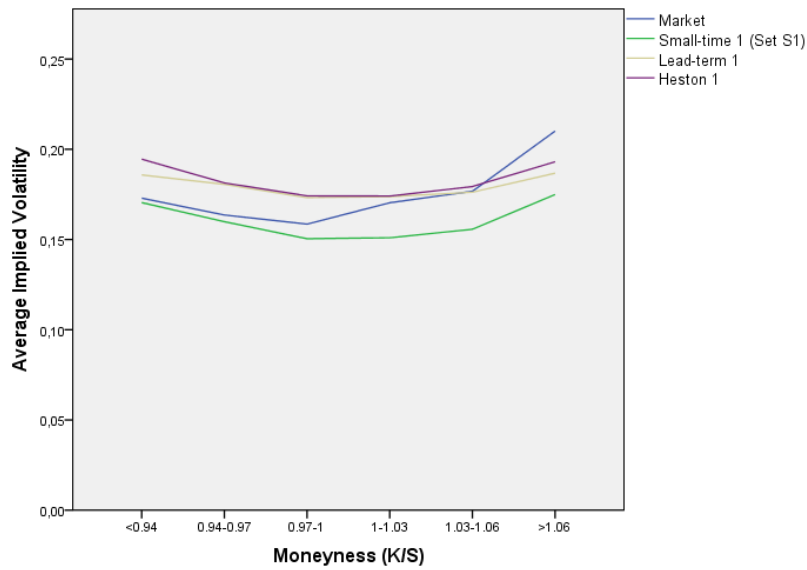


Figure 5.5: Implied volatility of both small-time calibration and corresponding Heston model calibration results per moneyness group

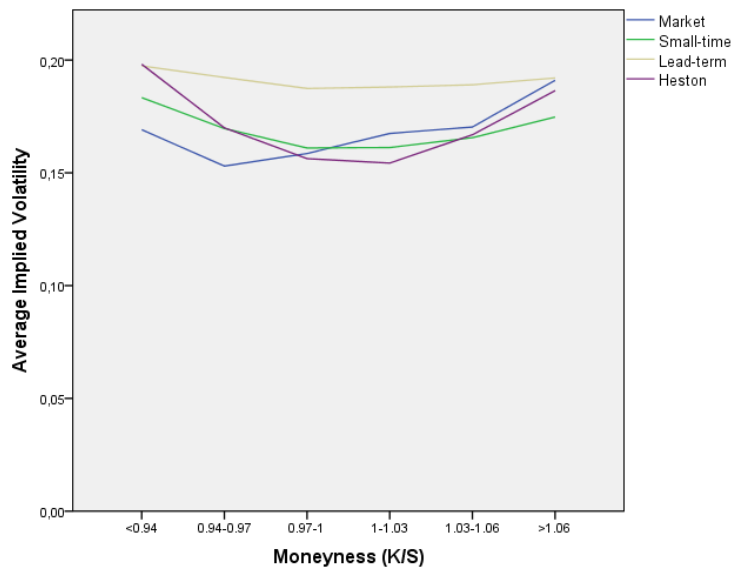


Figure 5.6: Implied volatility of both small-time calibration and corresponding Heston model calibration results per moneyness group, on sample data with maturities ranging from 0.08 to 0.16 years

Parameter	< 0.94	0.94-0.97	0.97-1.00	1.00-1.03	1.03-1.06	> 1.06	all
MAPE							
Small-time 1	0,0130	0,0310	0,0721	0,1497	0,2548	0,5104	0,2339
Small-time 2	0,0304	0,1176	0,2286	0,4821	0,7103	1,0367	0,5599
Small-time 3	0,0175	0,0340	0,0850	0,2260	0,4003	0,7411	0,3420
Lead-term 1	0,0131	0,0412	0,0691	0,0741	0,1058	0,3652	0,1533
Lead-term 2	0,0145	0,0606	0,1306	0,2213	0,3534	0,6053	0,3038
Heston 1	0,0154	0,0420	0,0799	0,1002	0,1309	0,3233	0,1525
Heston 2	0,0128	0,0539	0,0989	0,1230	0,1338	0,3941	0,1816
MPE							
Small-time 1	0,0043	0,0130	0,0422	0,1491	0,2548	0,3542	0,1814
Small-time 2	0,0304	0,1176	0,2259	0,4821	0,7103	0,5744	0,4263
Small-time 3	0,0155	0,0272	0,0752	0,2237	0,4003	0,3587	0,2290
Lead-term 1	-0,0073	-0,0364	-0,0530	-0,0359	0,0091	0,2608	0,0571
Lead-term 2	0,0116	0,0477	0,0897	0,2195	0,3534	0,5381	0,2759
Heston 1	-0,0130	-0,0373	-0,0567	-0,0601	-0,0707	0,1749	0,0132
Heston 2	-0,0069	-0,0523	-0,0923	-0,1190	-0,0794	0,2996	0,0299
MAE							
Small-time 1	3,0352	4,3070	6,7698	7,8120	6,2351	8,1014	6,6594
Small-time 2	7,0507	17,1938	22,4146	26,1285	20,9390	17,9041	19,5492
Small-time 3	4,0793	4,8398	7,1788	9,2847	8,0585	10,2964	8,0952
Lead-term 1	3,0655	5,6748	5,7490	3,4967	2,6454	5,8746	4,5652
Lead-term 2	3,3517	8,7823	13,1034	14,2441	11,4081	11,6858	11,2520
Heston 1	3,6630	5,6981	6,0345	3,5607	2,3525	5,5100	4,5317
Heston 2	2,9412	7,3971	7,8981	5,0336	3,2946	6,2944	5,5825
MSE							
Small-time 1	13,8975	29,8179	66,9096	80,1911	54,2565	119,1938	73,6250
Small-time 2	75,7073	378,8642	655,9842	797,7803	564,9768	465,8773	529,0791
Small-time 3	27,5576	37,8273	74,4067	103,5135	81,5246	168,9674	100,2579
Lead-term 1	16,0628	46,1124	49,6464	18,4064	13,7641	69,3591	39,7388
Lead-term 2	22,3553	104,3434	236,8109	280,2884	185,4299	215,9750	196,7194
Heston 1	22,6885	49,8070	56,1585	18,5756	10,9324	62,1077	39,2770
Heston 2	16,2853	72,9171	82,0007	36,1295	17,7745	75,4797	53,3016

Table 5.6: Pricing errors per moneyness group from calibrating whole sample data with both small-time formulas and Heston's formula

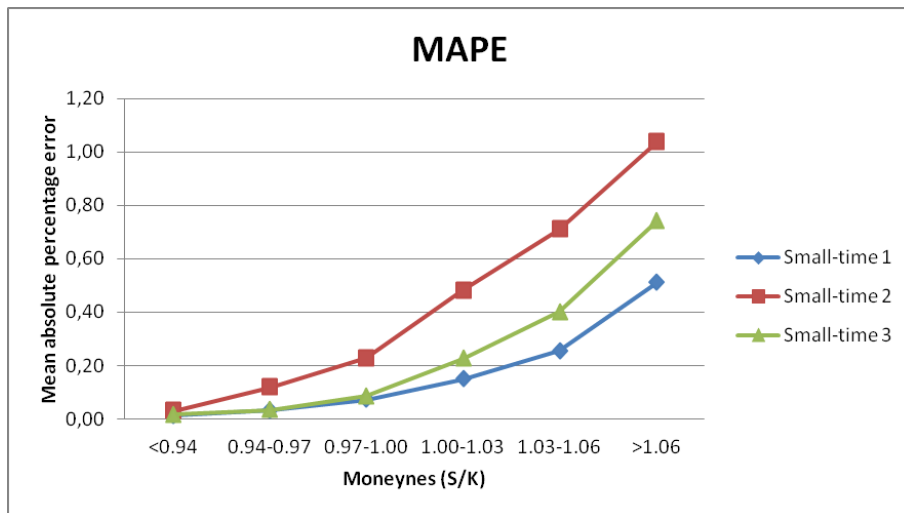


Figure 5.7: MAPE error per moneyes group from calibrating whole sample data with small-time formula and different initial parameters

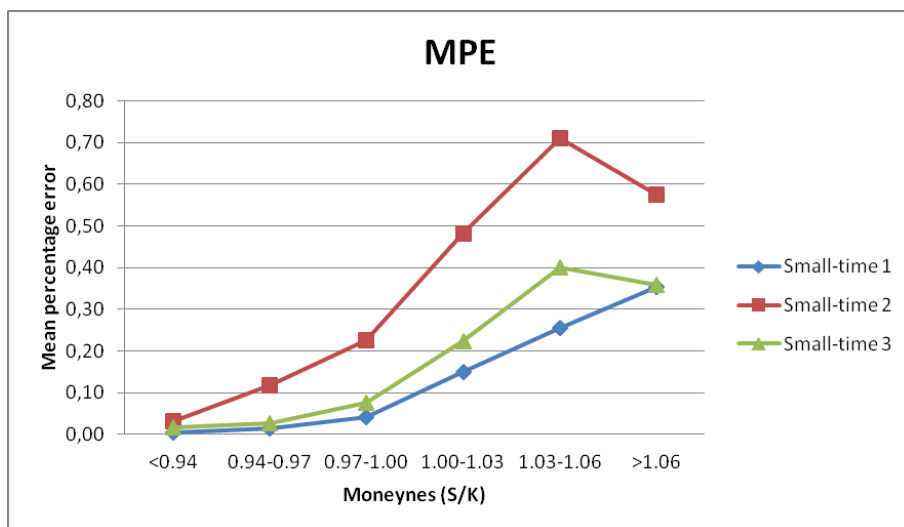


Figure 5.8: MPE error per moneyes group from calibrating whole sample data with small-time formula and different initial parameters

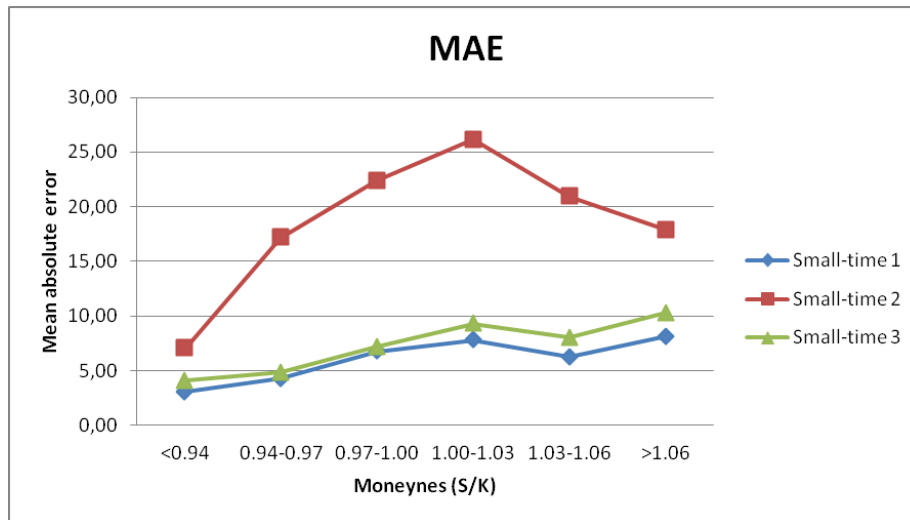


Figure 5.9: MAE error per moneyness group from calibrating whole sample data with small-time formula and different initial parameters

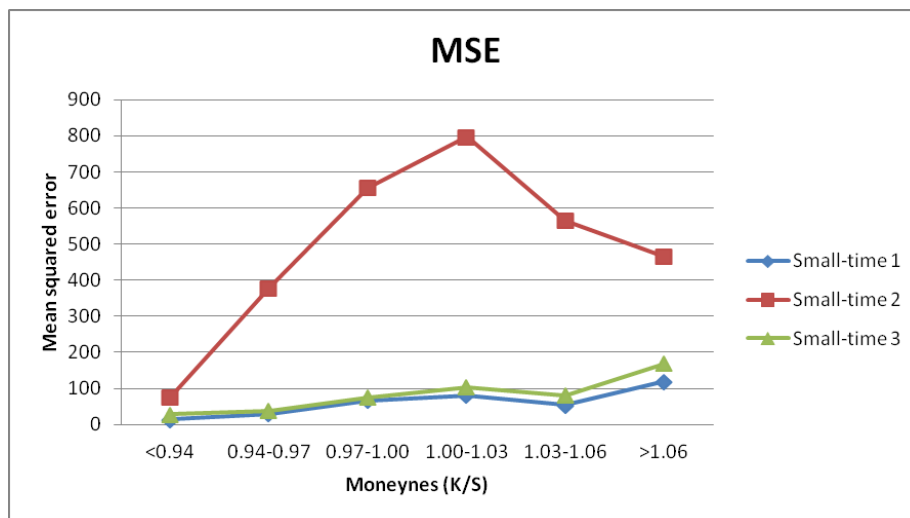


Figure 5.10: MSE error per moneyness group from calibrating whole sample data with small-time formula and different initial parameters

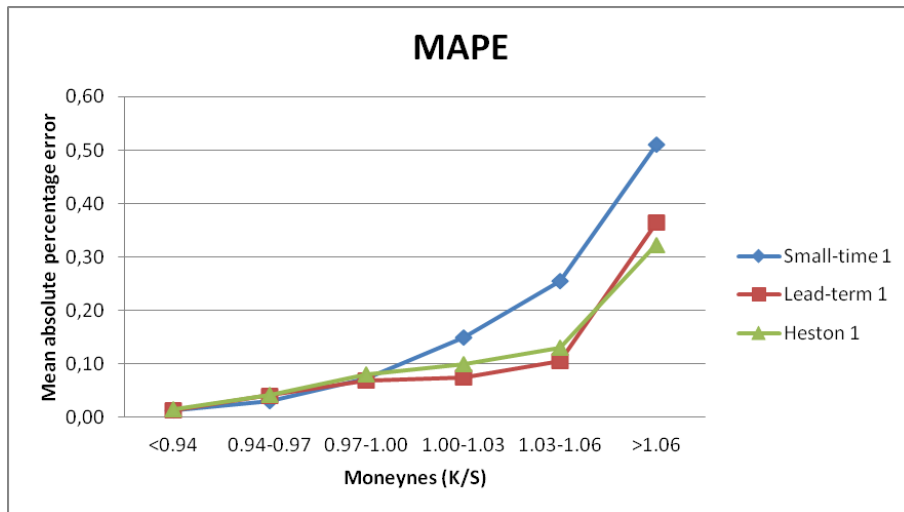


Figure 5.11: MAPE error per moneyness group from calibrating whole sample data with small-time and Heston formula

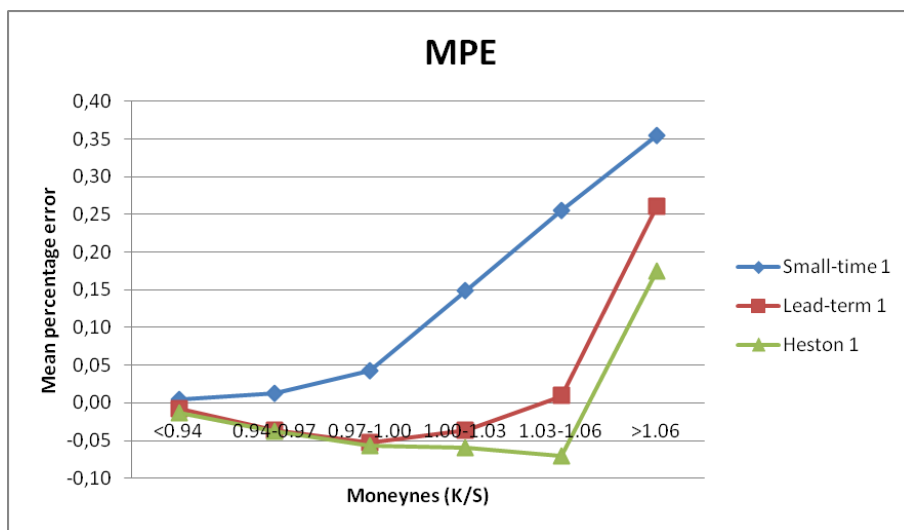


Figure 5.12: MPE error per moneyness group from calibrating whole sample data with small-time and Heston formula

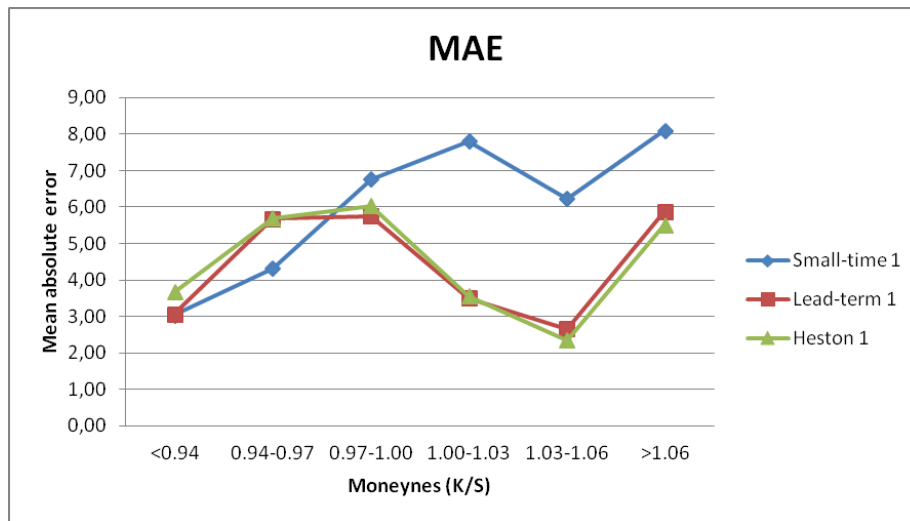


Figure 5.13: MAE error per moneyness group from calibrating whole sample data with small-time and Heston formula

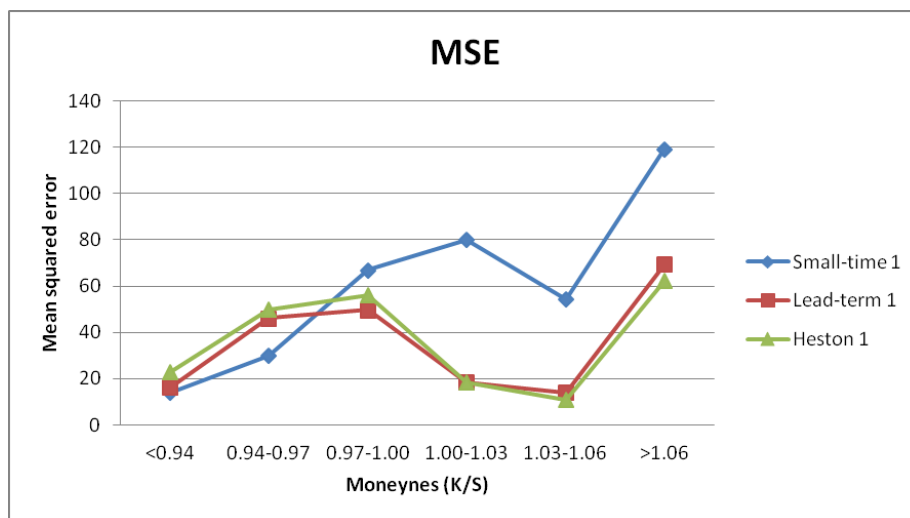


Figure 5.14: MSE error per moneyness group from calibrating whole sample data with small-time and Heston formula

Parameter	< 0.94	0.94-0.97	0.97-1.00	1.00-1.03	1.03-1.06	> 1.06	all
MAPE							
Small-time	0,0133	0,0398	0,0471	0,0616	0,0817	0,2920	0,0996
Lead-term	0,0202	0,0907	0,1247	0,1690	0,2774	0,3428	0,1795
Heston	0,0185	0,0414	0,0508	0,0909	0,0939	0,2228	0,0938
MPE							
Small-time	-0,0082	-0,0339	-0,0119	0,0376	0,0497	0,2290	0,0558
Lead-term	-0,0197	-0,0907	-0,1204	-0,1690	-0,2774	-0,0613	-0,1196
Heston	-0,0173	-0,0338	0,0100	0,0878	0,0219	0,0343	0,0201
MAE							
Small-time	3,1227	5,1355	4,2386	3,4071	1,9960	3,4811	3,4543
Lead-term	4,7017	11,9031	10,5193	7,6636	5,7426	4,2392	6,9473
Heston	4,4934	5,3597	4,6686	5,2586	2,1911	3,1239	4,0850
MSE							
Small-time	15,7962	38,3928	26,4827	16,1072	5,8521	22,4978	19,7854
Lead-term	37,2766	157,3386	127,8992	67,0734	36,1165	23,6136	66,1028
Heston	30,0256	42,1045	29,4617	38,8700	7,0630	14,8043	25,9548

Table 5.7: Pricing errors per moneyness group from calibrating with both small-time formulas and Heston's formula, using sample data with maturities ranging from 0.08 to 0.16 years

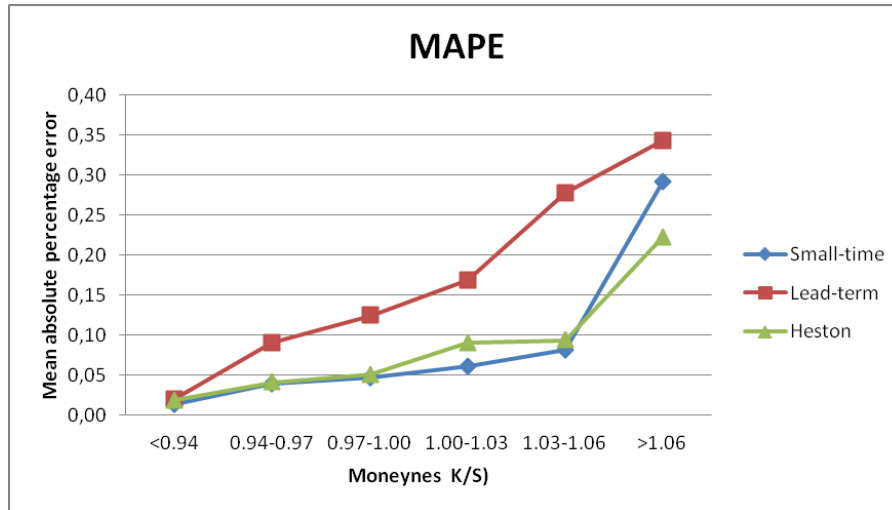


Figure 5.15: MAPE error per moneyness group from calibrating with small-time and Heston formula, using sample data with maturities ranging from 0.8 to 0.16 years

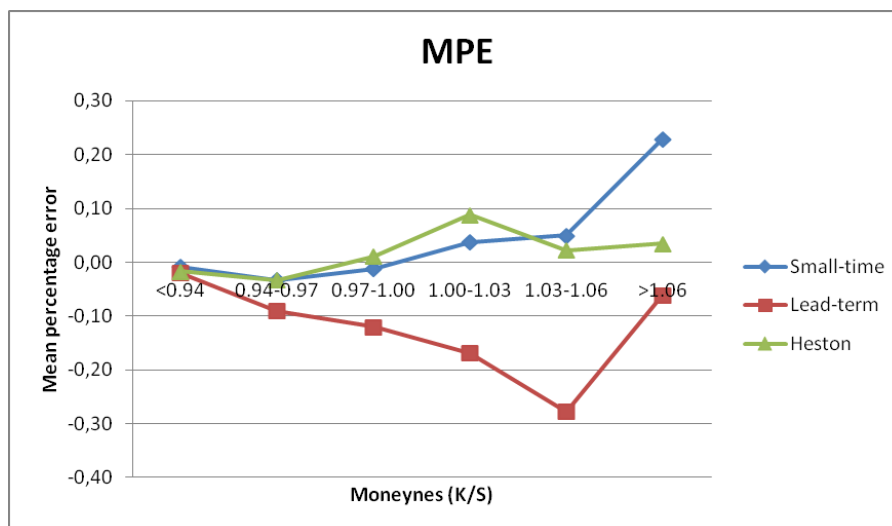


Figure 5.16: MPE error per moneyness group from calibrating with small-time and Heston formula, using sample data with maturities ranging from 0.8 to 0.16 years

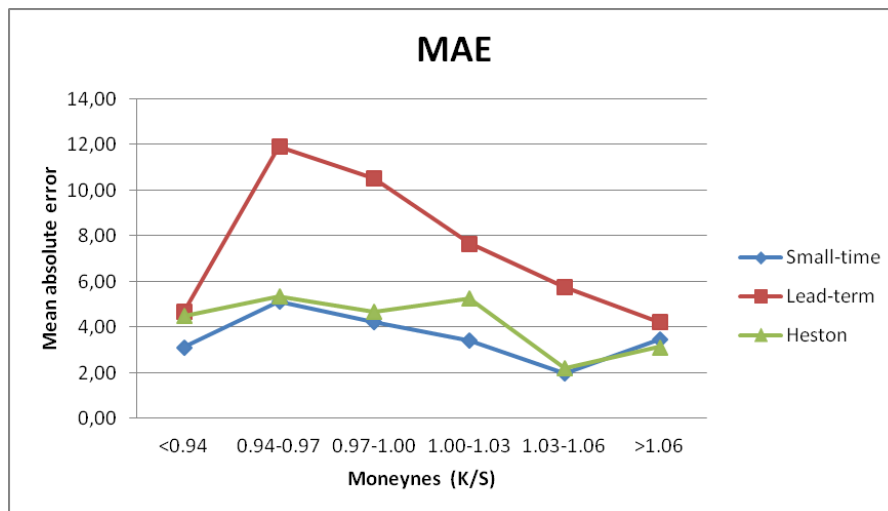


Figure 5.17: MAE error per moneyness group from calibrating with small-time and Heston formula, using sample data with maturities ranging from 0.8 to 0.16 years

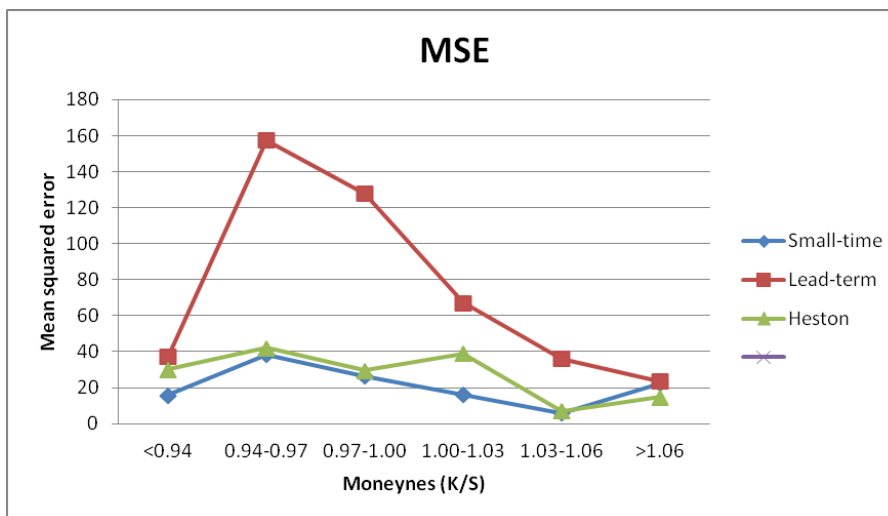


Figure 5.18: MSE error per moneyness group from calibrating with small-time and Heston formula, using sample data with maturities ranging from 0.8 to 0.16 years

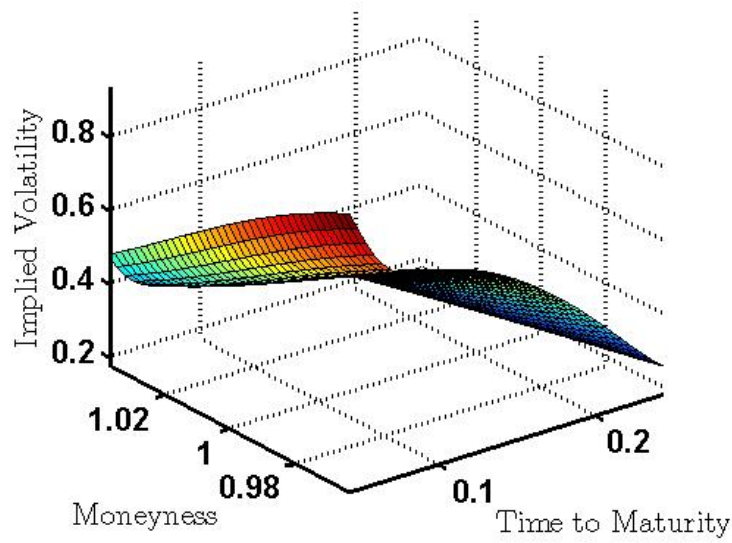


Figure 5.19: Implied volatility surface of call option **market data** for the underlying price 2700

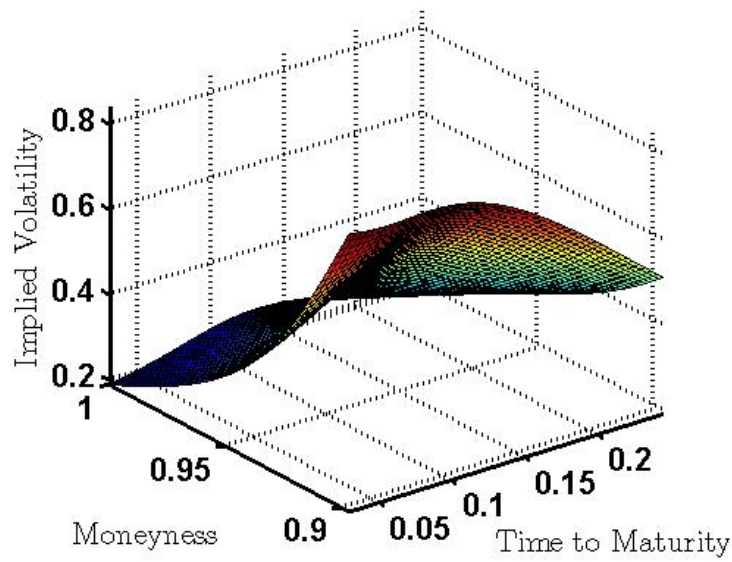


Figure 5.20: Implied volatility surface of call option **market data** for the underlying price 2900

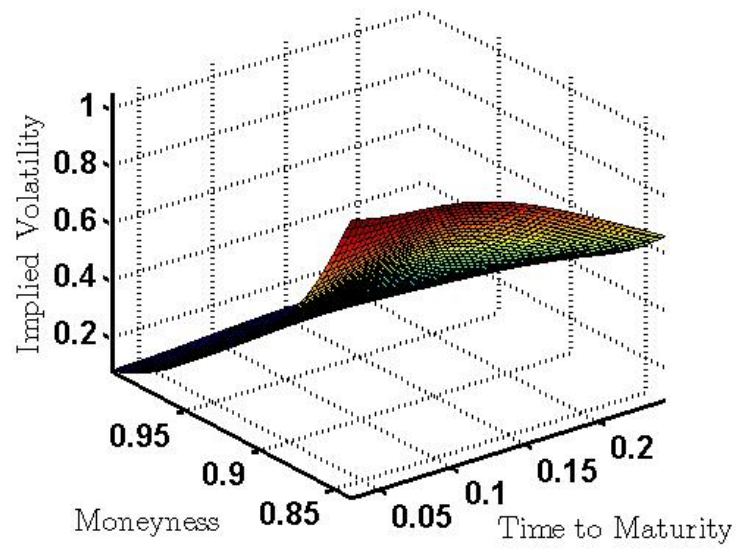


Figure 5.21: Implied volatility surface of call option **market data** for the underlying price 3100

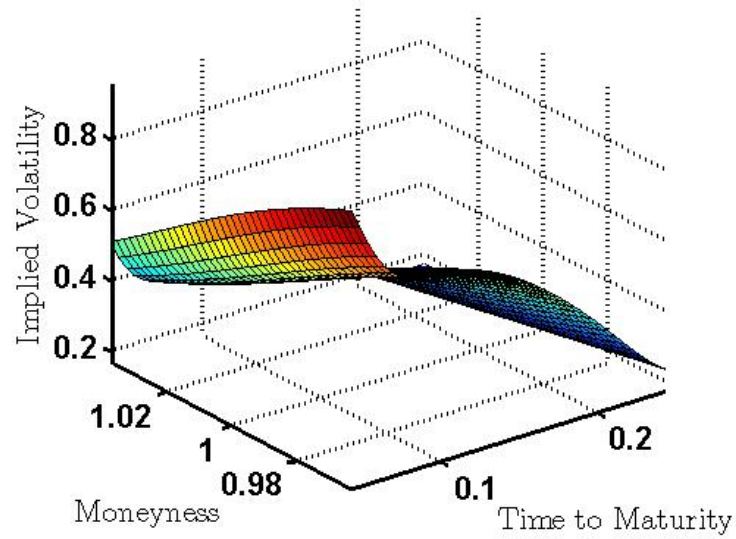


Figure 5.22: Implied volatility surface of **small-time calibration** result for call options with underlying price 2700

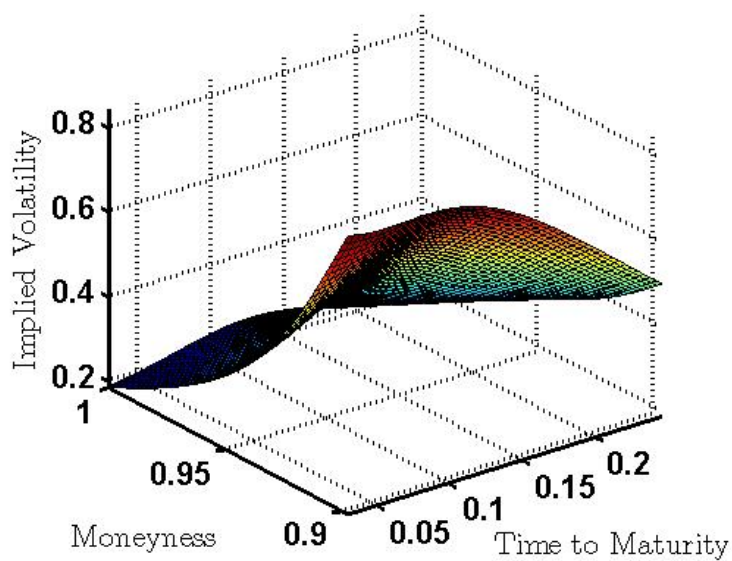


Figure 5.23: Implied volatility surface of **small-time calibration** result for call options with underlying price 2900

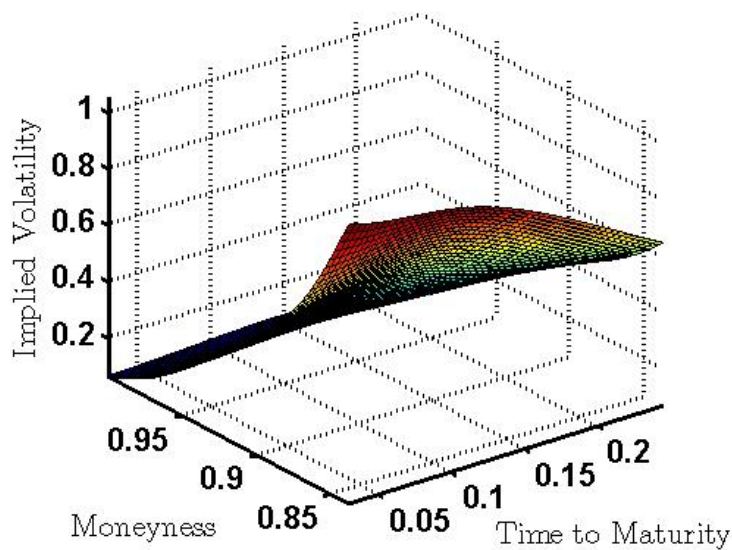


Figure 5.24: Implied volatility surface of **small-time calibration** result for call options with underlying price 3100

5.3.2 All Asymptotic Formulas

In this section the calibration results from the various implied volatility approximations from chapter 4 will be presented. For the small-time regime formula 4.5, for the large-time & large-strike regime formula 4.7, for the small-strike regime formula 4.11 and for the large-strike regime formula 4.13 were used without the error term.

Analogous to the previous section, the whole sample data of call options was calibrated at once. First, all call options (meaning all maturities) were calibrated and then only the call options with maturities ranging from 0.8 to 0.16 years were calibrated. The implied volatilities (figures 5.25 and 5.30) and the error measures (tables 5.8 and 5.9, figures 5.26 to 5.29 and 5.31 to 5.34) are displayed for the results from calibrating with the four different implied volatility approximations.

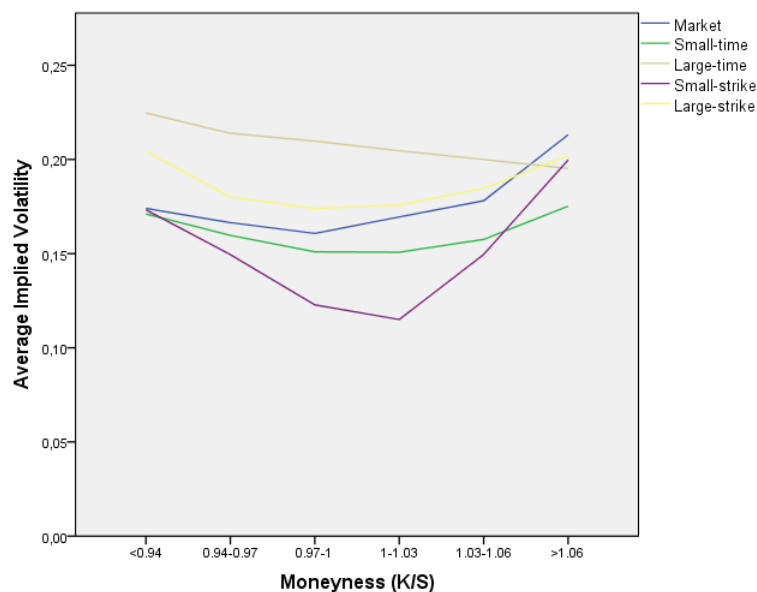


Figure 5.25: Implied volatility of various asymptotic formula calibration results per moneyness group, using whole sample data

Parameter	< 0.94	0.94-0.97	0.97-1.00	1.00-1.03	1.03-1.06	> 1.06	all
MAPE							
Small-time	0,0128	0,0321	0,0721	0,1497	0,2548	0,5104	0,2339
Large-time	0,0388	0,1247	0,2129	0,3593	0,4385	0,3641	0,2960
Small-strike	0,0137	0,0622	0,1915	0,4427	0,5868	1,0068	0,5101
Large-strike	0,0206	0,0524	0,1402	0,2480	0,3480	0,3139	0,2252
MPE							
Small-time	0,0044	0,0133	0,0422	0,1491	0,2548	0,3542	0,1814
Large-time	-0,0388	-0,1247	-0,2127	-0,3593	-0,4337	0,1280	-0,1534
Small-strike	0,0065	0,0385	0,1344	0,3703	0,1048	-0,3334	0,0173
Large-strike	-0,0196	-0,0371	-0,0633	-0,1179	-0,2316	0,0319	-0,0676
MAE							
Small-time	2,9745	4,4365	6,7698	7,8120	6,2351	8,1014	6,6594
Large-time	9,1571	17,1632	16,1941	11,9188	6,9144	6,5540	10,4085
Small-strike	3,2064	8,9729	18,8776	26,2776	17,0891	12,1628	15,5331
Large-strike	4,9698	6,9744	10,8148	9,1764	5,9687	5,8184	7,3078
MSE							
Small-time	13,4447	31,0767	66,9096	80,1911	54,2565	119,1938	73,6250
Large-time	104,1364	322,9477	315,0167	171,6854	58,9524	81,2544	156,4945
Small-strike	18,0347	115,8088	500,6586	895,0506	434,6833	240,4333	404,7159
Large-strike	35,5671	77,7865	150,1947	107,8304	47,2449	72,4465	84,2500

Table 5.8: Pricing errors per moneyness group from calibrating whole sample data with various asymptotic formulas

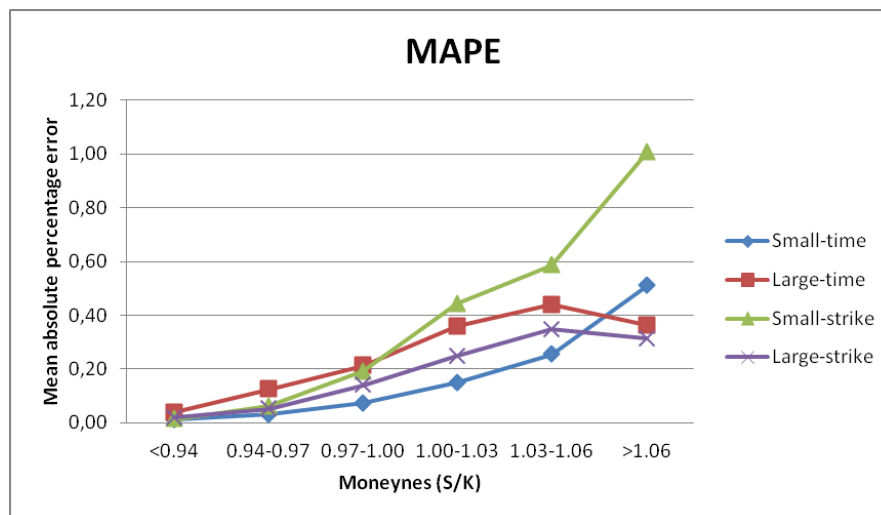


Figure 5.26: MAPE error per moneyness group from calibrating whole sample data with various asymptotic formulas

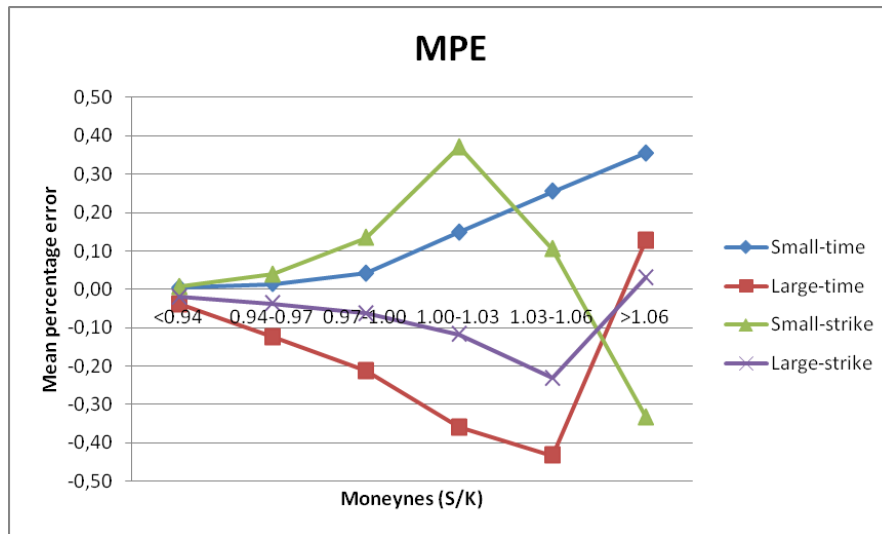


Figure 5.27: MPE error per moneyness group from calibrating whole sample data with various asymptotic formulas

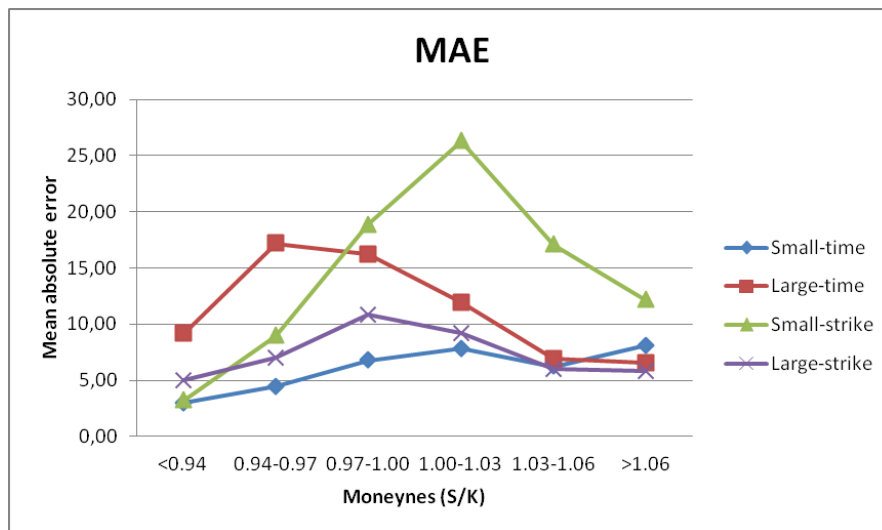


Figure 5.28: MAE error per moneyness group from calibrating whole sample data with various asymptotic formulas

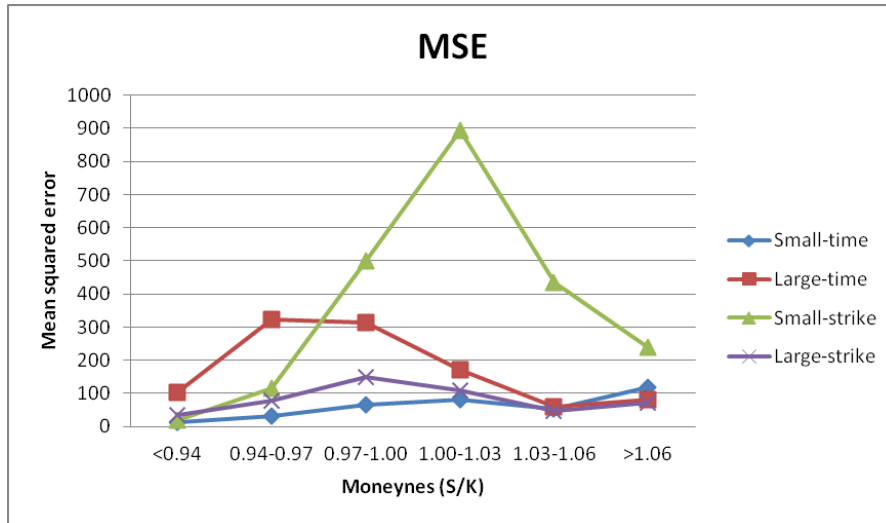


Figure 5.29: MSE error per moneyness group from calibrating whole sample data with various asymptotic formulas

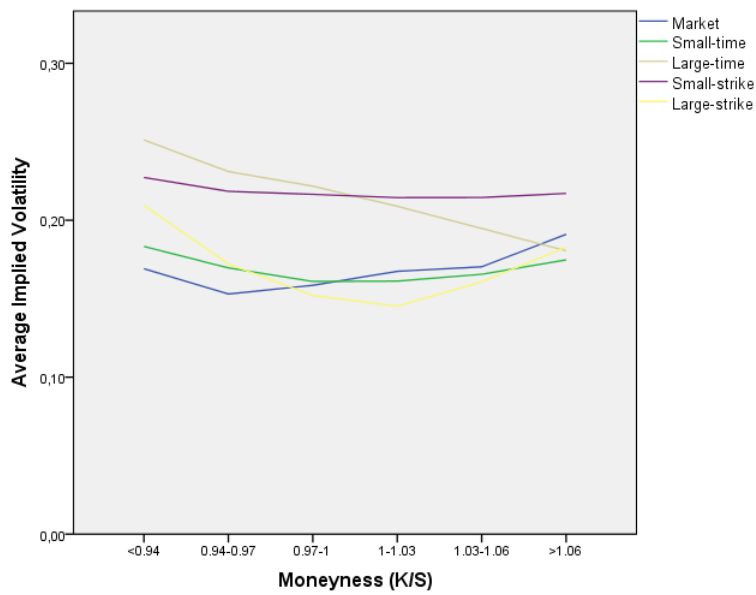


Figure 5.30: Implied volatility of various asymptotic formula calibration results per moneyness group, using sample data with maturities ranging from 0.08 to 0.16 years

Parameter	< 0.94	0.94-0.97	0.97-1.00	1.00-1.03	1.03-1.06	> 1.06	all
MAPE							
Small-time	0,0133	0,0398	0,0471	0,0616	0,0817	0,2920	0,0996
Large-time	0,0665	0,1913	0,2578	0,3280	0,3725	0,3529	0,2642
Small-strike	0,0442	0,1582	0,2388	0,3787	0,6887	0,5868	0,3641
Large-strike	0,0264	0,0447	0,0541	0,1602	0,1215	0,2177	0,1119
MPE							
Small-time	-0,0082	-0,0339	-0,0119	0,0376	0,0497	0,2290	0,0558
Large-time	-0,0665	-0,1913	-0,2578	-0,3280	-0,3725	0,1183	-0,1650
Small-strike	-0,0442	-0,1582	-0,2388	-0,3787	-0,6887	-0,5721	-0,3610
Large-strike	-0,0260	-0,0394	0,0285	0,1602	0,1084	0,0949	0,0600
MAE							
Small-time	3,1227	5,1355	4,2386	3,4071	1,9960	3,4811	3,4543
Large-time	15,9054	25,3024	22,1743	15,4718	7,4042	4,3595	13,9606
Small-strike	10,4323	20,7998	20,3235	17,5341	13,7893	6,5236	13,9895
Large-strike	6,4753	5,8633	4,9079	8,4377	3,3280	2,9519	5,2719
MSE							
Small-time	15,7962	38,3928	26,4827	16,1072	5,8521	22,4978	19,7854
Large-time	279,2723	658,1415	526,1456	254,3179	62,5581	27,3646	264,7532
Small-strike	129,3670	452,9656	450,2460	322,8830	195,3948	70,3056	243,8489
Large-strike	55,7443	48,1174	33,1507	82,6151	15,2773	15,1238	41,2528

Table 5.9: Pricing errors per moneyness group from calibrating with various asymptotic formulas, using sample data with maturities ranging from 0.08 to 0.16 years

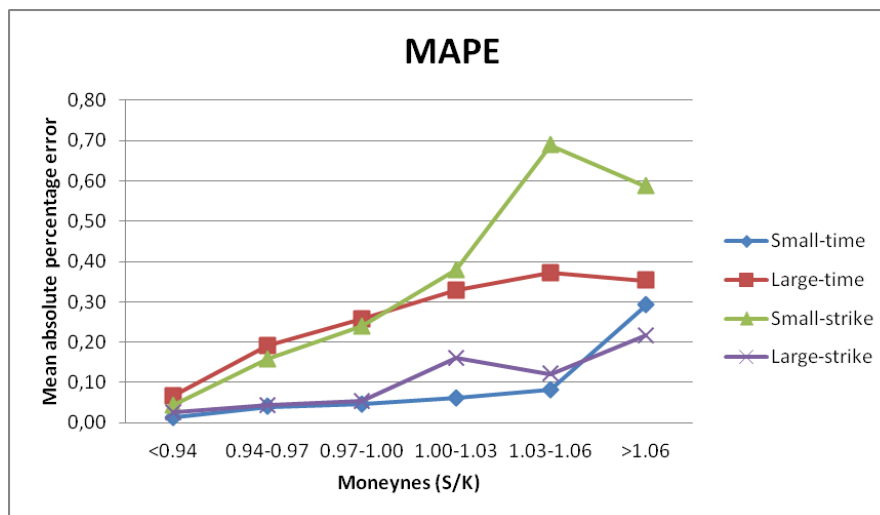


Figure 5.31: MAPE error per moneyness group from calibrating with various asymptotic formulas, using sample data with maturities ranging from 0.08 to 0.16 years

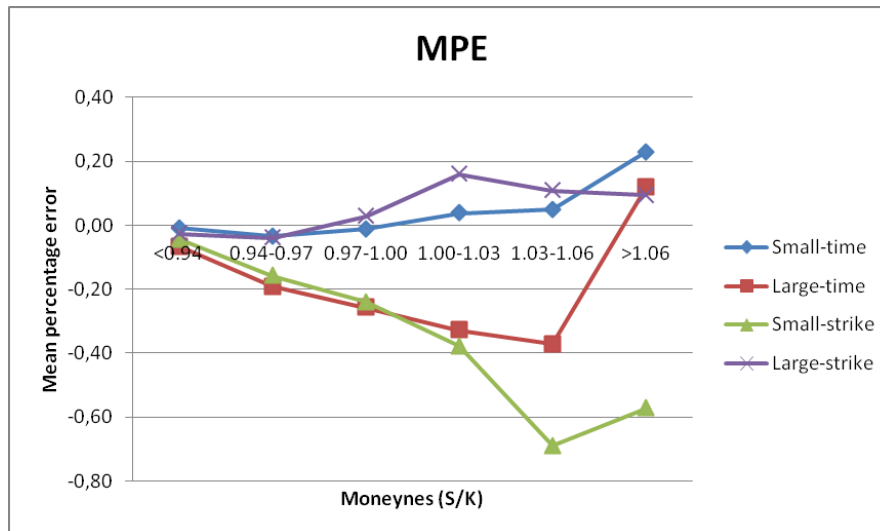


Figure 5.32: MPE error per moneyness group from calibrating with various asymptotic formulas, using sample data with maturities ranging from 0.08 to 0.16 years

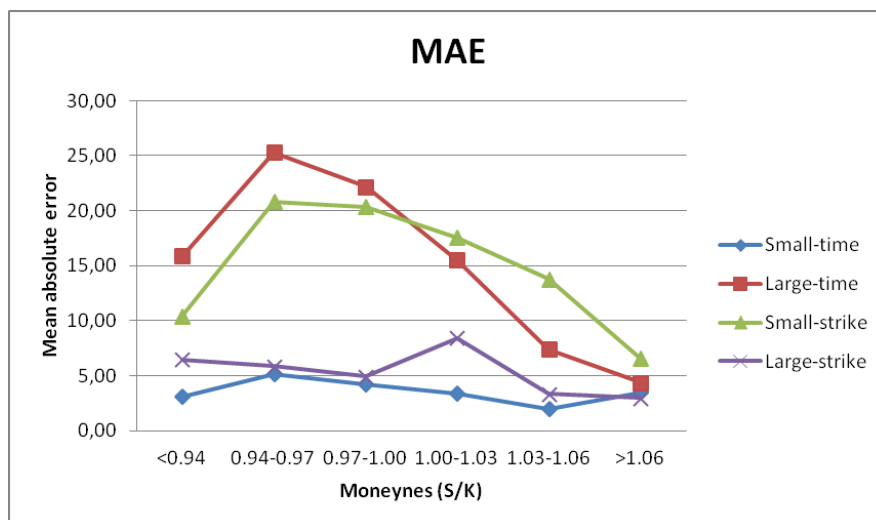


Figure 5.33: MAE error per moneyness group from calibrating with various asymptotic formulas, using sample data with maturities ranging from 0.08 to 0.16 years

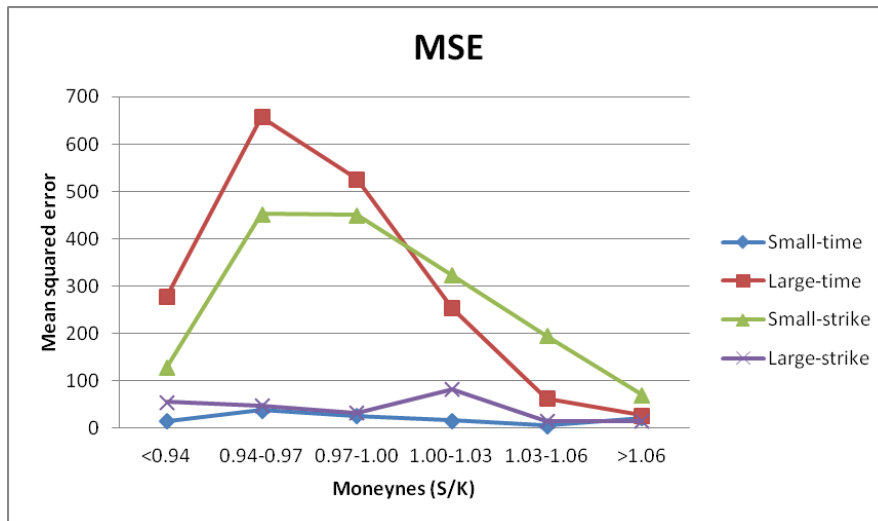


Figure 5.34: MSE error per moneyness group from calibrating with various asymptotic formulas, using sample data with maturities ranging from 0.08 to 0.16 years

Comparison on Time Periods of Sample Data

The sample data contains call options from March 10, 2011 to May 9, 2011 with maturity date May 20, 2011. In this section the call options have now been separated into four different time intervals (see table 5.10). The calibration with the implied volatility asymptotics was performed again on these time periods. For the results the implied volatility and the error measures are presented analogous to the previous sections.

Note, the sample data did not consist of any ITM call options in time period 4. Thus, calibration with the small-strike formula was not performed in this time period.

	Date		Maturity (days)	
	From	To	From	To
Time Period 1	10.03.2011	24.03.2011	71	57
Time Period 2	25.03.2011	07.04.2011	56	43
Time Period 3	08.04.2011	21.04.2011	42	29
Time Period 4	26.04.2011	09.05.2011	24	11

Table 5.10: Selected time periods for the calibration of the sample data

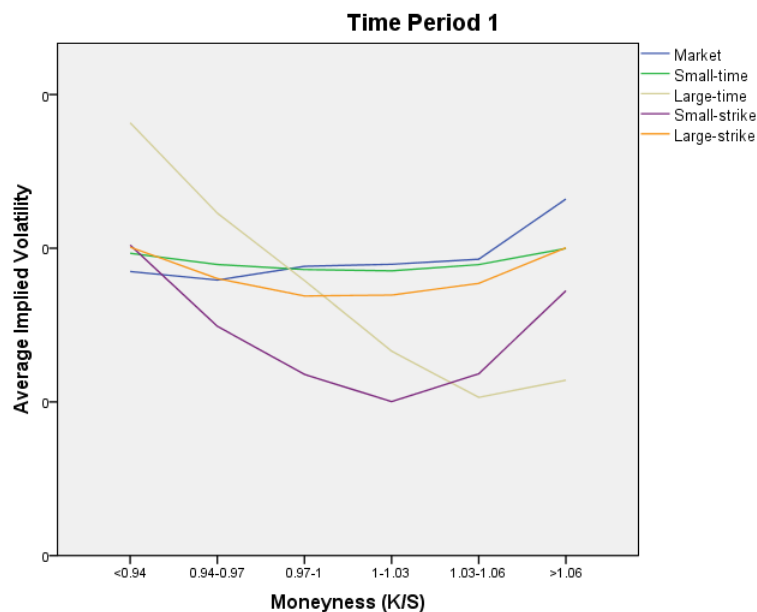


Figure 5.35: Implied volatility of various asymptotic formula calibration results per moneyness group, using options recorded in time period 1

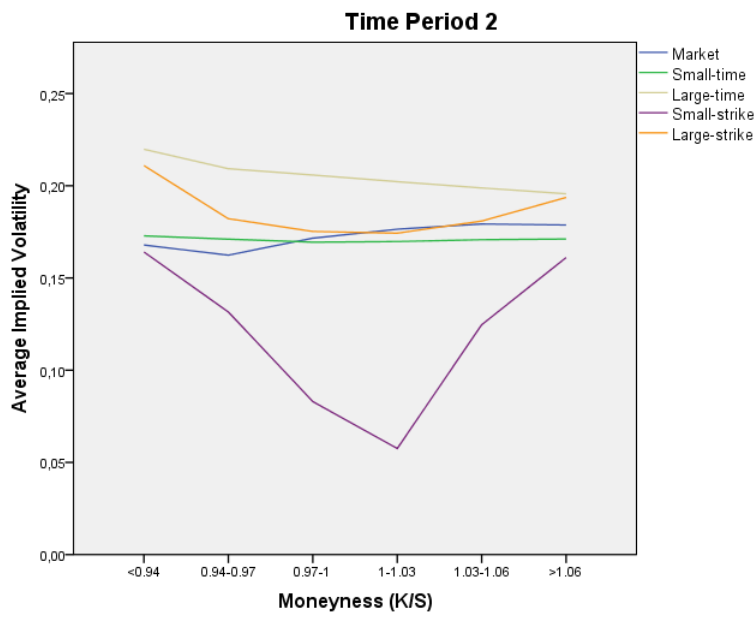


Figure 5.36: Implied volatility of various asymptotic formula calibration results per moneyness group, using options recorded in time period 2

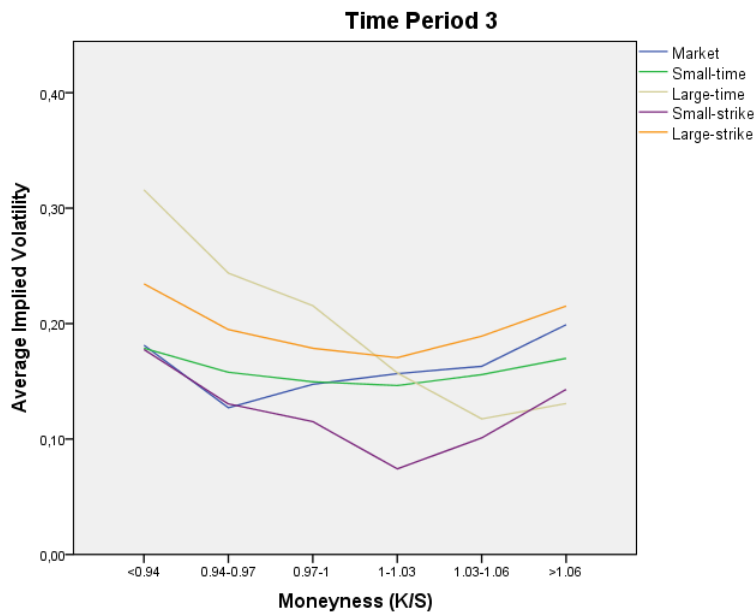


Figure 5.37: Implied volatility of various asymptotic formula calibration results per moneyness group, using options recorded in time period 3

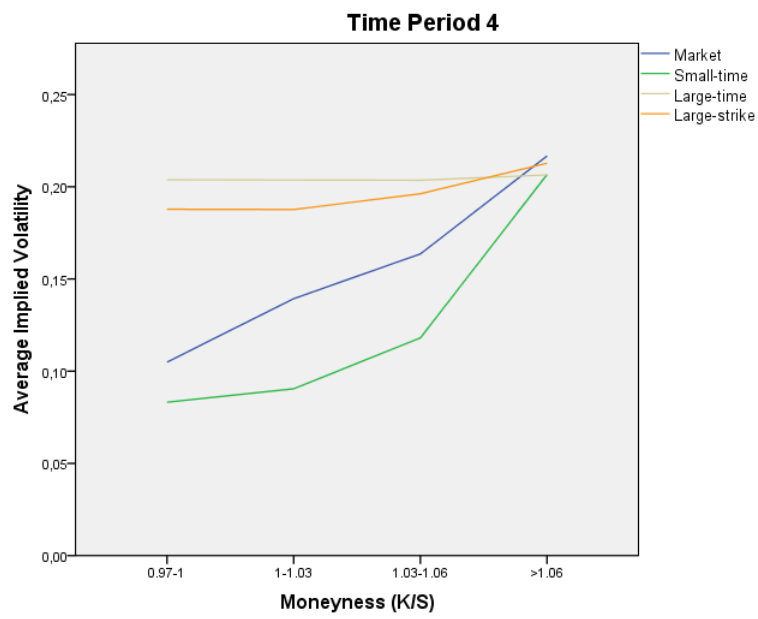


Figure 5.38: Implied volatility of various asymptotic formula calibration results per moneyness group, using options recorded in time period 4

Parameter	< 0.94	0.94-0.97	0.97-1.00	1.00-1.03	1.03-1.06	> 1.06	all
MAPE							
Small-time	0,0152	0,0310	0,0302	0,0332	0,0555	0,3364	0,1434
Large-time	0,1117	0,1025	0,0574	0,3722	0,7307	0,9019	0,5139
Small-strike	0,0197	0,0754	0,3048	0,5615	0,6173	0,5721	0,4228
Large-strike	0,0180	0,0241	0,0841	0,1250	0,1292	0,3127	0,1642
MPE							
Small-time	-0,0107	-0,0237	0,0090	0,0268	0,0242	0,3045	0,1139
Large-time	-0,1117	-0,1025	0,0439	0,3722	0,7307	0,9019	0,4632
Small-strike	-0,0132	0,0754	0,3048	0,5615	0,6173	0,5721	0,4196
Large-strike	-0,0139	0,0004	0,0841	0,1250	0,1292	0,3033	0,1545
MAE							
Small-time	3,4704	4,8109	3,1568	2,4762	2,8704	10,0799	5,7699
Large-time	26,8762	16,5274	5,8265	25,0977	34,4955	26,0348	23,3458
Small-strike	4,7605	11,4205	31,6062	40,0906	29,7288	17,4681	22,0551
Large-strike	4,1941	3,7451	8,7376	9,1614	6,6959	9,6401	7,7158
MSE							
Small-time	27,6029	26,9702	17,0628	11,2629	18,9574	159,1708	70,1698
Large-time	747,3431	320,4912	64,4588	702,1155	1224,4419	753,5985	668,5201
Small-strike	32,2431	166,5759	1047,3057	1618,0034	938,2289	391,7897	654,2946
Large-strike	33,6033	19,4455	95,3839	94,1242	67,2276	157,3207	97,3664

Table 5.11: Pricing errors per moneyness group from calibrating options recorded in **time period 1** with various asymptotic formulas

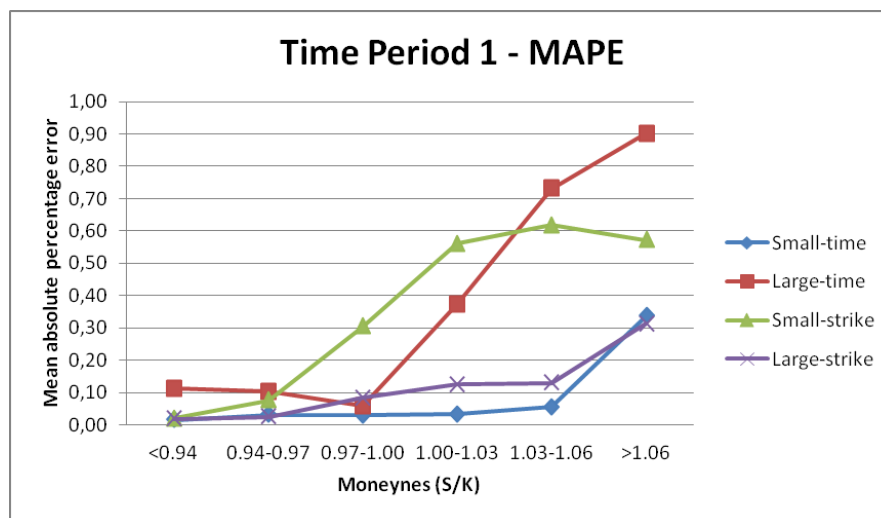


Figure 5.39: MAPE error per moneyness group from calibrating options from time period 1 with various asymptotic formulas

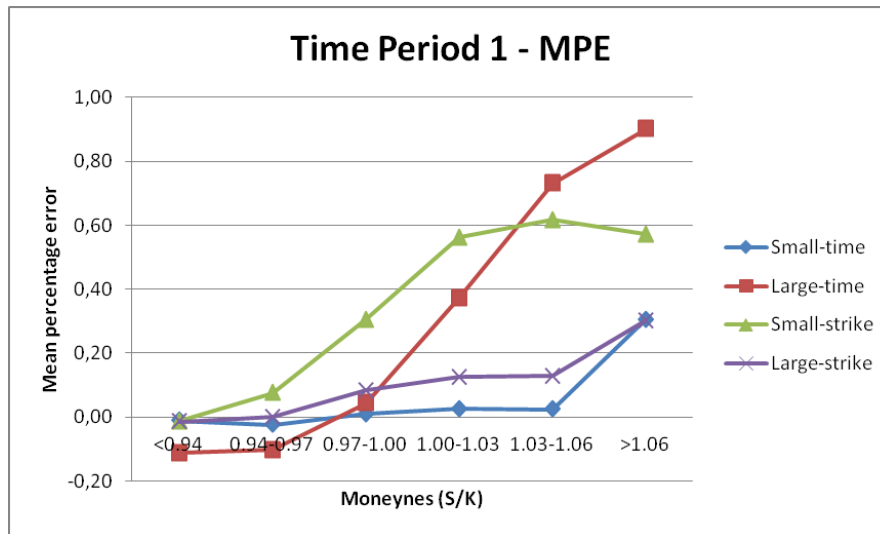


Figure 5.40: MPE error per moneyness group from calibrating options from time period 1 with various asymptotic formulas

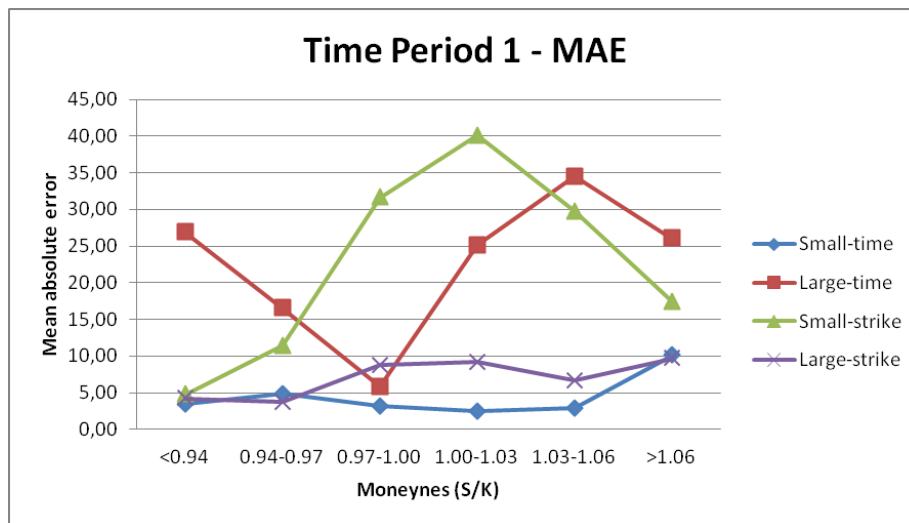


Figure 5.41: MAE error per moneyness group from calibrating options from time period 1 with various asymptotic formulas

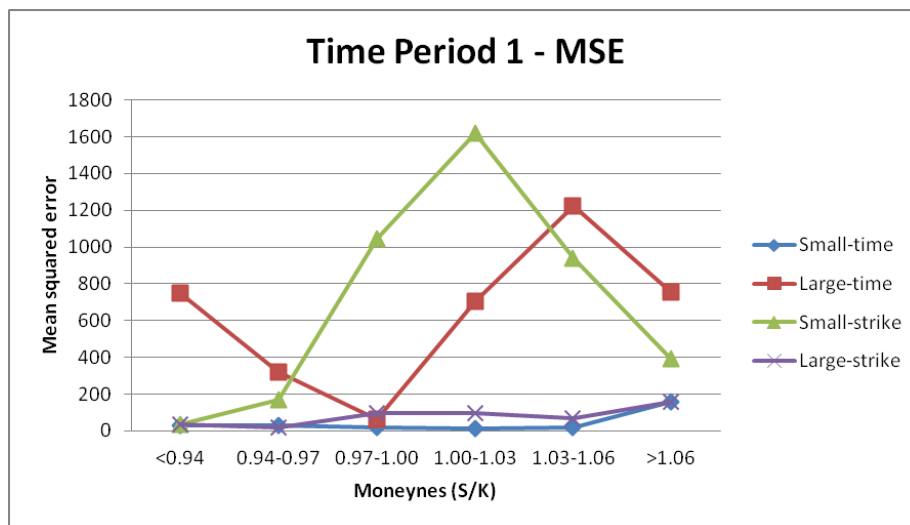


Figure 5.42: MSE error per moneyness group from calibrating options from time period 1 with various asymptotic formulas

Parameter	< 0.94	0.94-0.97	0.97-1.00	1.00-1.03	1.03-1.06	> 1.06	all
MAPE							
Small-time	0,0123	0,0309	0,0237	0,0483	0,0893	0,1356	0,0551
Large-time	0,0391	0,1191	0,1522	0,1907	0,2066	0,3655	0,1710
Small-strike	0,0347	0,0293	0,5040	0,7571	0,5216	0,2680	0,3121
Large-strike	0,0253	0,0474	0,0377	0,0553	0,0525	0,3305	0,0950
MPE							
Small-time	-0,0023	-0,0193	0,0055	0,0385	0,0875	0,1032	0,0340
Large-time	-0,0391	-0,1191	-0,1522	-0,1907	-0,2066	-0,3267	-0,1638
Small-strike	0,0300	-0,0293	0,5040	0,7571	0,5216	0,2334	0,3034
Large-strike	-0,0253	-0,0468	-0,0153	-0,0004	-0,0203	-0,2917	-0,0719
MAE							
Small-time	2,7505	4,1795	2,2130	3,3027	3,1829	2,5255	3,0089
Large-time	9,1343	16,2360	13,6465	10,5388	7,3540	5,5840	10,0336
Small-strike	7,5223	3,9297	37,7966	48,7500	19,4856	5,2002	19,3044
Large-strike	6,0877	6,4731	3,3230	3,1148	1,8210	4,9798	4,5839
MSE							
Small-time	12,0923	28,4260	8,4049	15,7003	11,9049	14,6956	15,1615
Large-time	97,5380	284,7849	199,3725	117,0069	56,3922	36,7451	123,2464
Small-strike	92,3128	15,4422	1428,5852	2660,8683	404,1454	46,4857	734,8361
Large-strike	46,3532	68,4287	18,1817	16,6906	3,9321	28,8522	32,8098

Table 5.12: Pricing errors per moneyness group from calibrating options recorded in **time period 2** with various asymptotic formulas

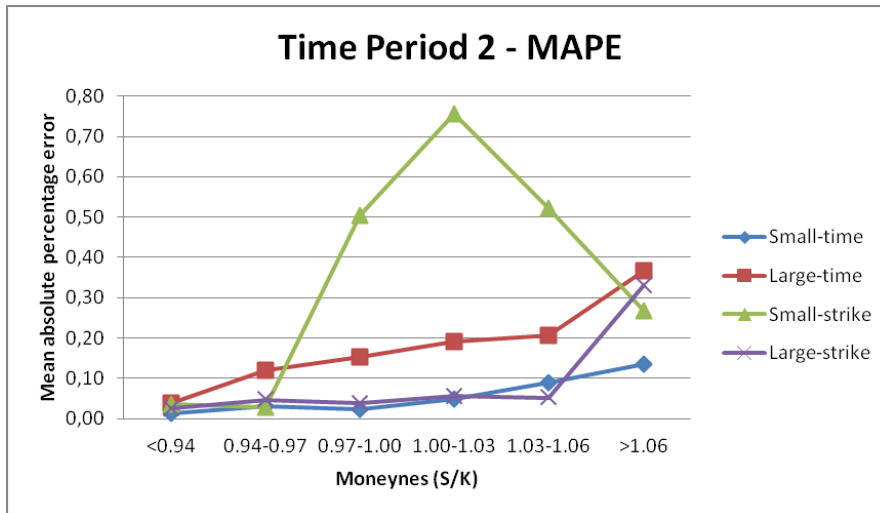


Figure 5.43: MAPE error per moneyness group from calibrating options from time period 2 with various asymptotic formulas

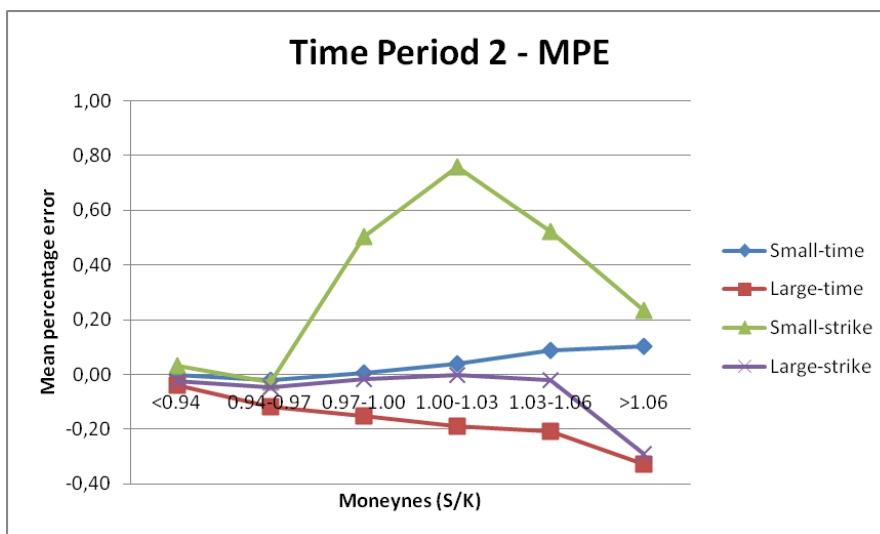


Figure 5.44: MPE error per moneyness group from calibrating options from time period 2 with various asymptotic formulas

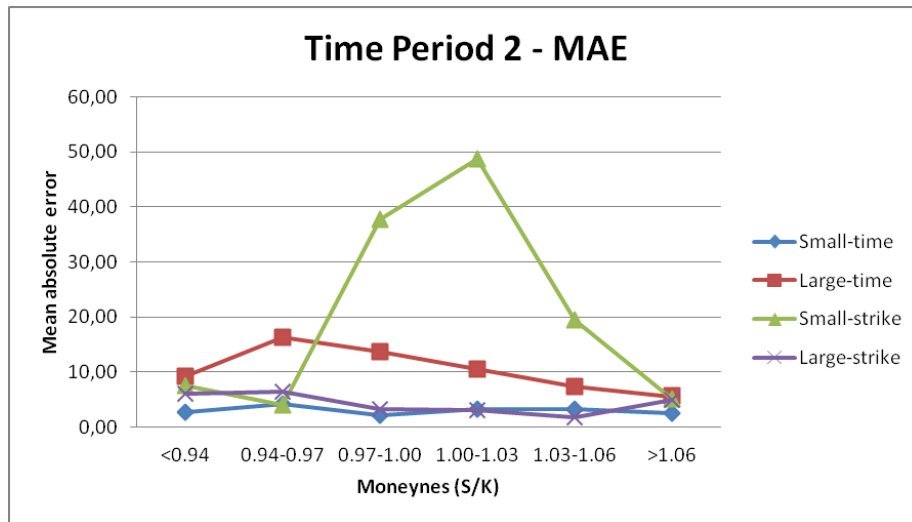


Figure 5.45: MAE error per moneyness group from calibrating options from time period 2 with various asymptotic formulas

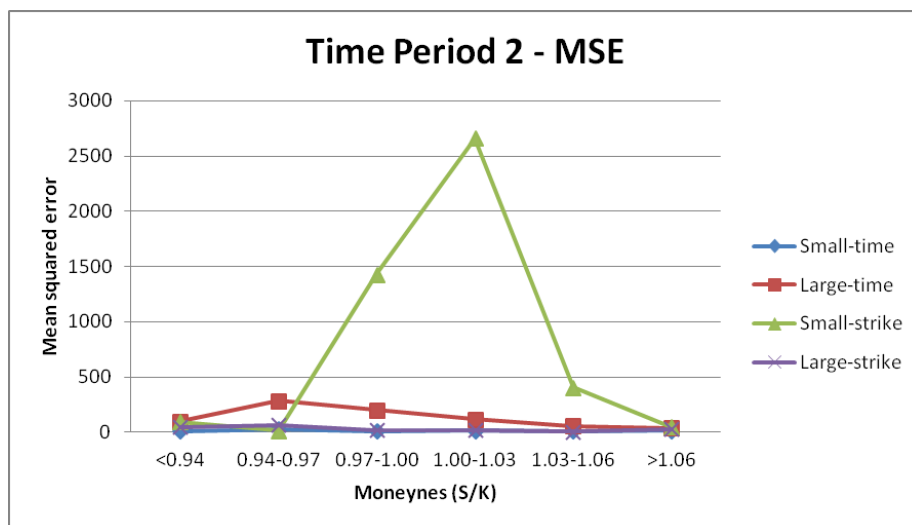


Figure 5.46: MSE error per moneyness group from calibrating options from time period 2 with various asymptotic formulas

Parameter	< 0.94	0.94-0.97	0.97-1.00	1.00-1.03	1.03-1.06	> 1.06	all
MAPE							
Small-time	0,0056	0,0571	0,0514	0,0852	0,1115	0,4611	0,1684
Large-time	0,0903	0,2583	0,2581	0,1139	0,6092	0,8366	0,4314
Small-strike	0,0044	0,0256	0,1259	0,6591	0,7705	0,6933	0,4810
Large-strike	0,0269	0,1417	0,1352	0,1303	0,4460	0,4826	0,2751
MPE							
Small-time	0,0031	-0,0571	-0,0130	0,0777	0,1003	0,4397	0,1388
Large-time	-0,0903	-0,2583	-0,2581	0,0084	0,6092	0,8366	0,2637
Small-strike	0,0026	-0,0023	0,1259	0,6591	0,7705	0,6933	0,4785
Large-strike	-0,0269	-0,1417	-0,1261	-0,1226	-0,4460	-0,4190	-0,2563
MAE							
Small-time	1,4355	6,8096	4,7496	3,7404	1,9184	4,0044	3,6107
Large-time	23,1518	31,4988	21,4327	4,7610	10,0518	7,1048	13,3717
Small-strike	1,0699	2,8915	10,2527	26,8163	13,0953	6,7491	11,5047
Large-strike	6,8903	17,1812	11,0808	5,0134	6,6984	3,4185	7,1864
MSE							
Small-time	2,7272	50,2819	33,9445	22,2004	6,0952	25,6596	21,9790
Large-time	543,0797	997,4518	507,2509	36,0105	111,3600	64,6994	270,3604
Small-strike	1,6580	11,0104	165,3617	731,3030	198,8030	65,6044	223,5882
Large-strike	50,0132	297,6535	135,9645	33,5561	49,9061	22,1820	74,9093

Table 5.13: Pricing errors per moneyness group from calibrating options recorded in **time period 3** with various asymptotic formulas

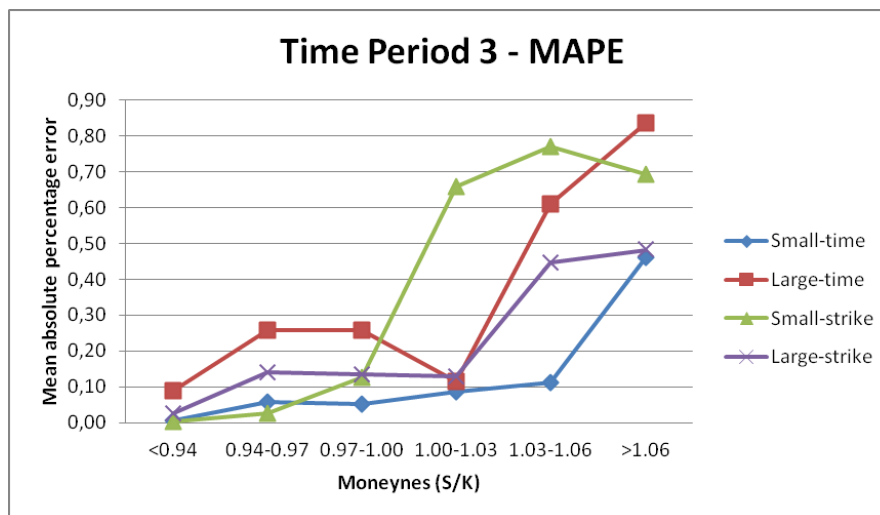


Figure 5.47: MAPE error per moneyness group from calibrating options from time period 3 with various asymptotic formulas

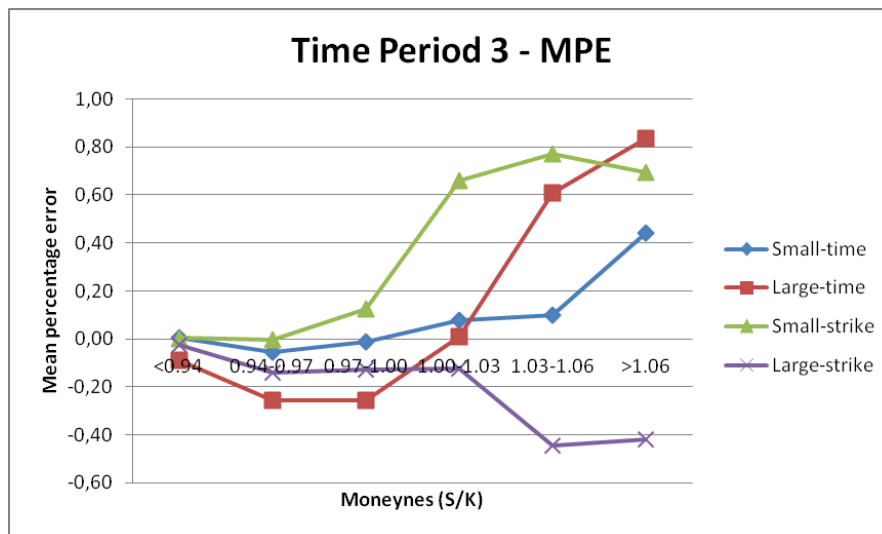


Figure 5.48: MPE error per moneyness group from calibrating options from time period 3 with various asymptotic formulas

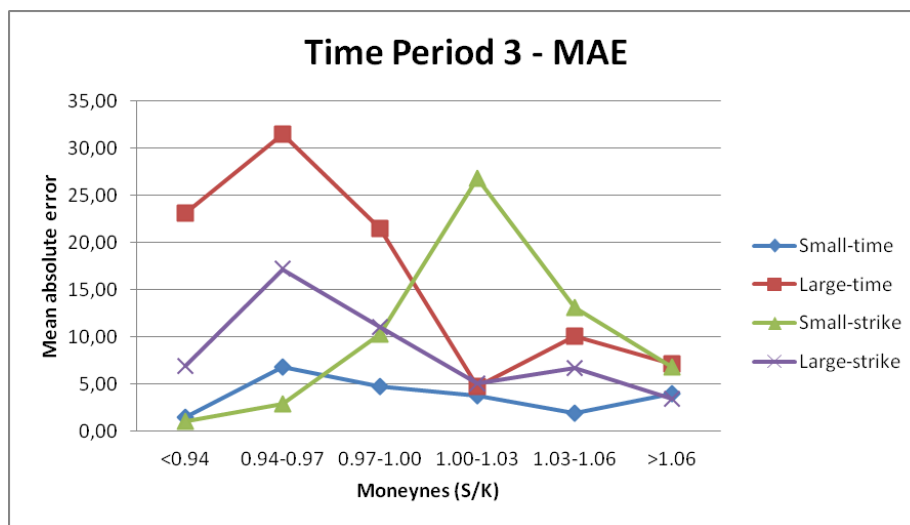


Figure 5.49: MAE error per moneyness group from calibrating options from time period 3 with various asymptotic formulas

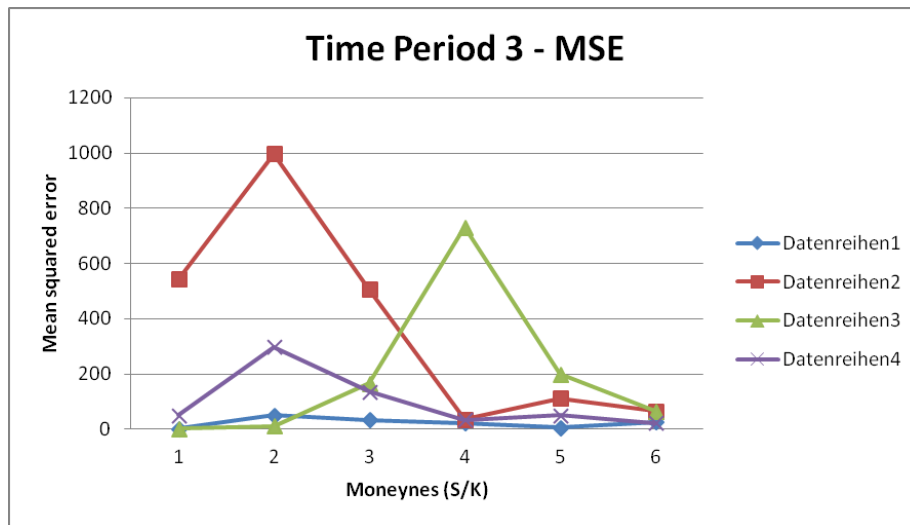


Figure 5.50: MSE error per moneyness group from calibrating options from time period 3 with various asymptotic formulas

Parameter	< 0.94	0.94-0.97	0.97-1.00	1.00-1.03	1.03-1.06	> 1.06	all
MAPE							
Small-time	-	-	0,1409	0,5831	0,7286	1,8154	0,8989
Large-time	-	-	0,3884	0,9324	1,0242	0,3938	0,6300
Small-strike	-	-	-	-	-	-	-
Large-strike	-	-	0,3158	0,6964	0,8266	0,3774	0,5158
MPE							
Small-time	-	-	0,1228	0,5831	0,7286	-1,0028	-0,0211
Large-time	-	-	-0,3884	-0,9324	-1,0242	0,1518	-0,4527
Small-strike	-	-	-	-	-	-	-
Large-strike	-	-	-0,3158	-0,6964	-0,8266	-0,0385	-0,4056
MAE							
Small-time	-	-	6,2413	10,6174	4,4408	2,4443	5,5337
Large-time	-	-	20,5618	14,8517	6,1610	0,9876	9,5306
Small-strike	-	-	-	-	-	-	-
Large-strike	-	-	16,9146	11,0274	4,9438	0,8526	7,5636
MSE							
Small-time	-	-	56,6695	132,0944	21,2300	8,8477	49,7277
Large-time	-	-	430,3289	234,8339	42,3527	1,3358	158,5699
Small-strike	-	-	-	-	-	-	-
Large-strike	-	-	295,3740	130,2575	27,9788	1,1760	101,7497

Table 5.14: Pricing errors per moneyness group from calibrating options recorded in **time period 4** with various asymptotic formulas

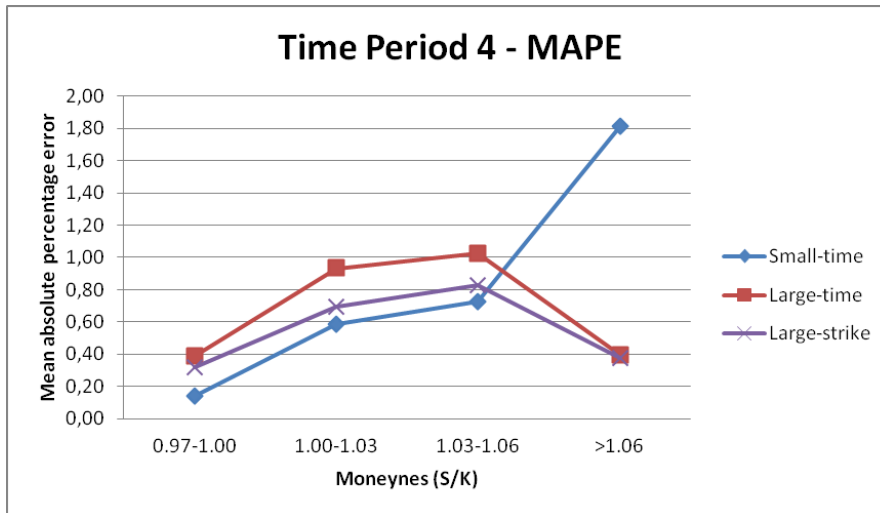


Figure 5.51: MAPE error per moneyness group from calibrating options from time period 4 with various asymptotic formulas

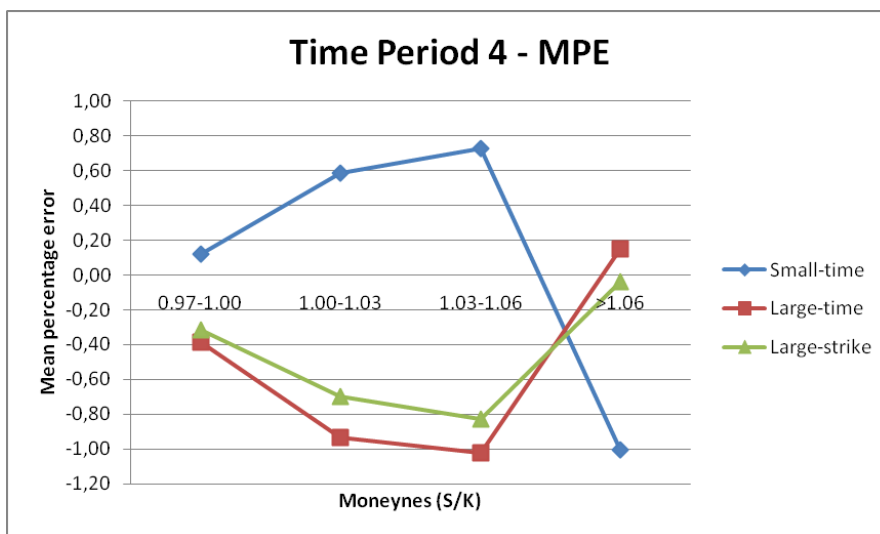


Figure 5.52: MPE error per moneyness group from calibrating options from time period 4 with various asymptotic formulas

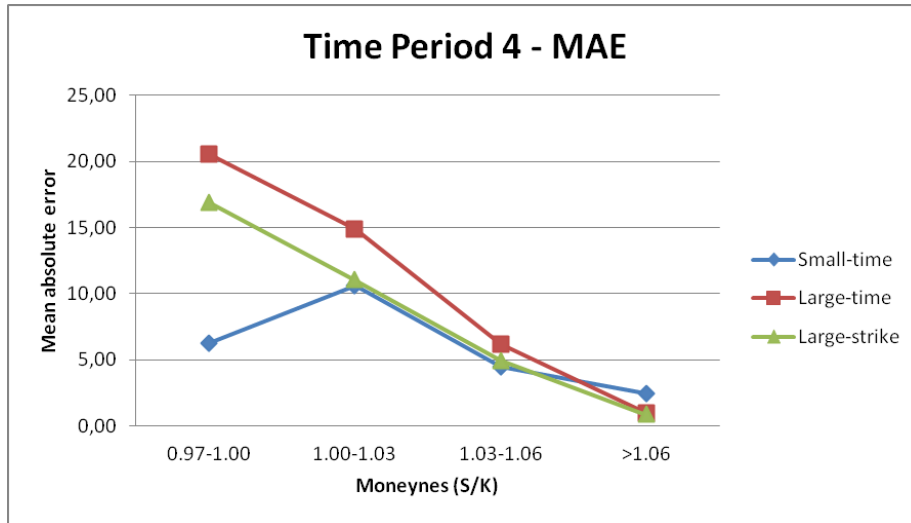


Figure 5.53: MAE error per moneyness group from calibrating options from time period 4 with various asymptotic formulas

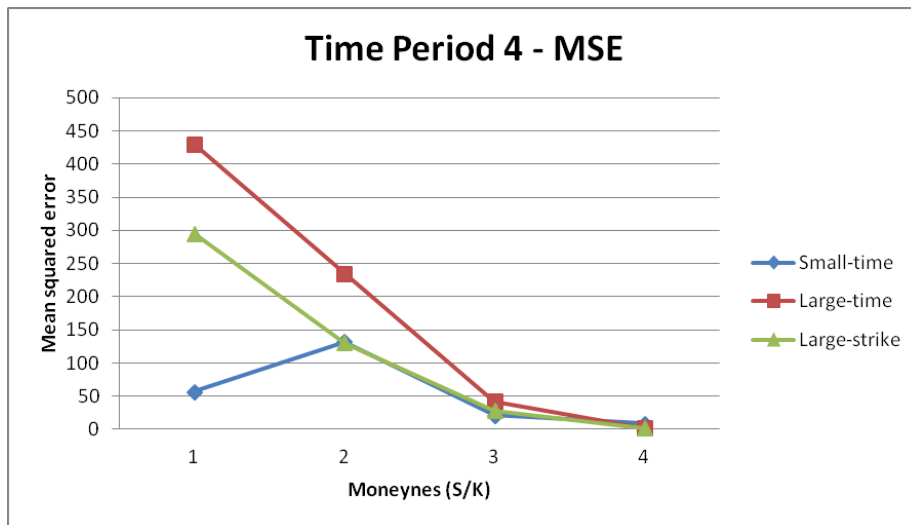


Figure 5.54: MSE error per moneyness group from calibrating options from time period 4 with various asymptotic formulas

5.4 Conclusion

As expected, the calibration results, using implied volatility asymptotics, depend on their starting point as well. It was observed, that the mean reversion rate κ and the volatility of variance σ vary more often in the results, than the other parameters. However, the different calibration results all served as good initial parameters for calibration with Heston's semi-closed form (3.11), as one can see in 5.3 and 5.4.

For the small-time regime was also observed that calibration, using only the leading order term, is quite accurate as well. The results serve as good initial parameters as one can see in table 5.6 (Lead-term 1 and 2).

Comparing the calibration results using the various implied volatility asymptotics, it is obvious that the small-time (4.5) and the large-strike (4.11) regime yield the best results. This was to be expected since the sample data consists of 45% OTM call options and quite short maturities, ranging from 10 to 90 days. Note, that slightly better results were received from the small-time regime, when calibrating the whole market data or only time periods of the data. The results from calibrating with the small-strike (4.13) and the large-maturity & large-strike (4.7) formulas are not so accurate. This is due to the mentioned fact, that the sample data consists of options with short maturities and only 29.2% ITM options.

The general conclusion of the thesis is, that it is necessary to take a look at the option data prior the calibration. Then one should choose the appropriate implied volatility asymptotic formula (see chapter 4) and reasonable starting values for calibrating the parameters. Following these guidelines, one will receive good initial parameters for the calibration with Heston's semi-closed form solution (3.11).

Appendix A

Software

The following software was used for various calculations throughout this thesis:

- Maple 15.00
- MATLAB 7.11.0.584 (2010b)
- Microsoft Excel 2007
- PASW Statistics 18.0.0

The calculations in chapter 5 were done in MATLAB (matrix laboratory). It is a numerical computing environment and fourth-generation programming language. It allows matrix manipulations, plotting of functions and data, implementation of algorithms, creation of user interfaces, and interfacing with programs written in other languages. MATLAB was also used to simulate the figures 2.1, 2.2 and the volatility surfaces 5.19 to 5.24.

Figure 2.11 and all the implied volatility per moneyness plots in chapter 5 were generated with the programme PASW Statistics (since 2010 named SPSS again). It is a statistics program used for survey authoring and deployment, data mining, text analytics, statistical analysis, and collaboration and deployment.

The differential calculus for the asymptotic formula in the large-time & large-strike regime was done in Maple. Maple is a general-purpose commercial computer algebra system. Users can enter mathematics in traditional mathematical notation and there is extensive support for numeric computations, to arbitrary precision, as well as symbolic computation and visualization.

Microsoft Excel was used to manage the sample data, and calculate and plot the error measures in chapter 5.

Appendix B

MATLAB Code

B.1 Calibration

```
function [x] = run ()

%Initial Parameter Set
%x0 = [kappa, theta, sigma, rho, v0]
x0 = [0.2542 0.9998 0.8096 -0.0001 0.0119]

%Lower and upper bound for optimisation
lb = [0 0 0 -1 0];
ub = [20 1 5 0 1];

datensatz = xlsread('Satensatz.xlsx', 'all', 'A2:I251');
% Maturity
T = datensatz(:,2);

% Strike price
strike = datensatz(:,4);

% Underlying price
Under = datensatz(:,3);

%Implied Volatility
implvol = datensatz(:,9);

tic; % start timer

% Optimisation
options = optimset('TolFun', 1e-8);
```

```

[x,resnorm,unused,exitflag]
    = lsqnonlin(@(x) costf3(x,T,strike,Under,implvol),x0,lb,ub,options);

%value of objective function
fprintf('resnorm = %.20f\n', resnorm);

%3: Change in the residual was less than the specified tolerance
fprintf('exitflag = %d\n\n', exitflag);

fprintf('kappa=%.20f\n theta=%.20f\n sigma=%.20f\n',x(1),x(2),x(3));
fprintf('rho=%.20f\n v0= %.20f\n',x(4),x(5));

fprintf('\nRechenzeit: %d s\n', int16(toc)); % stop timer and output

end

function [L] = costf3(x, T, strike, Under, implvol)
for i = 1 : length(T)

%L(i) depends on the regime one wants to use:
L(i)=((implvol(i)^2-SmallTime(x(1),x(2),x(3),x(4),x(5),money(i),T(i)))/implvol(i)^2);

%Small-time Leading Order Time:
((implvol(i)^2-SmallTimeLDT(x(1),x(2),x(3),x(4),x(5),money(i),T(i)))/implvol(i)^2);

%Large-time, Large-strike:
((implvol(i)^2-LargeTime(x(1),x(2),x(3),x(4),x(5),money(i),T(i)))/implvol(i)^2);

%Small-strike:
(implvol(i)-SmallStrike(x(1),x(2),x(3),x(4),x(5),T(i),strike(i),Under(i)))/implvol(i);

%Large-strike:
(implvol(i)-LargeStrike(x(1),x(2),x(3),x(4),x(5),T(i),strike(i),Under(i)))/implvol(i);

end
end

```

B.2 Small-maturity

```
function H = SmallTime(kappa,theta,sigma,rho,v0,money,T)

x = log(money);
alpha = kappa*theta;

term1 = 1 + (rho/2)*(sigma*x/v0) + (1-(7/4)*rho^2)* (sigma^2*x^2)/(12*v0^2);
term2a = (rho*sigma*v0)/2 - (sigma^2/6)*(1-rho^2/4) + alpha - kappa*v0;
term2b = sigma^2*(1-rho^2) + rho*sigma*v0 - 2*alpha - 2*kappa*v0;
term3a = (176 - 712*rho^2 + 521*rho^4)*sigma^2 + 40*sigma*rho^3*v0;
term3b = 80*(13*rho^2 - 6)*alpha - 80*kappa*rho^2*v0;

H1 = v0 * term1 + (term2a + (rho*sigma)/(12*v0) * term2b * x) * (T/2);
H2 = (sigma^2/(7680*v0^2)) * (term3a + term3b) * x^2*T;

H = H1 + H2;
end
```

B.3 Small-maturity Leading Order Term

```
function H = SmallTimeLDT(kappa,theta,sigma,rho,v0,money,T)

x = log(money);
alpha = kappa*theta;

term1 = 1 + (rho*sigma*x)/(4*v0);
term2 = (1/24)*(1 - 5*rho^2/2)*(sigma^2*x^2/v0^2);

H = v0*(term1 + term2)^2;
end
```

B.4 Large-maturity

```
function H = LargeTime(kappa,theta,sigma,rho,v0,money,T)
```

```

x = (1/T)*log(money);
kappa2 = kappa - rho*sigma;
theta2 = (kappa*theta)/kappa2;

%p corresponds to p*
pterm1 = (sigma-2*kappa*rho)/(2*(1-rho^2)*sigma);
pterm2a = (sigma^2+4*kappa^2 - 4*kappa*rho*sigma);
pterm2b = (x^2*sigma^2+2*x*kappa*theta*rho*sigma+kappa^2*theta^2);
pterm2 = sqrt(pterm2a/pterm2b);
p = pterm1 + (kappa*theta*rho + x*sigma)/(2*(1 - rho^2)*sigma) * pterm2;

Vterm = (kappa - rho*sigma*p - sqrt((kappa-rho*sigma*p)^2 + sigma^2*(p-p^2)));
V = (kappa*theta/sigma^2) * Vterm;
Vstern = p*x - V;

if ((x > theta2/2) || (x < -theta2/2) )
H = 2*(2*Vstern - x - 2*sqrt(Vstern^2 - Vstern*x));
else
H = 2*(2*Vstern - x + 2*sqrt(Vstern^2 - Vstern*x));
end
end
end

```

B.5 Small-strike

```

function [H] = SmallStrike(kappa, theta, sigma, rho, v0, T, strike, Under)

a = kappa*theta;
b = -kappa;
c = sigma;
k = log(strike/Under);

%root finding procedure
NullstelleGefunden = false;
Start = 100;
options = optimset('Display','off');

while ~NullstelleGefunden

```

```

fs = ExplosionTime(Startwert, rho, c, b, T);

if isfinite(fs) && isreal(fs)
[solution, fval, exitflag] = fzero(@(s) ExplosionTime(s, rho, c, b, T), Start, options);

if (exitflag == 1)
    if isreal(solution) & solution >= -1
        NullstelleGefunden = true;
        s = solution;
    end;
end;
end;

Start = Start + 100;

if (Start >= 5000)
    fprintf('Startwert schon bei %d\n', Start);
    disp(rho);
    disp(c);
    disp(b);
    disp(T);
end;
end

B3 = -(s+1);
B2 = 2* (2*v0)^(1/2)/(c * slope^(1/2));
rho1= 2^(1/2) * ((B3+2)^(1/2) - (B3+1)^(1/2));
rho2= B2*2^(-1/2) * ( 1/(B3+1)^(1/2) - 1/(B3+2)^(1/2));
rho3= 2^(-1/2) * (1/4 - a/c^2) * ( 1/(B3+2)^(1/2) - 1/(B3+1)^(1/2));

H = (1/T^(1/2)) * (rho1*(-k)^(1/2) + rho2 + (rho3 * log(-k))/((-k)^(1/2)));
end

function Tstern = ExplosionTime(s, rho, c, b, T)
term = (atan(sqrt(-(s*rho*c+b)^2 + c^2*(s^2-s))/(s*rho*c+b)));
Tstern = ((2/sqrt(-(s*rho*c+b)^2 + c^2*(s^2-s))) * term)-T;
end

```

B.6 Large-strike

```

function [H] = LargeStrike(kappa, theta, sigma, rho, v0, T, strike, Under)

a = kappa*theta;
b = -kappa;
c = sigma;
k = log(strike/Under);

%root finding procedure
NullstelleGefunden = false;
Start = 100;
options = optimset('Display','off');

while ~NullstelleGefunden
fs = ExplosionTime(Start, rho, c, b, T);

if isfinite(fs) && isreal(fs)
[solution, fval, exitflag] = fzero(@(s) ExplosionTime(s, rho, c, b, T), Start, options);

if (exitflag == 1)
if isreal(solution) & solution >= -1
NullstelleGefunden = true;
s = solution;
end;
end;
end;

Start = Start + 100;

if (Startwert >= 5000)
fprintf('Startwert schon bei %d\n', Start);
disp(rho);
disp(c);
disp(b);
disp(T);
end;
end

term1a = T*c^2*s*(s-1) * (c^2*(2*s-1) - 2*rho*c*(s*rho*c + b));
term1b = 2*(s*rho*c + b) * (c^2*(2*s-1) - 2*rho*c*(s*rho*c + b));
term1c = 4*rho*c * (c^2*s*(s-1) - (s*rho*c + b)^2);
R1 = term1a - term1b + term1c;

```

```

R2 = 2*c^2*s * (s-1) * (c^2*s*(s-1) - (s*rho*c + b)^2);

%slope corresponds to sigma in formula
slope = R1 / R2;

A2 = 2*(sqrt(2*v0))/(c*sqrt(slope));
A3 = s + 1;

beta1 = sqrt(2)*(sqrt(A3-1) - sqrt(A3-2));
beta2 = (A2/sqrt(2)) * (1/sqrt(A3-2) - 1/sqrt(A3-1));
beta3 = (1/sqrt(2)) * (1/4 - a/c^2) * (1/sqrt(A3-1) - 1/sqrt(A3-2));

H = (1/sqrt(T)) * (beta1*k^(1/2) + beta2 + (beta3 * log(k))/k^(1/2));
end

function Tstern = ExplosionTime(s, rho, c, b, T)
term = (atan(sqrt(-(s*rho*c+b)^2 + c^2*(s^2-s))/(s*rho*c+b)) + pi);
Tstern = ((2/sqrt(-(s*rho*c+b)^2 + c^2*(s^2-s))) * term)-T;
end

```

B.7 Heston Model

The MATLAB code for the semi-closed form solution of the Heston model is based on [51].

```

function call = HestonCallQuad(kappa,theta,sigma,rho,v0,r,T,s0,K,opt)
warning off;
if(opt==1)
call = s0*HestonP(kappa,theta,sigma,rho,v0,r,T,s0,K,1)
- K*exp(-r*T)*HestonP(kappa,theta,sigma,rho,v0,r,T,s0,K,2);
else
call= s0*HestonP(kappa,theta,sigma,rho,v0,r,T,s0,K,1)
- K*exp(-r*T)*HestonP(kappa,theta,sigma,rho,v0,r,T,s0,K,2)-s0+K*exp(-r*T);
end

function ret = HestonP(kappa,theta,sigma,rho,v0,r,T,s0,K,type)
ret=0.5+1/pi*quadl(@HestonPIntegrand,0,100,[],[],kappa,theta,sigma,rho,v0,r,T,s0,K,type);

```

```

function ret = HestonPIntegrand(phi,kappa,theta,sigma,rho,v0,r,T,s0,K,type)
ret = real(exp(-i*phi*log(K)).*Hestf(phi,kappa,theta,sigma,rho,v0,r,T,s0,type)./(i*phi));
function f = Hestf(phi,kappa,theta,sigma,rho,v0,r,T,s0,type);
if type == 1
u = 0.5;
b = kappa - rho*sigma;
else
u = -0.5;
b = kappa;
end
a = kappa*theta; x = log(s0);
d = sqrt((rho*sigma*phi.*i-b).^2-sigma^2*(2*u*phi.*i-phi.^2));
g = (b-rho*sigma*phi*i + d)./(b-rho*sigma*phi*i - d);
C = r*phi.*i*T + a/sigma^2.*((b- rho*sigma*phi*i + d)*T -2*log((1-g.*exp(d*T))./(1-g)));
D = (b-rho*sigma*phi*i + d)./sigma^2.*((1-exp(d*T))./(1-g.*exp(d*T)));
f = exp(C + D*v0 + i*phi*x);

```


Appendix C

Curriculum Vitae

Rudolf Bauer

Lindenweg 5 • 3632 Bad Traunstein • Austria
E-mail: bauer.r@hotmail.com

▣ EDUCATION

- Oct. 2005 to Mar. 2012 **Vienna University of Technology**
Diploma study in Technical Mathematics (equivalent to M.Sc.)
• Main subject: Financial and Actuarial Mathematics
• Thesis: Fast Calibration in the Heston Model
- Feb. – May 2009 **University of Bath (UK)**
Exchange Semester at the Department of Mathematical Sciences
- 1996 – 2004 **Bundesrealgymnasium Zwettl**
A-levels passed with distinction

▣ INTERNSHIPS

- July 2010 – Feb. 2011 **Pioneer Investments Austria GmbH, Vienna – Risk Management**
• Daily analysis, validation and reporting of Value-at-Risk results
• Further improvement of programs
• Data monitoring and processing: e.g. CDS, Benchmarks
- July – Sept. 2009 **Centrum Bank AG, Vaduz (LI) – Risk Controlling**
• Support in implementation of Focus ALM (risk managing software)
• Preparation of a tool for the replication of variable products
• Statistical evaluation and data maintenance: e.g. ratings
- Sept. 2008 **BA-CA Versicherung AG, Vienna – Actuarial Mathematics and Reinsurance**
• Various Calculations (e.g. cash values)
• Support in balancing of accounts, establishing business plans
- Aug. 2008 **Verbund AG, Vienna – Optimisation of Hydropower Application**
• Support in implementation of a software for resource optimisation
• Preparation of diagrams and statistics

▣ OTHER EMPLOYMENTS

- Summer 2003,04,06,07 **Brantner & Dürr, Zwettl – Waste disposal**
- Jan. – Sept. 2005 **Military Service, Lager Kaufholz**
- Summer 2001,02 **Hotel St. Georg, Bad Traunstein – Hotel and restaurant industry**

▣ COMPUTER SKILLS

- Advanced MS Office, LaTeX
- Intermediate Bloomberg, MATLAB, SPSS, Visual Basic
- Basics C, Maple, R

▣ LANGUAGE SKILLS

- German Mother tongue
- English Fluent spoken and written

▣ ADDITIONAL INFORMATION

- Driving licence Austrian driving licence, categories B and C
- Voluntary associations
• Buddynetwork of TU Vienna: Responsible for exchange students
• Brass band of Bad Traunstein: Playing drum kit
• Sports Union Bad Traunstein: Coach of football youth teams
- Other leisure activities Travelling, skiing, volleyball

Bibliography

- [1] ALBRECHER, H., MAYER, P., SCHOUTENS, W., AND TISTAERT, J. The Little Heston Trap. Working Paper, Linz and Graz University of Technology, K.U. Leuven, ING Financial Markets, 2006.
- [2] ALÒS, AND EWALD, C. O. Malliavin differentiability of the Heston volatility and applications to option pricing. *Advances in Applied Probability*, 40 (1), (2008), 144-162.
- [3] AMIN, K. I., AND JARROW, R. A. *Pricing Options On Risky Assets In A Stochastic Interest Rate Economy*. Mathematical Finance, Wiley Blackwell, 2(4), (1992), 217-237.
- [4] BAJEUX, I., AND ROCHET, J. C. Dynamic Spanning: Are Options an Appropriate Instrument. *Math. Finance* 6, 1, (1996), 1-17.
- [5] BAKSHI, G., CAO, C., AND CHEN, Z. Empirical performance of alternative option pricing models. *Journal of Finance*, 52, (1997), 2003-2049.
- [6] BERESTYCKI, H., BUSCA, J., AND FLORENT, I. Computing the Implied Volatility in Stochastic Volatility models. *Communications in Pure and Applied Mathematics*, 57, (2004), 1352-1373.
- [7] BJÖRK, T. *Arbitrage Theory in Continuous Time*. Oxford University Press, 3, 2009.
- [8] BLACK, R. Studies of Stock Price Volatility Changes. *Proceedings of the 1976 Meetings of the American Association, Business and Economic Statistic Section*, (1976), 177-181.
- [9] BLACK, F., AND SCHOLES, M. The Valuation of Options and Corporate Liabilities. *Journal of Political Economy*, 81, (1973), 637-654.
- [10] CARR, P. P., CHANG, E. C., AND MADAN, D. B. The Variance-Gamma Process and Option Pricing. *European Finance Review*, 2, (1998), 79-105.
- [11] CARR, P. P., AND MADAN, D. B. Towards a theory of volatility trading. In R. Jarrow (Ed.), *Volatility*, Risk Publications, (1998), 417-427.
- [12] CONT, R. Empirical properties of asset returns: stylized facts and statistical issues. *Quantitative Finance* 1, (2001), 223-236.

- [13] COX, J. C., AND ROSS, S. A. The Valuation of Options for Alternative Stochastic Processes. *Journal of Financial Economics*, 3, (1976), 145-166.
- [14] COX, J. C., INGERSOLL, J. E., AND ROSS, S. A. A theory of the term structure of interest rates. *Econometrica*, 5, (1985), 385-407.
- [15] DETEMPLE, J., AND SELDEN, L. A General Equilibrium Analysis of Option and Stock Market Interactions. *Inter. Econ. Rev.* 32, 2, (1991), 279-303.
- [16] DRĂGULESCU, A. D., AND YAKOVENKO, V. M. Probability distribution of returns in the Heston model with stochastic volatility. *Quantitative Finance* 2, 6 (2001), 443-453.
- [17] DURRLEMAN, V. From implied to spot volatilities. PhD dissertation, Princeton University, 2004.
- [18] FAMA, E. F. Mandelbrot and the Stable Paretian Hypothesis. *The Journal of Business*, 36, (1965), 420-429.
- [19] FENG, J., FORDE, M., AND FOUQUE, J. P. Short maturity asymptotics for a fast meanreverting Heston stochastic volatility model. *SIAM Journal on Financial Mathematics*, 1, (2010), 126-141.
- [20] FINCAD The Heston Model of Stochastic Volatility: Fast Option Pricing and Accurate Calibration, available at: <http://www.fincad.com/derivatives-resources/articles/heston-model-stochastic-volatility.aspx>, 2007.
- [21] FORDE, M., AND JACQUIER, A. Small time asymptotics for the implied volatility under the Heston model. *International Journal of Theoretical and Applied Finance*, 12(6), 2009.
- [22] FORDE, M. StocVol smile toolpack documentation: a survey of asymptotic results for stochastic volatility and exponential Lévy models. Formula Sheet, Dublin City University, available at <http://webpages.dcu.ie/~fordem/research/FormulaSheet.pdf>, 2011.
- [23] FORDE, M., AND JACQUIER, A. The large-maturity smile for the Heston model. *Finance and Stochastics*, In Press, 2010.
- [24] FORDE, M., JACQUIER, A., AND LEE, R. The small time smile and term structure of implied volatility under the Heston model. Available at <http://math.uchicago.edu/~rl/FJL.pdf>, 2011.
- [25] FORDE, M., JACQUIER, A., AND MIJATOVIĆ Asymptotic formulae for implied volatility in the Heston model. *Proceedings of the Royal Society A*, 466 (2124) (2010), 3593-3620.
- [26] FOUQUE, J.-P., PAPANICOLAOU, G., AND SIRCAR K. R. *Derivatives in Financial Markets with Stochastic Volatility*. Cambridge University Press, 2000.

- [27] FRIZ, P., GERHOLD, S., GULISASHVILI, A., AND STURM, S. On refined volatility smile expansion in the Heston model. *Quantitative Finance*, In Press, 2011.
- [28] GATHERAL, J. *The Volatility Surface, A Practitioner's Guide*. Wiley, 2006.
- [29] GAUTHIER, P., AND RIVAILLE, P.-Y. H. Fitting the smile: Smart parameters for SABR and Heston. Available at http://papers.ssrn.com/sol3/papers.cfm?abstract_id=1496982, 2009.
- [30] GULISASHVILI, A., AND STEIN, E. M. Asymptotic behavior of the stock price distribution density and implied volatility in stochastic models. *Appl. Math. Optim.*, 61, 3 (2010), 287-315.
- [31] HART, O. D. On the Optimality of Equilibrium when the Market Structure is Incomplete. *Journal Economic Theory*, 11, (1975), 418-443.
- [32] HENRY-LABORDÈRE, P. A General Asymptotic Implied Volatility for Stochastic Volatility Models. *Proceedings of the Petit déjeuner de la Finance*, <http://ssrn.com/abstract=698601>, 2005.
- [33] HESTON, S. A closed-form solution for options with stochastic volatility with applications to bond and currency options. *Review of Financial Studies* 6 (1993), 327-343.
- [34] HULL, J. C. *Options, Futures, And Other Derivatives*, Pearson Prentice Hall, 8th edition, 2011.
- [35] HULL, J., AND WHITE, A. The Pricing of Options on Assets with Stochastic Volatilities. *Journal of Finance*, 42, (1987), 281-300.
- [36] JACKWERTH, J. C., AND RUBINSTEIN, M. Recovering Probability Distributions from Option Prices. *The Journal of Finance*, 51, (1996), 1611-1631.
- [37] JACQUIER, A., AND MARTINI, C. Heston 2010. *Zeliade Systems*, White Paper, available at <http://www.zeliade.com/whitepapers/zwp-0004.pdf>, 2010.
- [38] KARATZAS, I., AND SHREVE, S. *Brownian motion and Stochastic Calculus*. Springer-Verlag, 1991.
- [39] KARLIN, S., AND TAYLOR, H.M. A second course in stochastic processes. Academic Press, 1981.
- [40] KARLSSON, P. The Heston Model: Stochastic Volatility and Approximation, Departement of Economics, Lund University, 2008.
- [41] KIM, I. J., AND KIM, S. Empirical comparison of alternative stochastic volatility option pricing models: Evidence from Korean KOSPI 200 index options market. *Pacific-Basin Finance Journal*, 12, (2004), 117-142.

- [42] LEE, R. W. The moment formula for implied volatility at extreme strikes. *Math. Finance* 14, 3 (2004), 469-480.
- [43] LUCIC, V. Forward start options in stochastic volatility models. *Wilmott Magazine*, September Issue, 2003.
- [44] MANDELBROT, B. The variation of certain speculative prices. *The Journal of Business*, 36, (1963a), 394-419.
- [45] MANDELBROT, B. New methods in statistical economics. *Journal of Political Economy*, 61, (1963b), 421-440.
- [46] MEDVEDEV, A., AND SCAILLET, O. A Simple Calibration Procedure of Stochastic Volatility Models with Jumps by Short Term Asymptotic. *FAME Research Paper Series*, rp93, International Center for Financial Asset Management and Engineering, 2004.
- [47] MERT, M. C. Ein Empirischer Vergleich von Stochastischen Optionswertungsmodellen. Institute of Mathematical Methods in Economics, Vienna University of Technology, 2011.
- [48] MERTON, R. C. The Theory of Rational Option Pricing. *Bell Journal of Economics and Management Science*, 4, (1973), 141-183.
- [49] MERTON, R. C. Option Pricing When Underlying Stock Returns Are Discontinuous. *Journal of Financial Economics*, 3, (1976), 125-144.
- [50] MIKHAILOV, S., AND NÖGEL, U. Heston's Stochastic Volatility Model: Implementation, Calibration, and some Extensions. *Wilmott*, (2003), 74-94.
- [51] MOODLEY, N. The Heston Model: A Practical Approach. Faculty of Science, University of the Witwatersrand, Johannesburg, South Africa, 2005.
- [52] MUSIELA, M., AND RUTKOWSKI, M. *Martingale Methods in Financial Modelling*. Springer-Verlag, 1997.
- [53] ROMANO, M., AND TOUZI, N. Contingent Claims and Market Completeness in a Stochastic Volatility Model. *Math. Finance* 7, 4, (1997), 399-410.
- [54] SAMUELSON, P. Mathematics of speculative prices. *SIAM Review*, 15, (1973), 1-39.
- [55] SCHOUTENS, W., SIMONS, E., AND TISTAERT, J. A perfect calibration! Now what? *Wilmott Magazine*, 2, (2004), 66-78.
- [56] SCOTT, L.O. Option Pricing When the Variance Changes Randomly: Theory, Estimation, and an Application. *Journal of Financial and Quantitative Analysis*, 22, (1987), 419-438.
- [57] STEIN, E. M., AND STEIN, J. C. Stock Price Distributions with Stochastic Volatility: An Analytic Approach. *Journal of Financial and Quantitative Analysis*, 4, (1991), 727-752.

- [58] VARADHAN, S. R. S. On the behavior of the fundamental solution of the heat equation with variable coefficients. *Communications in Pure and Applied Mathematics*, 20, (1967), 431-455.
- [59] WIGGINS, J. B. Option Values under Stochastic Volatilities. *Journal of Economics*, 19, (1987), 351-372.
- [60] WILMOTT, P. Chichester: John Wiley & Sons. *Paul Wilmott on Quantitative Finance*, 2000.
- [61] WIENER BÖRSE History of the exchange operating company, available at <http://en.wienerborse.at/static/cms/sites/wbag/media/en/pdf/about/history.pdf>, 2009.
- [62] ZELIADÉ SYSTEMS Heston 2009. *Zeliade Systems White Paper*, available at <http://www.zeliade.com/whitepapers/zwp-0004.pdf>, 2009.